Rapid Fluorescence Amplified Biofilm Detection

Herzog, Dylan Benjamin

Awarding institution:
King's College London

Rapid Fluorescence Amplified Biofilm Detection

Dylan Benjamin Herzog

A thesis submitted for the degree of

Doctor of Philosophy

Tissue Engineering and Biophotonics

Dental Institute, King's College London

September 2016

Abstract

Bacterial biofilms are the cause of many diseases linked to persistent bacterial infection. When remaining in the root canal space following endodontic treatment, bacteria can lead to a secondary infection, resulting in treatment failure and the subsequent need for re-intervention. Currently, there are no methods in use to detect bacterial presence within the root canal space in a fast and reliable manner. Such methods would be especially beneficial in determining the end point of root canal treatments.

Here, we make use of molecular fluorescent dyes and fluorescent microscopy/spectroscopy to optically detect remnant live bacteria within the root canal space. Calcein AM was evaluated as a fast acting vital cell stain, suitable for rapid staining of stressed and mature biofilms. Calcein AM staining produced fluorescence only when vital bacteria were present and showed significantly higher ratios for vital/non-vital bacteria as well as vital bacteria/ substrates when compared to other stains tested ($p<0.001$).

Detection was achieved with an *ex-situ* approach, where root canals were sampled with endodontic paper points for subsequent staining and analysis using a spectrometer coupled to a fluorescence microscope. Detection of vital cells in a stressed *in-vitro* endodontic biofilm was shown to be more sensitive than culturing: fluorescence detection was achieved for up to 40 seconds of 1% NaOCl exposure, compared to 15 seconds for culturing. The methodology was then applied to clinical trial involving 53 teeth and 114 roots. Detection immediately pre-obturation was achieved in 18.4% of roots and in 35.8% of teeth.

The feasibility of remote *in-situ* spectral analysis was shown with preliminary studies using fluorescent beads as well as *in-vitro* studies using a 200 µm diameter probe on biofilms. Ratiometric analysis of live/dead stained nutritionally starved endodontic biofilms provided a simple alternative to conventional live/dead staining.

Using software for spectral unmixing provided a method for fast and objective detection. The creation of a prototype, which couples a fluorescence spectrometer to a wide-field microscope, allowed for a successful patient trial, demonstrating the potential of this system to be miniaturised and commercialised for a chair-side use.

Table of Contents

Table of Figures

Table of Tables

Acknowledgements

I would firstly like to thank my supervisors Dr. Frederic Festy, Professor Tim Watson and Professor Francesco Mannocci for offering scientific guidance and support, whilst having faith in my ability to work independently. Specifically, I wish to thank Dr. Frederic Festy for his continued support and time invested in this project and helping me over the past four years, both for general issues as well as imaging and microscopy questions. I would also like to express my gratitude to Professor Francesco Mannocci for all his help with the clinical trial as well as any endodontic related issues and questions. My gratitude also goes to Professor Tim Watson for his guidance and help, especially for his help with my thesis. I would also like to thank Federico Foschi for his supervision and guidance, especially early on in the project.

Further, I am very grateful for all the help and support I was offered both in and outside the lab by other members of the dental institute. My sincere gratitude goes to Dr. Sadia Niazi for all her training with bacterial culturing and fluorescence staining in the microbiology lab, as well as support outside of the lab and her work on the establishment and confirmation of the endodontic biofilms used in the *in-vitro* studies. I would also like to thank Dr. Chris Chong, Dr. Garrit Koller and especially Dr. Liisa Hirvonen for all the help and support early on in my PhD. My gratitude also goes to Dr. Neveen Hosny for her general help and guidance in writing. I am also very grateful for the help provided in the labs by Steve Gilbert, Richard Mallet and Peter Pilecki, with special thanks to Peter Pilecki for proofreading the thesis. I would further like to thank Riyaz Sogiawalla and Rohit Chaturvedi for their assistance with the proof of concept studies.

I owe sincere gratitude to my funding bodies, the EPSRC as well as the Guy's and St Thomas' NHS Trust.

A huge amount of gratitude also goes to my girlfriend Eva, for being very patient and supportive throughout this PhD and for being on the receiving end of a substantial amount of practice presentations. Finally, I would like to thank my parents for all their support over the years, in all my endeavours and especially in my academic career.

Abbreviations

Abbreviation	Meaning
AF	Autofluorescence
CAM	Calcein AM
CBCT	Cone Beam Computed Tomography
CFU	Colony Forming Unit
CP	Cold Plasma
DMSO	Dimethyl Sulfoxide
Em	Emission
EPSRC CASE	Engineering and Physical Sciences Research Council Collaborative Awards in Science and Engineering
EPS	Extracellular Polymeric Substance
Ex	Excitation
FITC	Fluorescein Isothiocyanate
HA	Hydroxyapatite
mFUM	Modified Fluid Universal Medium
NaOCl	Sodium Hypochlorite
OCT	Optical Coherence Tomography
PAD	Photo Activated Disinfection
PBS	Phosphate Buffered Saline
PI	Propidium Iodide
RC	Root Canal
RCT	Root Canal Treatment
RGB	Red Green Blue
SHG	Second Harmonic Generation
2P	Two-Photon

Thesis overview

Interactions between bacteria and their human hosts are constantly occurring, from the countless commensal bacteria in our gastrointestinal tract, to the daily contact we have with contaminated surfaces and air. It is the pathogenic and opportunistic bacteria that cause disease in us. Their ability to adapt to various treatments and environments make bacterial infections a continuous challenge. Many bacterial infections involve multiple species interacting together, adhering to surfaces and creating a protective exopolysaccharide matrix. Such microcolonies are termed biofilms and are far more resistant to treatment than their planktonic counterparts. Biofilm infections play a large role in persistent bacterial infections. From a dental standpoint, a very common microbial biofilm presents itself in plaque formation on teeth. Further, less visible biofilm infections occur during implant placement, or in root canal infections, when pathogenic or opportunistic bacteria get access to the root canal space. In the UK alone about one million root canal treatments are carried out each year. The resilient nature of biofilms means many of these require secondary disinfection due to residual vital bacteria.

This PhD focuses on using fluorescent staining and micro-spectroscopy to rapidly detect vital cells in mature bacterial biofilms, primarily focused on endodontic biofilms but with distinct implications in a broader use for biofilm detection. The term ‘vital’ will be used throughout this thesis to describe any bacterial cells that are still alive, including viable but non-culturable cells.

Bacterial biofilms are microcolonies, most commonly consisting of multiple bacterial species. They are far more resistant to antimicrobial agents than planktonic bacteria, due to the formation of their own microenvironment, protected by an exopolysaccharide matrix: they, therefore, play a large role in persistent bacterial infections. Being able to survive in nutrient-poor hostile environments, they can colonise and survive in dental root canals, even following chemo-mechanical disinfection, creating the need for complicated re-interventions.

Two main approaches for the detection of remnant bacteria in the root canal space were initially explored: firstly, *in-situ* sampling using endodontic paper points (already in use in clinics) followed by *ex-situ* staining and detection (*ex-situ* approach) and secondly *in-situ* staining and detection where the fluorescent stain is applied directly into the root canal followed by *in-situ* detection using a small probe (*in-situ* approach). *In-vitro* proof of concepts using

fluorescent beads were carried out for both of these approaches. The fluorescent beads were seen as simulations of fluorescently stained bacteria and were applied to root canals of extracted teeth to simulate the *in-situ* approach and to endodontic paper points for the *ex-situ* approach.

Following these proof of concept studies, suitable fluorescent dyes for rapid detection of mature biofilms were evaluated. The stains were evaluated for fluorescence intensity, specificity to live cells and incubation time. In order to be seen as a clinically relevant stain, the incubation time was chosen to be a maximum of 5 minutes. The fluorescent stains were evaluated on an established mature endodontic biofilm. The biofilm consists of strains of typical root canal colonisers, confirmed using 16SrRNA gene sequencing as well as CFU counting. Evaluation of the fluorescent dyes was carried out using confocal scanning laser microscopy, a widely used imaging method for stained microbes. Various types of stains differing in binding method and fluorescent wavelengths were tested. We then investigated the correlation of the number of vital bacteria to the fluorescence intensity, by comparing CFU counting of a dilution series of *Enterococcus faecalis,* a common, persistent root canal pathogen, to live fluorescent staining.

In order to increase the sensitivity of detecting vital cells within a biofilm, we created a prototype setup that coupled a spectrometer to a fluorescence microscope with a custom filter cube allowing for spectral analysis. The fluorescent dyes had a very distinct spectrum, distinguishable from the autofluorescence of a given substrate and can thus be detected even at low fluorescence intensities. Spectral unmixing software determined the contribution of the fluorescent stain to a measured spectrum. We applied this prototype for the rapid detection of vital cells in a sodium hypochlorite (NaOCl) stressed *in-vitro* grown biofilm to simulate bacteria surviving during a root canal treatment.

The approach taken, to develop a rapid system for biofilm detection in the RC system, can be broadly split into four main steps.

1. Proof of concept studies assessing the feasibility of detection of fluorophores in relation to clinical settings.
2. Characterisation of fluorescent dyes on a multispecies nutritionally starved endodontic biofilm, which represents conditions found in the RC space.
3. Choice and development of an appropriate optical detection system including fluorescence microscopy and spectroscopy, for both an *in-situ* and *ex-situ* approach.
4. Choice of *in-vitro* studies to assess bacterial detection and comparison to culturing, using the detection system.
5. The evaluation of a final detection system in a patient trial.

Given the nature of the EPSRC CASE (Engineering & Physical Sciences Research Council, Cooperative Awards in Science & Technology) studentship, this project had the aim to increase the impact of the studies carried out by applying them to clinical settings. Following the *in-vitro* studies, a clinical trial was rolled out utilising the *ex-situ* method, that is, paper point sampling followed by fluorescent staining with the viability stain calcein AM. Fifty-three patients undergoing primary root canal treatment were recruited and signed informed consent. During the root canal treatment, samples were taken at three time-points: Immediately after accessing the root canal space, following the shaping process of the canals and pre-obturation of the root canal space. With the pre-obturation sample indicating whether the canal space was sufficiently disinfected at the end of the treatment.

A further application of this prototype presented itself in the assessment of various disinfection methods used to remove biofilms from dental implants. The rapid detection using spectral un-mixing was compared to various other detection methods by removing a relevant mature biofilm from titanium surfaces.

Overall, we demonstrate a rapid, easy to use method based on vital fluorescent staining, which has been shown to detect vital cells in stressed biofilms both using *in-vitro* and *in-vivo* sampling of root canals. The assessment of disinfection methods in the removal of biofilms from implants indicates how this method could have a very broad application in rapid detection of biofilms and assessment of removal techniques in various situations.

Chapter 1 *Literature Review*

1.1 Microbial biofilms

Bacteria are often viewed and studied as independent single-celled organisms. Despite having the ability to function as single cells, it has become more apparent just how common it is for bacteria to co-interact and form multi-cellular, interdependent communities. When bacteria form such populations, we speak of biofilms. Biofilms typically, but not exclusively, form on surface areas, often at a liquid – solid interface (Davey et al., 2000; Hall-Stoodley et al., 2004). The bacteria within a biofilm excrete an extracellular polymeric substance (EPS) which, together with other substances, largely contributes to the EPS matrix (Flemming and Wingender, 2010). The extracellular matrix has various roles in providing the biofilm with structure, suitable environment for anaerobic bacteria, nutrient absorption, protection against antibacterial agents and environmental stress as well as bringing about homeostasis. A microbial biofilm can consist of multiple single cell organisms of a single species of bacteria. More commonly, however, it consists of multiple, co-dependent, interacting species (Davey et al., 2000; Hall-Stoodley et al., 2004).

The following aspects are associated with and are used to characterise bacterial biofilms involved in host infections:

- The bacteria must be adherent to a surface or substratum.
- The bacteria must be in microcolonies/cell clusters embedded in EPS matrix.
- Infection is local to a particular area, unless dissemination occurs.
- The infection must be partially/completely resistant to antibiotic treatment although the planktonic form of the species is responsive to the antibiotic drug (Parsek and Singh, 2003).

Biofilm infections are involved in a large amount of bacteria associated infections. Any medical devices or implants inserted into patients have the potential for biofilm infections: from joint replacements and catheters to contact lenses. The infection interfaces can also be native, such as in wound or respiratory infections.(Drago et al., 2012; Wu et al., 2015; Roy et al., 2014)

1.1.1 Development

Broadly speaking biofilm development is the transition of planktonic microbes into a resistant mature biofilm, surrounded by an extracellular matrix. The processes and environmental cues for biofilm formation vary depending on species, however, the developmental steps from initial attachment to a surface, formation of microcolonies, and maturation into an EPS matrix covered biofilm, followed by dispersion are steps that can generally be applied. Figure 1 illustrates formation, maturation and dispersion of a biofilm (Davey et al., 2000).

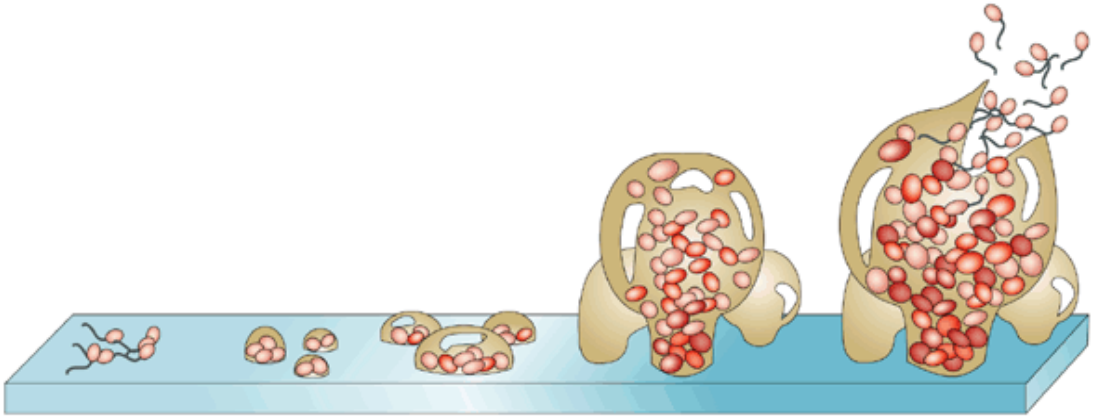

Figure 1: Illustration of initial attachment, formation of microcolonies surrounded by EPS matrix and finally dispersion of planktonic cells (Davies, 2003). Permission of use granted by Nature Publishing Group.

Attachment and adhesion

Initial attachment of biofilms and subsequent biofilm formation occurs when microbes encounter conditions favourable for the transition from a planktonic state to surface attached colonisation. It is important to note that favourable conditions and mechanisms of attachment vary from species to species (Toole et al., 2000).

Using crystal violet staining, genetic approaches and *Pseudomonas fluorescens* as a model organism, O'Toole *et al*. explored attachment mechanisms and environmental influences on the initial attachment of the biofilm (O'Toole and Kolter, 1998). They demonstrated the need for protein synthesis in initial biofilm formation. *P. fluorescens* incubated in the presence of the tetracycline (a protein synthesis inhibitor) was shown to be strongly inhibited in the biofilm.

Inhibition only applied to initial attachment, cells previously attached for 30 mins showed no negative response to the same exposure to tetracycline. Further, adding a protease to the assay demonstrated the importance of extracellular proteins during attachment. Environmental conditions such as osmolality and nutrition also influenced biofilm attachment. However, conditions promoting cell growth do not necessarily favour biofilm formation. Genetic approaches revealed 37 mutant strains which were defective in biofilm formation but unhindered in planktonic proliferation in medium. The mutants included strains with defects in flagellum synthesis as well as in proteins with functions in degrading misfolded proteins. Many of the mutants could be rescued: supplementation of iron, citrate or glutamate resulted in the strains being able to form biofilms, suggesting multiple pathways for surface attachment dependent on environmental conditions (O'Toole and Kolter, 1998).

A more recent study exploring attachment of *Escherichia coli* found that the laboratory strain, despite having genes for adhesins such as flagella pili and curli, are unable to attach to glass surfaces and form biofilms. In contrast, four out of eight tested environmental strains of *E.coli* showed the ability to attach and form biofilms when compared to the laboratory strain. Interestingly, attachment was temperature dependent, with growth at 28 degrees but not at 37. Only the strains able to form a biofilm expressed curli fibres (protein structures involved in adhesion). Further, a co-dependant adhesion was demonstrated: laboratory strains of *E.coli* and *Pseudomonas putida,* each individually unable to form biofilms, showed significantly increased attachment when co-cultured (Castonguay et al., 2006).

Attachment surfaces and preconditioning of these surfaces are also factors to consider in biofilm attachment. A review of the literature by Teughels *et al*. concludes that increase in surface roughness above a threshold R_a of 0.2 µm aids biofilm formation on implant materials (Teughels et al., 2006). Surface coating also has an important role in initial attachment: Surfaces exposed to growth medium or human bodily fluids form an initial film of minerals, proteins and polysaccharides, depending on the initial film and the microbial strains, this can increase or inhibit biofilm formation. A recent study shows increased biofilm formation not only on rougher surfaces but on more hydrophobic surfaces, thought to favour initial protein aggregation and thus induce biofilm growth (Lüdecke et al., 2014).

These studies demonstrate initial biofilm attachment to be made up of many varying mechanisms (which differ between strain), show beneficial multispecies interactions and multiple environmental dependent adhesion pathways. Attachment of the biofilm to a surface is the first step leading to maturation of the biofilm, and, to the upregulation of factors in favour of life as a sessile colony (Kostakioti et al., 2013). One of the main shifts in the formation of a mature biofilm being the establishment of robust biofilm structure, including the extracellular polymeric substance, as will be discussed in the following sections (Flemming and Wingender, 2010).

1.1.2 Structure and extracellular matrix

The extracellular polymeric substance (EPS) matrix is a fundamental part of the biofilm nature and can make up over 90% of the dry mass in a biofilm. It surrounds the microbes in a biofilm, giving it structure, including physical micro-domains within and increasing cell interactions. Further, extracellular enzymes are kept in close proximity, aiding in digestion of nutrients and recycling of debris. The matrix provides protection against physical and antimicrobial actions, as well as fluctuations in the environment by active retention of water (Flemming and Wingender, 2010). The EPS matrix consists of various polymers, excreted by the microbes within the biofilm themselves, predominantly including the following:

- Exopolysaccharides: the main component of the matrix, commonly they are long linear or branched molecules involved in initial surface attachment, biofilm formation as well as structure (Colvin et al., 2011).
- Proteins: also a large component of the EPS (Toyofuku et al., 2012), are involved in enzymatic digestion of nutrients within the biofilm, they also have roles in the digestion and rearrangement of the EPS matrix itself. Further, they facilitate dispersion of bacterial cells, often in response to a change in nutrient availability. Non-enzymatic proteins such as lectins, which bind to carbohydrates are involved in formation, crosslinking and stabilisation of the biofilm.
- Matrix DNA: has been shown to function as an adhesion as well as for intercellular connection (Harmsen et al., 2010; Flemming and Wingender, 2010)

Part of the virulence presented by the EPS matrix is simply the protection and enhanced interaction provided to the cells within the biofilm (Flemming and Wingender, 2010). However, it has been shown to play a more active role in virulence as demonstrated by Xiao *et al.,* who used a mixed species biofilm, analysed by confocal microscopy and gene sequencing (Xiao et al., 2012. The EPS matrix was shown to promote local accumulation of bacteria and connect forming microcolonies. Facilitating the 3D structure of the biofilm, heterogeneous pH environments were found with accumulations of acidogenic bacteria and virulence on the surface (Xiao et al., 2012). Supplementation with sucrose was shown to trigger EPS matrix formation, It was also found that EPS matrix related gene expression was significantly upregulated in mixed species biofilm compared to individual strains, highlighting the importance of environmental triggers on the EPS formation (Xiao et al., 2012)**.**

Communications between bacteria in biofilms, or bacteria in general, occur primarily through quorum sensing systems: small signalling molecules produced and excreted by bacteria increase in concentration as the population density increases and once these molecules reach a certain threshold, they trigger a change in gene expression in the quorum-sensing bacteria. These signalling molecules are often referred to as pheromones or auto-inducers. Quorum sensing regulates the behaviour of bacteria within a population, and by reacting to internal and external changes, can aid a biofilm in survival. Signal excretion and reaction is often studied on single species, but interactions in between different strains of bacteria within a population have been shown to influence biofilm behaviour (Miller and Bassler, 2001; Solano et al., 2014). The disruption of quorum sensing in biofilms has been shown to reduce biofilm formation on various species and has been suggested to be applied to combat biofouling issues as shown in a study by Paul *et al*. (Paul et al., 2009). Interestingly, quorum sensing has also been harnessed to control biofilm formation in beneficial biofilms: applications such as bioremediation (use of microbes to break down pollutants) and bio refineries (conversion of biomass to fuel) could use the multispecies, robust nature of biofilms for more efficient complex transformation than possible with their planktonic counterparts could. Hong *et al*. demonstrate an artificial quorum sensing circuit for this purpose, allowing for the establishment and removal of a two-species biofilm at will (Hong et al., 2012).

1.1.3 Biofilm formation as a bacterial defence mechanism

It has been long known that biofilm resistance to antibiotics increases significantly when bacteria form biofilms (Gristina et al., 1987; Evans and Holmes, 1987; Sedlacek and Walker, 2007), in addition to this, maturity of the formed biofilm has been shown to play a role in resistance, resulting in a lesser effect of antibiotic treatment than in young biofilms (Anwar et al., 1992). Antibiotics are often applied to keep bacterial and biofilm infections at bay, however, studies suggest that antibiotic treatment, especially when the doses are insufficient, can lead to a shift in the microbiota and increase biofilm and extracellular matrix formation (Bleich et al., 2015; Mart et al., 2014). Moreover, largely due to EPS production, biofilm formation can protect its community from other chemical disinfection, the host immune response, germicides and even from physical removal, as biofilm structures can offer resistance to mechanical disruption when grown in challenging environments (Donlan and Costerton, 2002). EPS production and other defence mechanisms are often increased when the biofilm community is confronted with unfavourable environmental conditions, such as starvation or toxic stress (Donlan and Costerton, 2002; Fux et al., 2005).

Adaption to the environment

An important part of biofilm survival is the ability to adapt to a large range of environments, including changes in availability of nutrients, change in pH and even presence of antimicrobial agents. Biofilm communities can trigger a stress response which can lead to physiological changes resulting in a biofilm phenotype more suited to the change in environment (Poole, 2012; Fux et al., 2005). As shown by Xiao *et al*., challenges introduced by changes in environment can also favour or shift the numbers of vital bacteria of different species within a biofilm. Shifts in the dominant species within a biofilm can have profound effects and lead to higher virulence factors, such as an increase in acidogenic bacteria like *Streptococcus mutans* in response to the availability of sucrose (Xiao et al., 2012). Bacteria have long been known to react to nutritional starvation by a so called ‘stringent response’ which involves conservation of energy by downregulation of protein and nucleic acid synthesis, whilst upregulating the degradation of protein by the synthesis of signalling molecules which hinder synthesis of nucleic acids (Chatterji and Kumar Ojha, 2001). Nguyen *et al*. demonstrate that the

same applies to biofilm starvation: They demonstrated that this active response to starvation is directly linked to antibiotic resistance (Nguyen et al., 2011). Dormancy has also been shown as a response to various unfavourable environments, such as nutritional or chemical stress, extreme temperatures and oxygen availability. Entering such a dormant and non-culturable state can also result in such bacteria remaining undetected (Li et al., 2014). These are some of many means of biofilms to adapt to hostile environments, their ability to adapt is as a result of the multispecies nature and interaction, as well as inherent bacterial survival mechanisms that are a large part of their success and prevalence during infections.

Extracellular Polymeric Substance Matrix

The EPS matrix, as a first barrier, impedes diffusion of large and positively charged molecules into the biofilm, both by physical obstruction and molecular binding. Smaller molecules, however, are not significantly hindered from diffusing into the biofilm, suggesting that defence to smaller antimicrobial molecules relies on more specific binding or neutralisation (de Beer, 1997). Neutralisation or removal of antibiotics in the matrix can occur due to antibiotic-degrading enzymes, such as β-lactamases expressed by *Pseudomonas aerugionsa* (Anwar et al., 1992; Umadevi et al., 2011) or via active transport of efflux pumps (Köhler et al., 1999; Taylor et al., 2014). Defence mechanisms against other disinfectants such as hydrogen peroxide by catalase enzymes in the matrix also aid biofilm survival (Stewart et al., 2000).

Polysaccharides in the EPS matrix have been shown to provide protection from the host immune system: Alginate or alginic acid, an exopolysaccharide, has shown to prevent phagocytosis of biofilm cells by leukocytes (Leid et al., 2005). Upregulation of biofilm formation, and thus matrix production has been shown to increase in bacterial populations exposed to antibiotic treatment (Mart et al., 2014). In a study by Bleich *et al*. the EPS matrix formation in *Bacillus subtilis* was shown to not necessarily just occur as a non-specific response to antibiotics, perceived competition or environmental stress. Using a fluorescent transcription reporter, they were able to monitor matrix gene expression and using thiopeptide antibiotics, demonstrated that biofilm promoting genes could be triggered in the absence of any

antimicrobial effect: thus suggesting a direct signalling and matrix gene activation by these thiopeptides (Bleich et al., 2015).

The close proximity of the bacteria within a matrix surrounded biofilm increases cell interactions, which also leads to an increase in horizontal gene transmission and the rate of mutations. Accelerated horizontal gene transfer can lead to biofilms resistant to multiple antibiotic drugs by the expression of numerous evasion methods (Hoiby et al., 2010).

Dormancy

Within biofilms, most of the activity and growth occurs close to the surface, with only little growth and cell activity in the centre. These largely inactive bacterial don't grow, or die in the presence of antimicrobial agents and are often termed 'persister cells', it has been suggested that their state of dormancy prevents antibiotic killing (Keren et al., 2004). Viable but non-culturable (VBNC) cells are well known phenomenon and are common to both planktonic and biofilm bacteria. A VBNC state can be induced by environmental factors such as toxic stress or starvation, despite their inability to grow using standard culturing methods and having downregulated functions, they are still vital and metabolically active. With the right conditions certain VBNC strains have been shown to be resuscitated to their culturable state (Li et al., 2014).

From the EPS matrix as a barrier to fast response mechanisms, mutating colonies and excretion of protective enzymes, the formation of such multispecies communities with the ability to rapidly respond to environmental cues results in a far more resistant and permanent infection.

1.1.4 Biofilm removal

Being significantly more resistant to antimicrobial treatments and the host immune system, biofilms produce a unique challenge for disinfection. Thorough antimicrobial treatment in patients can keep biofilm infections at bay, however, concentrations high enough to completely eliminate biofilm infections are challenging to reach. Wu *et al*. provide a recent summary of biofilm removal techniques in clinical settings (Wu et al., 2015). A broad distinction is made between infection of foreign bodies such as implants and infections of the host directly. For infections which don't involve implants or foreign bodies, high doses of combined antibiotics

may be sufficient to eliminate the biofilm. Importance lies both in selection of appropriate antibiotics (systemic and topical where possible), as well as correct duration and dosage.

Infections involving implants often require removal and replacement of the implant or surgical treatment involving exposure of the infected surface combined with administration of antibiotics (Schwarz et al., 2014; Wu et al., 2015). Surfaces of dental implants are often ideal for bacterial colonisation, especially when rough surfaces are used to aid osseointegration. A review of the literature by Teughels *et al*. concludes that increase in surface roughness above a threshold R_a of 0.2 µm aids biofilm formation on implant materials (Teughels et al., 2006). Therefore, implant placements not only increase the probability of a biofilm infection occurring, but established biofilms will also be more challenging to remove.

Removal techniques, much like biofilm infection, vary depending on the type and area of infection. Dedicated disinfection techniques are applied for management and ultimately removal of biofilm infections. The following sections will discuss endodontic and implant related methods for biofilm removal in more detail. However, where possible a combination of physical removal and antimicrobial agents is of benefit, as antibiotics or disinfecting irrigant solutions will often not remove established biofilms(Taylor et al., 2014; Metzger et al., 2013). In certain cases, antibiotic treatment has even shown to have a detrimental effect, Bleich *et al*. demonstrate that thiopeptide antibiotics lead to upregulated biofilm formation in *Bacillus subtilis* (Taylor et al., 2014; Sedlacek and Walker, 2007; Bleich et al., 2015). More detailed descriptions of biofilm removal in endodontic and implant related therapy will be discussed in section1.2.2 and 1.3.3, respectively.

1.1.5 Biofilms in dentistry and root canals

Substrates as well as microbes exposed to an organic matter containing solution, such as saliva, immediately become covered in an acellular film, known as the pellicle (Teughels et al., 2006). In the oral cavity, this pellicle is formed of numerous salivary proteins and other macromolecules (Yao et al., 2003). Oral pellicles show supporting functions to the teeth in providing lubrication, which, by reducing friction of the teeth to the surrounding tissue, maintains essential functions such as speech and mastication (Berg et al., 2003). Salivary pellicles have also shown to provide protection of the enamel from stresses such as acid erosion (Hannig and Balz, 2001). However, pellicle formation can also produce favourable conditions for biofilm

formation. For early bacterial colonisers such as streptococci, molecules contained in the pellicle, such as proline-rich proteins and mucins, act as receptors allowing them to bind and create conditions that are more favourable for later colonisers. Subsequent recruitment and build-up of a mature multispecies biofilm results in the structures commonly referred to as dental plaque. (Rosan and Lamont, 2000; Kolenbrander et al., 2006). Figure 2 illustrates the composition of an oral biofilm adherent to a pellicle on an enamel surface.

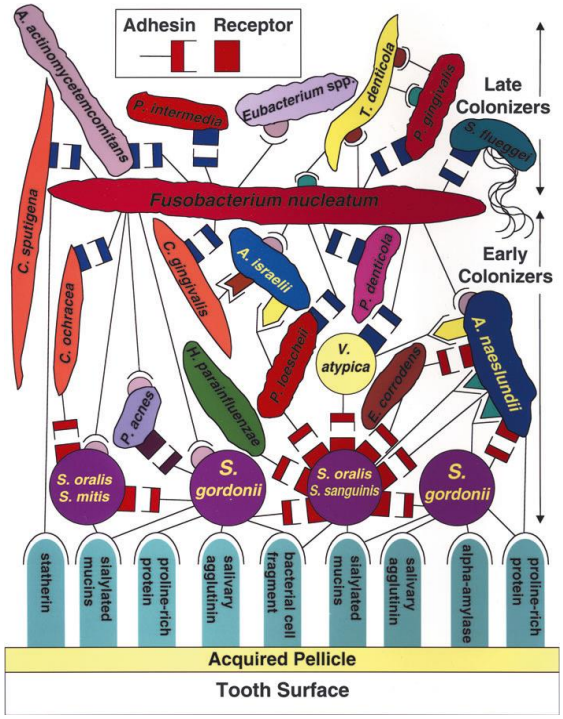

Figure 2: Diagram illustrating the attachment of early colonisers to receptor molecules in the pellicle as well as the co-attachment of late colonisers, resulting in an interconnected multispecies plaque biofilm (Kolenbrander et al., 2006). Permission of use granted by John Wiley and Sons.

Opportunistic or pathogenic bacteria are therefore able to attach to the mucosa and especially the non-shedding dental surfaces within the oral cavity. Given the opportunity and correct virulence factors, such microbes can enter the pulpal tissue and cause a root canal (RC) inflammation (pulpitis) and following this, periapical disease. Typically, bacteria will enter the RC space through a deep caries lesion, following crown placement or root trauma leading to cracks or fractures. Factors such as oral hygiene procedures reduce the virulence of pathogenic microbial communities (Orstavik and Thomas, 2007). However, other environmental factors, such as availability of nutrients in the oral cavity can boost the formation of pathogenic biofilms (Xiao et al., 2012). Although the initial infections of caries are similar to the ones occurring in the pulp, the microbial flora and biofilm species differ, presumably due to nutritional availability

and survival responses of certain species (Orstavik and Thomas, 2007). The RC system, due to its physiological nature, has a limited amount of oxygen and nutrients, making it a very selective environment with conditions leading to it being uninhabitable for most species (Chávez de Paz, 2007).

If the infection of the RC is not removed or halted, necrosis of the pulp tissue within the RC occurs. Once the tissue is necrotic, infection of the entire RC space occurs and the host defence retracts to the periapical tissue (Zehnder and Belibasakis, 2015). Periapical disease normally involves an inflammatory lesion around the RC apex and can presents itself as an acute or chronic inflammation. However, in most cases, especially when the tooth is necrotic, the inflammation is of chronic nature. This lesion is the site of bacterial interaction with the host immune response. The RC space, when necrotic, provides a safe space for the bacterial biofilms, as the various cells of the host response only have limited access to the infection. Varying extents of tissue destruction and retreat of bone tissue from the source of the infection occur as a result of the interactions between the bacterial and the host response. Therefore, a number of host cells (from both the specific and non-specific host defence) get recruited to the site of inflammation including polymorphonuclear leukocytes, macrophages, eosinophils, plasma cells, mast cells and epithelial cells (Gulabivala and Ng, 2014; Zehnder and Belibasakis, 2015).Biofilm presence is a common cause for secondary infections, even in high-standard root canal treatments (RCTs). The bacteria can be located in deltas or irregularities and be unaffected by the mechanical instrumentation of the RC. In such circumstances, the biofilm must also be able to withstand canal disinfecting measures and survive in an environment even more depleted of nutrients. Bacteria with these abilities may cause secondary infections despite high standard RCTs (Siqueira, 2001)(See Table 1 for summary). It is to be added that there is a substantial overlap in the microbiota of primary and persistent infections, the strains detected will also vary depending on the methods of investigation used. An example of this is a recent study using molecular techniques by Siqueira et al., which found *Proteobacteria,* commonly known for primary infections, to be one of the most prevalent phyla in persistent infections (Siqueira et al., 2016). A commonly isolated strain from secondary/persistent infection is *E. faecalis.* Whilst being receptive to antimicrobial agents in its planktonic form, in a biofilm, resistance can increase up to a factor of 1000 (Distel et al., 2002). With increasing

understanding of biofilm formation, it has become more evident that bacteria isolated in a large number from an infected site need not necessarily be the sole causative agent of the infection, rather the accumulation could be a result thereof (Chávez de Paz, 2007). Most RC infections, much like other biofilm infections *in-vivo,* are caused by multiple species, a biofilm infection can host a large number of interacting bacteria, aiding the survival of the biofilm (Chávez de Paz, 2007).

Table 1: Summary of microbial characteristics in root canal infections, determined using both culture and molecular based techniques (Anderson et al., 2012; Gomes et al., 2004; Niazi et al., 2010; Ito et al., 2012; Murad et al., 2014). *Detected species per root canal can vary largely depending on sampling method, growth media used, incubation conditions and identification methods.

Root Canal Infection	Characteristics	Common species
Primary	- Mixed microbiota of gram-positive and gram-negative organisms. - Mostly anaerobes. - Typically 3-10* species per canal recovered (Culturing).	*Fusobacterium necrophorum,* *Fusobacterium nucleatum,* Olsenella profuse, *Porphyromonas gingivalis,* *Prevotella intermedia,* Pseudoramibacter alactolyticus, *Streptococcus constellatus,* *Streptococcus oralis,* *Peptostreptococcus micros,* *Peptostreptococcus prevotii,*
Persistant/Secondary	- Microbiota of largely gram positive organisms. - Mostly facultative anaerobes. - Typically 1-12* species per canal recovered.	*Actinomyces naeslundii,* *Bradyrhizobium japonicum,* *Enterococcus faecalis,* *Enterococcus faecium,* *Eubacterium Saburreum,* *Methylobacterium mesophilicum,* *Propionibacterium acnes,* *Pseudomonas putida,* *Rhodococcus erythropolis,* *Streptococcus mitis,* *Staphylococcus epidermidis,*

Biofilm development, leading to the formation of dental plaque, implant infections and RC infections, therefore present an ongoing challenge in dentistry: in particular, due to resistance of the biofilm to antimicrobial disinfection, removal and virulence factors. Endodontic infections are often especially difficult to deal with, considering the technical challenges of the RCT procedures and complicated RC morphology.

1.2 Endodontics

A tooth can be macroscopically divided into two main parts, the visible crown and the root, which anchors the root into the jaw by extending into the jaw bone. The general structure of the tooth consists of enamel, dentine, cement and the pulp as shown in Figure 3a. Located inside the root is the dental RC system, which is surrounded by dentine. It leads from the pulp chamber down to the apical foramen (root-end opening) and contains within it the connective tissue, referred to as the pulp. The pulp tissue is responsible for the blood and nerve supply to the tooth. Odontoblasts are cells originating in the pulp which form dentine during tooth growth as well has having functions in maintenance and repair. Throughout the lifespan of a tooth physiologic secondary dentine is laid down, additionally, in response to caries or tooth wear tertiary dentine can be laid down (Banerjee and Watson, 2015). A further function of the pulp is the sensory response to pressure, changes in temperature and inflammation. Due to the innervated nature of the pulp tissue combined with the very limited space, inflammation can lead to severe pain in the case of endodontic infections. Dental RCs come in varied numbers, shapes and thicknesses and can have elaborate curvatures and ramifications which are often difficult to access and clean in the context of a RC (Figure 3 b).

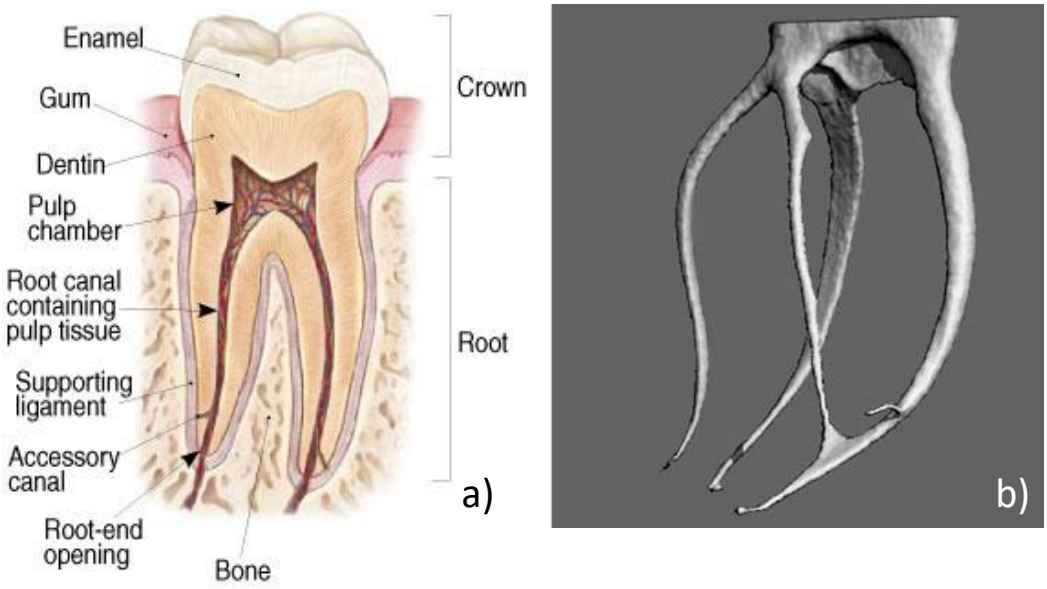

Figure 3: a) Diagram showing the anatomy of a human tooth, including the RC containing the pulpal tissue. b) A µCT image showing the RC anatomy of a maxillary human tooth (Peters et al., 2003). Permission of use granted by John Wiley and Sons.

1.2.1 Root canal treatment

Overview

The goal of an endodontic RCT is the removal of the pulp tissue and biofilm infection from the RC space, followed by thorough sealing of the RC space to avoid any potential re-infection. Ideally, as much of the natural tooth as possible is retained during this procedure. The RC preparation is one of the most important steps of the RCT. It is during this procedure that the debridement, disinfection and removal of infectious agents as well as the shaping of the RC takes place. The quality of the RC preparation will determine the success of the entire treatment (Metzger et al., 2013). The main difficulties in RC preparations lie in the varying, unpredictable RC anatomy, the inability to visualise this anatomy and subsequent lack of penetration of irrigation solutions (Peters, 2004). In most cases RCTs are undertaken using, a chemo mechanical approach including the use of nickel-titanium files/rotary instruments and irrigation with sodium hypochlorite (NaOCl). The combination of mechanical and chemical approaches combines the physical disruption and removal of the bacterial load with irrigant disinfection for the best possible outcome. In many cases the roots are additionally dressed with an antimicrobial medication such as calcium hydroxide which is left in the RC space for a week before completing the treatment (Peters, 2004; Ruddle, 2005; Shuping et al., 2000)

The preparation of the infected canals is a very important factor for the success of the RCT to sufficiently reduce bacterial infection (Metzger et al., 2013; Byström and Sundqvist, 1981). It determines the effectiveness of subsequent debridement, providing access for antimicrobial agents and the final obturation of the canals. The first step of the mechanical treatment is the creation of the access cavity, gaining access to the pulp chamber to expose and access all the root openings, this also involves removing of any present caries and pulp whilst conserving sound tooth structures (Hargreaves and Berman, 2015; Prichard, 2012). Once access to the root system has been achieved, there are various methods in use to prepare the RC space, modern day endodontics typically rely on nickel titanium rotary instrumentation. A popular method which is also used at the King's College Dental institute is the ProTaper Universal method.

Figure 4: Rotary instruments of the ProTaper Universal method: Following coronal scouting with hand files or pathfinders (PF), S1 is passively inserted along the canal to cut and remove dentine before repeating with S2. This allows for scouting of the apical part of the root to establish the working length. S1 and S2 can then be used to achieve working length (SX is used where additional coronal shaping is required). F1 (or F2-F5 where necessary) can then be used to working length. Following successful use of the F files the canal is ready for obturation.

The ProTaper method is characterised by the use of shaping (S) and finishing (F) instruments, the taper of the shaping instruments increases towards the top end of the instrument. First, hand held pathfinder files are introduced into the RC space, establishing a reproducible path into the root. Following this different sized shaping files are inserted whilst applying irrigant solutions such as NaOCl. Using a hand file, the apical part of the RC is then scouted to determine the working length (using an apex locator) and enlarge the apex. The shaping files are then applied to the full length of the roots followed by final instrumentation with finishing files as described in Figure 4 (Ruddle, 2005).

Failure

The highly variable shapes and curvatures of the RC in combination with the treatment being a “blind” procedure lead to a RCT being a challenging undertaking. RCT failures are caused by persistent bacterial biofilms or by the penetration of bacteria via leaking restorations and RC fillings (Chávez de Paz, 2007). Chemo-mechanical techniques are a powerful tool in bacterial removal, however, the resilient nature of bacterial biofilms as well as the morphology and characteristics of dental RCs leads to a considerable amount of secondary infection.

Failure rates of root canal treatments can vary largely, depending on the method of assessment and the time period of observation. A ten-year study on the outcome of RC fillings in the General Dental Services in England revealed that only 74% of RCTs pass through ten

years without the need of a secondary treatment or extraction. As an example of the costs generated by this; in the year to March 2004 1,001,675 RC fillings at a cost of £50.5 million were placed in the General Dental Services (Lumley et al., 2008). A one year follow up study by Patel *et al.,* making use of cone beam computed tomography (CBCT) indicated similar success rates of 73.9 or 89.4% depending on criteria. The strict criterion (73.9%) refers to roots that show a complete lack of periapical radiolucency. The lose criterion (89.4%) refers to where the radiolucency has reduced in size (Patel et al., 2012). They were further able to demonstrate, in a cadaver study with histologic controls, that conventional periapical radiography may not always have sufficient sensitivity and specificity to achieve a correct diagnosis, as CBCT scans resulted in a significantly higher rate of detection (Kanagasingam et al., 2016). It is to be noted that CBCT is not currently recommended as a method for routine check-up by the European Society of Endodontics due to radiation exposure. However, it should be considered to gain additional information in complex or unusual treatments and is a valuable tool in research (Patel et al., 2014).

Fabricius *et al.* demonstrated in an animal study, that, where residual bacteria remained in the RC space following treatment, failure rates of the treatments were very high (79% based on both histology and radiographs, 67% based on radiographically absence of a lesion only) and were even more likely to fail in the presence of a mixed species bacterial culture (Fabricius et al., 2006). This has previously been shown by culturing bacteria sampled immediately pre-obturation. A study by Sjogren *et al.* shows a significantly lower success rate for teeth with positive bacterial sampling when compared to teeth with a lack of culturable bacteria (Sjögren et al., 1997).

Peters *et al*. demonstrated the effect of initial canal anatomy on the final outcome of RC shaping by superimposing an X-ray micro tomography (µCT) image of pre-shaped RC on the same RC post treatment (Figure 5). Especially wide canals showed areas unaffected by mechanical treatment. It has also been noted that, despite the use of flexible files, in curved canals there is an uneven distribution of force leading to uneven removal of the RC surface. Flexible files manufactured as straight instruments still exert forces towards being straight (Peters, 2004).

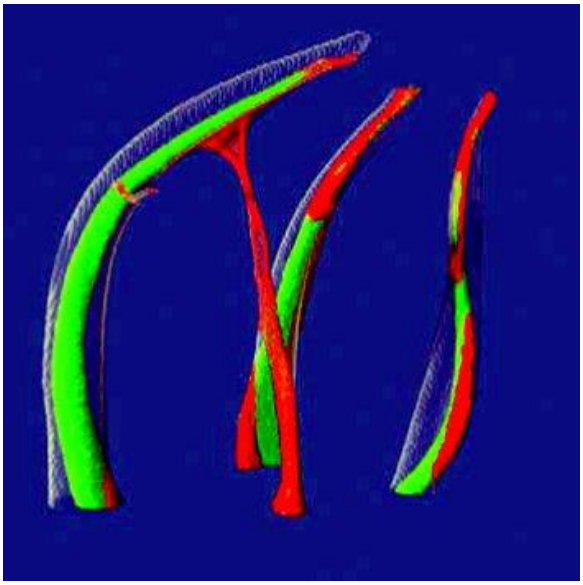

Figure 5**:** Superimposed µCT images of a RC pre- and post-treatment, showing treated areas in green and unaffected areas in red (Peters et al., 2003) Permission of use granted by John Wiley and Sons.

A successful RCT requires thorough removal/debridement of necrotic pulp tissue, organic material and most importantly bacteria from the canal before obturation.

1.2.2 Mechanisms of biofilm removal

A combination of both chemical and mechanical disinfection, as described above, gives the clinician the best chance of the successful reduction in bioburden within an infected RC. The following section gives an overview of the mechanisms by which the bacterial load is reduced during treatment.

Mechanical biofilm removal and disruption

The key factors of mechanical preparation are the removal of the infected pulp and dentine as well as the widening and shaping of the canal to allow for more effective irrigation and to facilitate obturation (Metzger et al., 2013). Biofilms adherent to the RC walls can be challenging to remove due to their relative resistance to antimicrobial agents: as shown in studies using *in-vitro* biofilm models with Staphylococcus aureus and Listeria monocytogenes, biofilms can survive treatment with NaOCl (Almatroudi et al., 2016; Norwood and Gilmour, 2000). Mechanical removal and disruption of biofilms and infected pulp and dentine is therefore a vital part of the successful RCT (Metzger et al., 2013). Siqueira et al. demonstrate this effect,

by showing significant decrease in vital bacteria following treatment even when using saline without any anti-microbial agents as rinsing solution (Siqueira et al., 2002).

Ideally this preparation of the root would result in debridement of each entire canal, centred around the original root structure. As shown in Figure 5 and outlined in the literature, in practice this is rarely the case (Peters et al., 2003; Hargreaves and Berman, 2015; Peters, 2004).

Chemical disinfection and irrigation of endodontic biofilms

Endodontic irrigation solutions are used in combination with the mechanical removal of bioburden from the RC space. The disruption and removal of parts of the biofilms and bacterial load is achieved through mechanical instrumentation; however, a study by Siqueira et all shows that the addition of irrigant solutions into the treatment leads to a significant reduction in residual bacteria following RCT (Siqueira et al., 2002). In addition to their antimicrobial effects, irrigant solutions aid the successful treatment by dissolving residual organic matter, lubrication of the root walls and the rinsing out of detached debris from the RC space (Giardino et al., 2007).

Sodium Hypochlorite (NaOCl)

NaOCl is a commonly used irrigant solution in endodontics where concentrations of use range between 1% and 5.25%, it is classified as a chlorine-releasing agent (CRA), meaning it has highly oxidising properties leading to severe impairment of protein activity, it has also been shown to degrade bacterial DNA (Young et al., 2007). Hypochlorous acid, which is produced when chlorine is dissolved in water can penetrate outer walls of bacteria, further, NaOCl has been shown to degrade bacterial nucleic acid (Donnell, 1999). In endodontics NaOCl is a very popular irrigant due to its potent bactericidal properties, as well having been shown to degrade endodontic biofilms. However, it has also been shown, both through *in-vitro* studies and case reports, to be toxic to the periapical tissues, especially when applied at high concentrations (Gernhardt et al., 2004; Önçağ et al., 2003). In modern dentistry, the use of NaOCl is often limited to 1% to minimise potential damage when reaching the periapical tissue. The bactericidal effects of 1% NaOCl have shown not to be significantly lower than concentrations as high as 5.25%, when using sufficient volumes (Siqueira et al., 2000). An animal study conducted on rats has further suggested that lower concentrations of NaOCl exposure are more

biocompatible, showing more acceptable levels of inflammatory response (Gomes-Filho et al., 2008).

Chlorhexidine

Chlorhexidine is an alternative popular irrigant solution in endodontic treatment, having the advantage of being more biocompatible than NaOCl whilst having shown some effectivity in biofilm removal and RC disinfection (Ercan et al., 2004). Chlorhexidine has hydrophobic and lipophilic properties and thus interacts with bacterial cell membranes, which can lead to alteration of the permeability of the bacterial cells as well as altering their osmotic equilibrium. These properties lead to chlorhexidine's antimicrobial effects at high enough concentrations (Mohammadi et al., 2014).

Studies regarding the superiority of either NaOCl or chlorohexidine as an irrigant solution for endodontic treatment are divided in their outcome, a recent systematic review of clinical trials concludes that the comparable evidence remains too scarce and suggests the needs for additional clinical trials on the matter (Önçağ et al., 2003; Gonçalves et al., 2016).

Calcium Hydroxide

Calcium hydroxide was originally described as a pulp-capping agent, but has since become more widespread in use. In RCT it is often used as a disinfecting dressing which remains in the RC space between visits. Calcium hydroxide has a very high pH (up to 12.5), the effect of providing such an alkaline environment has been shown to have bactericidal effects as well as preventing acidic dissolution of dentine (Carrotte, 2004). Due to the slow release of hydroxyl ions, the antibacterial effects of calcium hydroxide are long lasting and have been shown to further aid bacterial disinfection, following initial treatment (Sjögren et al., 1991).

1.2.3 Current methods for detection of residual microbes

Current clinical methods are highly subjective and include detection of clean dentine on the files, white dentine along visible portion of the RC or clear irrigant solution flushed from the

RC area. Additionally, smell or the lack of dry paper points taken from the canals may be regarded as indicators for residual bio burden.

Endodontic paper points or other means of bacterial sampling from the RC may be cultured to give evidence of remaining microorganisms, however, this is very time consuming (magnitude of weeks) and gives no information concerning the area of persistence. Unfortunately, bacterial infection may redevelop between the sampling and culture or molecular test result collection, for example, as a result of bacterial leakage of temporary restorations. In addition, certain bacterial species may be non-culturable or in non-culturable states, therefore there is a possibility for false negatives. Microbial sampling is of use in research but cannot be seen as a clinically relevant method (Sathorn et al., 2007).

Means to reliably quantify or detect bacteria are generally limited to research studies, including molecular biology methods such as polymerase chain reaction (PCR) (Anderson et al., 2012; Sathorn et al., 2007; Kato, a Yoshida, et al., 2007) which are not clinically feasible, due to being too time consuming and, in the case of PCR, do not give information on vitality. Other proposed methods using auto-fluorescent readings of the RC system, show the ability to differentiate between infected and sound dentine, however, due to the lack of viability staining there is no indication to the presence of vital bacteria. It is unclear whether the analysis of weak auto-fluorescent signals would be sufficient to detect small accumulations of bacteria (Sainsbury et al., 2009a; Ho et al., 2010; Giana et al., 2003). Sato *et al*. propose the application of a system using live/dead staining and a membrane filter for bacterial counting (Sato et al., 2012). Unfortunately the procedure, despite being comparatively rapid, takes 30 minutes and requires additional collection and preparation of dentine samples, making it unfeasible for routine use in a clinical setting. A recent concept that proposes the detection of vital bacteria by ATP activity has been suggested to be a rapid and sensitive method, which can be performed within 5 minutes. The sample collection and analysis for this approach, however, also requires additional steps of scraping the RC and vortexing the samples taken from the RC space before application the ATP assay and analysis in a luminometer (Tan et al., 2015).

1.3 Periodontitis/Implant dentistry

1.3.1 Dental implants

Placing dental implants has become a well-established procedure when dealing with tooth loss. First developed in 1965 by Brånemark, they are now placed for reasons ranging from trauma, to the impossibility of restoration due to severe caries and RC infection (Osman and Swain, 2015; Brånemark et al., 1977). The dental implant can be thought of as a replacement of the tooth root which screws into the jaw bone and is coupled to an artificial tooth crown (British Dental Health Foundation, n.d.). A dental implant consists of the implant screw, the abutment and a crown, as shown in Figure 6. The implant screw most often consists of a titanium alloy (Ti-6-Al-4V). It has higher strength than commercially pure titanium with similar corrosion resistance (Anusavice et al., 2013). A rough surface increases the osseointegration of the implant, surfaces will often be exposed to acid etching, particle blasting or other treatments to create a favourable surface topography (Malet, Mora, and Bouchard, 2011). The abutment, which extends from the implant screw through the gingiva to support the crown, is screwed to the titanium alloy implant, either internally or externally, allowing for load distribution and stability. The connection between these components can be cause for issues with implant placement by allowing for early microbial cell infiltration into the dental implant. Further, the loosening of this connection is one of the most common mechanical issues facing single tooth implants (Malet, Mora, and Bourard, 2011).

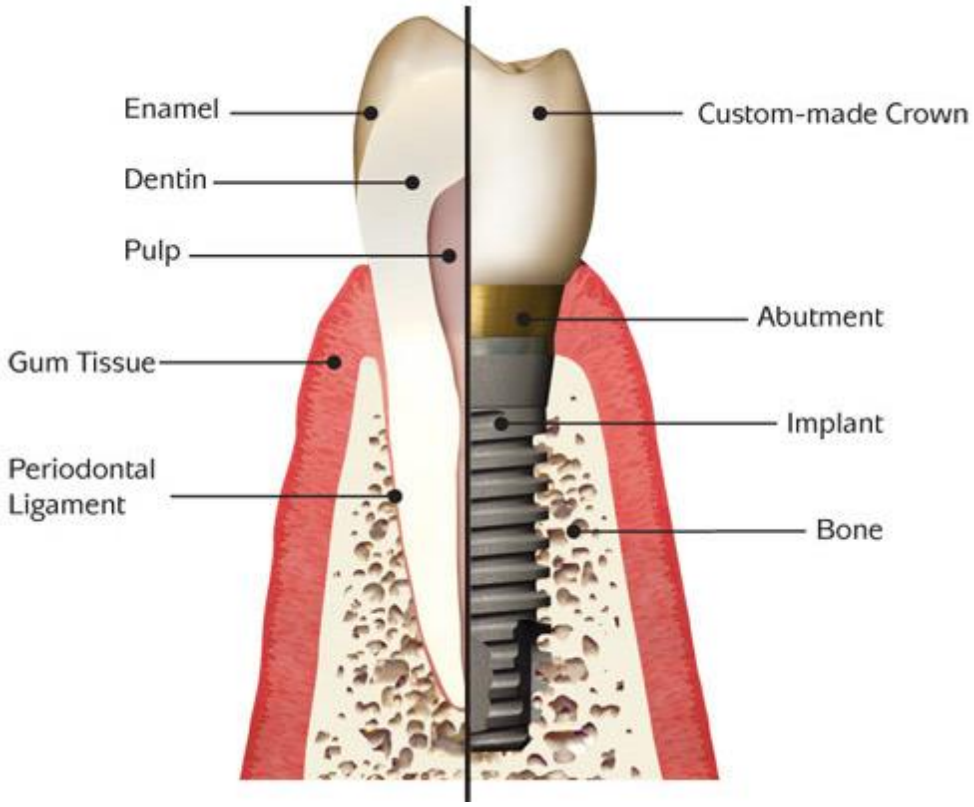

Figure 6**:** Image showing side-by-side comparison of a dental implant to a natural tooth (Zhang and Zheng, 2015). Permission of use granted by InTech (© 2015 Zhang D, Zheng L. Published in 'Emerging Trends in Oral Health Sciences and Dentistry' under CC BY 3.0 license. Available from: http://dx.doi.org/10.5772/59258).

Implant success

According to the American Academy of Implant Dentistry, 3 million people have implants, a number which is growing by 500,000 every year, with the US and European market expected to reach $4.2 billion by 2022 (Dentistry, n.d.). Reported success rates of placed dental implants vary, depending on the monitoring period and the used definition of success. Albrektsson et. al. provided an early set of criteria which are still commonly used (Albrektsson et al., 1986). However, self-defined criteria as well as criteria based on other studies are also applied: a review of various criteria used in implant dentistry by Papaspyridakos et. al. provides a summary of these (Papaspyridakos et al., 2012). Typically, the criteria will involve guidelines such as amount of bone loss after one year, probing depth into the soft tissue and patient satisfaction. In addition, there is often a distinction made between success and survival, where

survival is defined by the implant being present in the mouth and success refers to the absence of complications.

Failure of dental implants is often linked to lack of initial stability, trauma or infection and can be broadly categorised into being either of mechanical or biological nature (Norowski and Bumgardner, 2009; Sakka et al., 2012), in the latter instance, infection of the implant site may develop as peri-mucositis or peri-implantitis. Simionis et. al. investigated long-term survival and success of dental implants 10-16 years after placement. They found the success rate to be 82.94 %, however, they also reported a 48.03% complication rate (both biological and technical), meaning patients required additional treatment following the placement of the implant (Simonis et al., 2010). A more recent study evaluating patients 2 – 7 years after placement founds success rates between 90 and 97.95 %, indicating that complications can occur years after implant placement and long term success is not guaranteed (Bazrafshan and Darby, 2014).

1.3.2 Peri-implant pathology

Implant mucositis and peri-implantitis

Bacterial infection of dental implants can lead to an inflammatory host response and hinder osseointegration or even lead to loss of the bone tissue. Depending the on severity of the disease this can be broadly categorised into peri-implant mucositis or peri-implantitis (Norowski and Bumgardner, 2009). Peri-implant mucositis can be compared to gingivitis around teeth and often involves redness and swelling in the tissue surrounding an implant. Assessment involves checking for bleeding mucosa, following probing. Peri-implant mucositis is reversible and less serious than implantitis (Norowski and Bumgardner, 2009; Lang and Lindhe, 2015). Peri-implantitis involves lesions in the surrounding mucosal tissue and loss of osseointegration and surrounding bone. Here, assessment also requires probing as symptoms such as implant mobility may only occur in late stages of the disease. Upon probing the mucosa affected by peri-implantitis, puss is commonly exposed from the inflammatory lesions (Lang and Lindhe, 2015). Figure 7 depicts radiographic evidence of a case of peri-implantitis with associated pus formation and the establishment of a deep probing depth (Smeets et al., 2014).

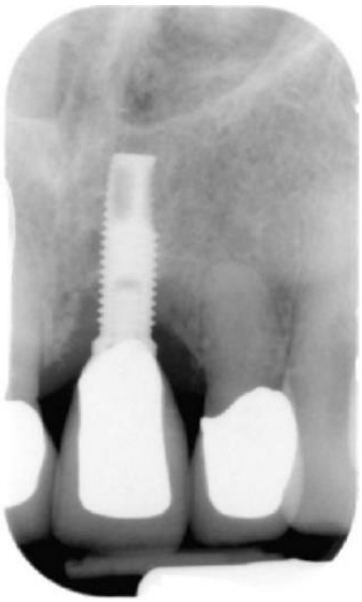

Figure 7**:** Photo of peri-implantitis case showing bone loss 8 years post implant placement (Byrne, 2014). Permission of use granted by John Wiley and Sons.

Biofilm infection

The microflora associated with implant disease, much like in periodontal disease is dominated by gram negative microbes, with infection resulting through opportunistic oral bacteria (Ata-Ali et al., 2011). As seen during the formation of plaque biofilms, the rapid establishment of a salivary pellicle on titanium surfaces provides receptors for early bacterial colonization. Papaioannou *et al*. demonstrated the presence of a pellicle on various surfaces to favour biofilm formation by *Porphyromonas gingivalis* (commonly associated with peri-implantitis) as well as an increase the number of vital cells present (Papaioannou et al., 2012). Fürst *et al*. show that immediate colonization of placed implants can occur, by taking sub-gingival samples immediately after suturing, such early colonisation may lead to development of biofilms and peri-implant disease at a later stage (Fürst *et al*. 2007). Formation of mature and treatment resistant biofilms submucossally show the same patterns of early colonisers and multispecies interactions as seen in other biofilm formations. In addition, compared to biofilms adhering to enamel surfaces, the submucosal environment lacks the effects of sheer forces (Busscher et al., 2010). Subgingival pockets have been shown to provide niches for microbial growth and offer protection as well as providing a hard, non-shedding surface (tooth or implant related) for bacterial attachment (Kuboniwa and Lamont, 2013)

The roughness of the surface of the infection site also plays a significant role in colonisation. Various studies have looked specifically into the matter of surface roughness indicating that increased roughness is favourable for bacterial growth and leads to greater biofilm growth and retention (Bürgers et al., 2010; Teughels et al., 2006). A study by Bollen *et al*. suggested that smoothening the roughness bellow a threshold of R_a = 0.2 µm had no further deterrent effect on microbial growth and termed this the 'threshold R_a' (Bollen et al., 1996). Many *in-vitro* studies use pooled, filter sterilised saliva in order to form a pellicle on the titanium discs as would occur in the oral cavity (Bürgers et al., 2010; Sánchez et al., 2014). Use of salivary pellicles is not universally agreed on, as the collected saliva from volunteers, even when it is not pooled, can vary in its protein and enzymatic composition. In order to remain as comparable and reproducible as possible not all *in-vitro* biofilm models rely on pellicle formation (Bürgers, Witecy, Hahnel, & Gosau, 2012).

P. gingivalis, as mentioned previously, is one of the species linked to peri-implant as well as periodontal disease and has been suggested to be the most representative strain involved in serious peri-implantitis (Persson and Renvert, 2014; Di Giulio et al., 2015). In addition, *P. gingivalis* is known to be present in common dental plaque as one of the late colonisers (Kolenbrander et al., 2006). *P. gingivalis* biofilms have therefore been used in multiple *in-vitro* studies relating to colonisation and removal in settings relating to peri-implantitis (Di Giulio et al., 2015; Park et al., 2014; Amoroso et al., 2006; Gosau et al., 2010)

1.3.3 Treatment

General Procedure

Thorough care and frequent monitoring of dental implants is of great importance in order to identify any occurring complications or disease at an early stage. The general aim when treating peri-implantitis is the removal or reduction of submucosal biofilms causing inflammation, as well as the creation of an immediate environment that is unfavourable for bacterial growth.

Generally, treatment can be divided into either surgical or non-surgical. With the treatment of early peri-implant mucositis being less intrusive than that of advanced peri-implantitis. Treatment in both cases involves mechanical removal of tartar (hardened plaque)

and bacterial biofilms/plaque. The hardened plaque is often scraped away with a curette or ultrasonic instruments.

In cases of non-surgical treatment, removal or tartar and plaque is often limited to the coronal area of the implant, above the mucosal margin. Scraping away below the mucosal margin, due to the threads and irregular shapes of implants, would result in a blind procedure, which could lead to a negative outcome. Hence, in cases of more advanced mucositis or even peri-implantitis, non-surgical treatment even in combination with antimicrobial agents is insufficient.

Surgical treatment involves gaining access to the infected surfaces of the implant. Once established that surgical treatment is necessary (based on bone loss and probing depth), access is normally achieved by raising a flap of the mucosal tissue. The exposed dental implant is then mechanically cleaned, in addition to applying antimicrobial agents to the implant and surrounding tissue. Where possible treatment could involve reconstruction of the surrounding bone tissue (Lang et al., 2015).

Disinfection methods

Treatment of implant infection relies on a thorough biofilm removal to avoid re-colonization and the subsequent need for further treatment. The mechanical surface debridement of an infected area forms the basis of the treatment. However, implant shape and surface roughness may not only provide a surface for biofilm attachment but hinder efficient mechanical debridement thereof, leading to the exploration of additional antimicrobial agents (Gosau et al., 2010). The following section discusses disinfection methods applied within the scope of this thesis.

1) Air abrasion

The use of air abrasion in the dental field dates back to 1945 (Black, 1945) when it was pioneered to supplement the available methods for caries removal. In essence, air abrasion involves high velocity firing of abrasive particles at a hard surface and has therefore been described as a pseudo mechanical minimally invasive cutting technique. The most common abrasives for cutting teeth is aluminium oxide. To avoid scattering of the abrasive powder systems may include a nozzle which guides water into a curtain surrounding the powder stream (Black, 1945; Banerjee and Watson, 2002). Using particles such as sodium bicarbonate

powders or glycine, air abrasion has shown suitability for the disinfection of dental implants without causing significant damage (Schwarz et al., 2009). *In-vitro* studies show strong promise for this method, however, there is a lack in clinical data to make conclusions on the long term suitability as well as the comparison to other new approaches for treatment (Froum et al., 2016). Alteration of the implant surface by the abrasive particles may have an effect on the treatment and future osseointegration and due to residual abrasive material from the treatment, it is suggested that the use of biocompatible materials may be beneficial (Tastepe et al., 2012)

2) Photo activated disinfection (PAD)

PAD, as the name suggests, makes use of photosensitising drugs, which are activated by light in the visible spectrum. Photosensitising drugs may be predominantly taken up by diseased tissue and bacterial cells (Mang, 2004). Initially developed for cancer therapy, due to the increase in bacterial antibiotic resistance, the antimicrobial potential of PAD has increased in importance (Yin and R. Hamblin, 2015). PAD requires the presence of oxygen, a photosensitising drug and activation light. Directing the activation light at cells which have accumulated a photosensitising drug will lead to rapid formation of reactive oxygen species (ROS), highly reactive molecules which bring about oxidation and cell death (Yin and R. Hamblin, 2015).

An *in-vitro* study by Eick *et al*. demonstrated the reduction of vital cells in both planktonic cells as well as on *P.gingivalis* and mixed species biofilms, they also stress the potential benefits of combining PAD with other peri-implantitis treatments (Eick et al., 2013). Reviews comparing peri-implantitis management recommend the use of PAD in treatment only in combination with other methods, due to being relatively new and lacking clinical outcome studies (Smeets et al., 2014).

3) Cold Plasma

Disinfection occurs predominantly through UV light and generation of reactive oxygen/nitrogen species, as well as electric fields. Plasma is defined as an ionized gas with overall neutral properties (Moisan et al., 2001). Cold plasma, also known as atmospheric plasma, is created through electric discharge at atmospheric pressure (Duan et al., 2007; Moisan et al., 2001). Disinfection of planktonic microbes is a well-established procedure, and the potential for biofilm removal has also been suggested (Joaquin et al., 2009; Rupf et al.,

2011). Joaquin *et al*. demonstrated a reduction in vital cells of an *in-vitro* biofilm model after exposure to cold plasma at different treatment times, and, using fluorescence imaging they also established that treated biofilm that lost the ability to form CFUs were not necessarily dead (Joaquin et al., 2009). Rupf *et al*. highlight the potential of cold plasma for removal of *in-situ* formed oral biofilms from rough titanium surfaces as are used in implant dentistry. Vitality and bacterial presence were confirmed using CFU, fluorescence microscopy and scanning electron microscopy and revealed a significant decrease in vital bacteria and biofilm following the plasma treatment. They further showed that the treatment had no effect on the titanium structure and that they were able to show increased removal success when the cold plasma was paired with intermittent rinsing. (Rupf et al., 2011).

With the emergence of hand piece cold plasma devices (Figure 8), cold plasma treatment provides a simple to use disinfection technique, which is assumed to be a safe to use method for both patients and practitioners, as the biocidal effects are only present where electrical discharge occurs, and end milliseconds after removal of the electric field (Moisan et al., 2001).

Figure 8: Dipiction of cold plasma handpiece (PZ2 cold plasma brush, Reylon Plasma , Germany) (GmbH, 2017)

1.4 Theory of fluorescence and imaging

1.4.1 Principle of fluorescence imaging and detection

Fluorescence is one of many interactions that can occur between electromagnetic radiation (light) and matter. Fluorescence is one of the two categories of luminescence, defined by the emission of light from any substance. The definition of fluorescence is dependent on the nature of the excited state of a molecule or fluorophore emitting light. When a light beam is directed at a molecule, given that the photons are of the right energy, a photon can get absorbed, transferring the molecule to an excited state. When absorption occurs, electrons move from their ground state (S0) to an excited state (S1). Electrons lose non-radiative vibrational energy, moving down through vibrational levels associated with the excited state, followed by de-excitation from S1 to S0 which is coupled with the release of a photon. Typically, the emitted photon will be of lower energy and thus higher wavelength, due to the lost vibrational energy. (Valeur and Berberan-Santos, 2013; Ball, 2006; Croneya et al., 2001; Lakowicz, 2006). Figure 9 depicts a form of a Jablonski diagram, illustrating such an electron excitation, followed by de-excitation coupled to a photon. The gap between the maximum absorption/excitation (Ex) and emission (Em) spectrum is known as the Stokes shift, as demonstrated in Figure 9a, with the Ex and EM spectra of calcein (Valeur and Berberan-Santos, 2013; Lakowicz, 2006). Absorption occurs in around 10^{-15} s and Internal conversion 10^{-12} or less. The de-excitation and photon emission, also known as fluorescence lifetime is around 10^{-8}. The time between the electron excitation and return to the ground state can be much slower for certain molecules (milliseconds to seconds), in such cases the phenomenon is termed phosphorescence (Lakowicz, 2006).

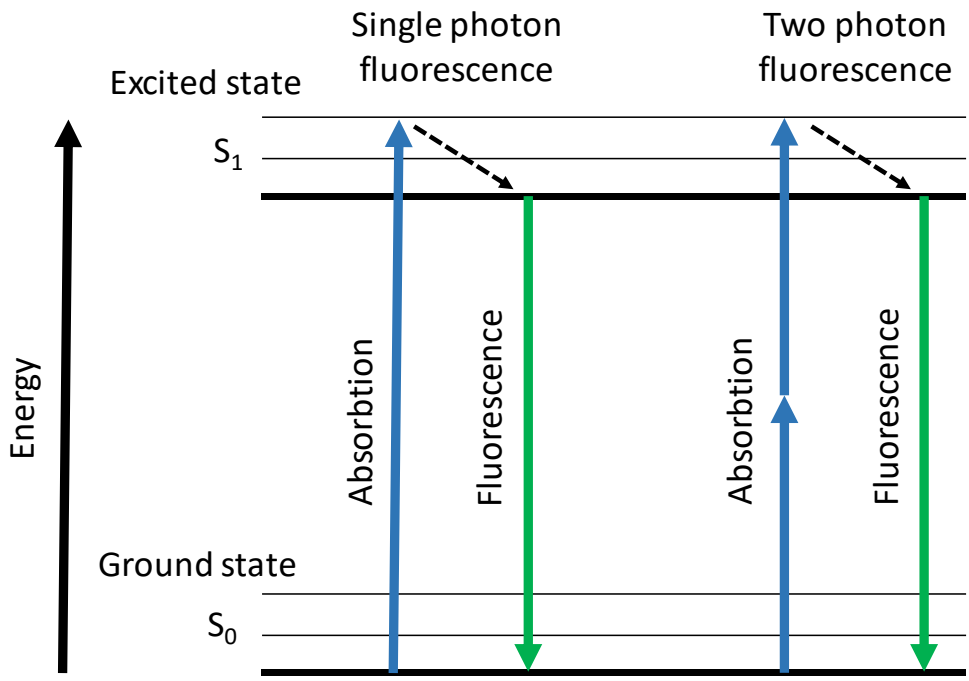

Figure 9: Jablonski diagram illustrating the principle of energy transfers in fluorescence, shown for both single and two-photon fluorescence.

The intrinsic autofluorescence (the natural fluorescence emitted from a substance when irradiated with light) of certain tissues may be strong enough for fluorescence measurements. Alternatively, as autofluorescence is typically weak in intensity, fluorophores (compounds with strong fluorescent properties) can be used to label desired biological structures. Both fluorescence spectroscopy and microscopy are commonly used methods in the biological and chemical sciences, and can be a powerful technique for biofilm detection (Bachmann, 2006; Takenaka et al., 2008; Wakamatsu et al., 2013; Moter and Göbel, 2000). In fluorescence microscopy, a fluorophore gets irradiated and excited at a wavelength of high absorption. To separate the excitation light from the longer wavelength emission light, a dichroic mirror is used alongside excitation and emission filters. Therefore, the excitation light gets discarded whilst only the emitted fluorescence is detected by the eye or other detection devices (Figure 10b), producing an image containing only the light within the bandwidth of the chosen emission filter. The methods of fluorescence microscopy used in this project utilise either wide-field, laser scanning or two-photon (2p) excitation as described in Table 2.

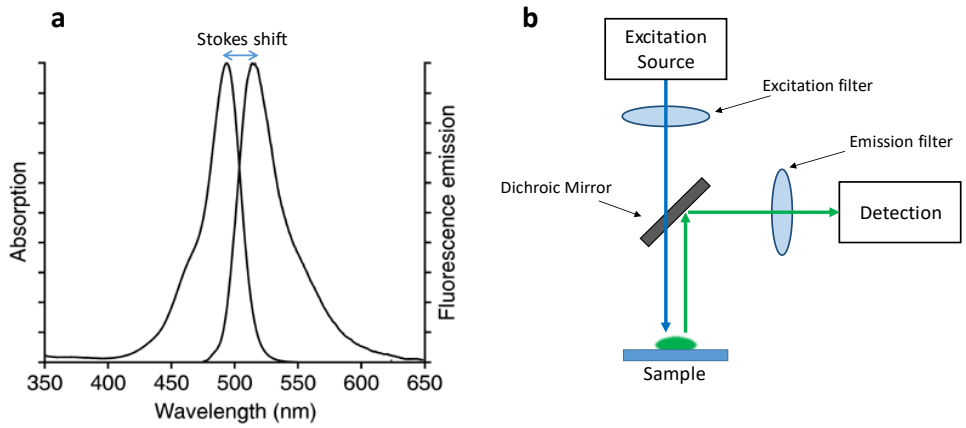

Figure 10: a) Diagram showing the Stokes shift between the maximum absorption and emission of calcein (Lifesciences, 2013). b) Example of a setup using filters and a dichroic mirror as used in fluorescence microscopy to separate and detect emitted light from the excitation light.

Table 2: Outline of types of fluorescence microscopy used in this project.

Fluorescence Microscopy	**Technology**	**Advantages/Disadvantages**	**Application to the project**
Wide-Field	Irradiation of entire sample, commonly with a xenon or mercury light source. Detection commonly by a CCD camera.	+Inexpensive, fast detection and imaging. -Interference by out of focus fluorescence.	Final device will utilise LED wide-field excitation.
Confocal	Scanning of sample by focused laser. Detection through adjustable pinhole by a photo multiplier tube or avalanche photodiode (Amos and White, 2003).	+ Pinhole discards out of focus fluorescence, improving 3D imaging. -Need for laser excitation and scanning with pinhole.	Evaluation of molecular dyes.
Two-Photon	Scanning of sample by pulsed laser beam of higher wavelength. Two photons must be absorbed in order to excite an electron. Detection through a photomultiplier tube (Zipfel et al., 2003).	+No Pinhole required as the rare event of two-photon absorption occurs only at focal plane. Photobleaching occurs only in focal plane. -Need for pulse laser excitation and scanning.	Proof of concept, allowing high resolution imaging under ideal conditions.

1.4.2 Fluorescence spectroscopy and spectral unmixing/curve fitting

Recording a fluorescent spectrum requires the use of a fluorescence spectrometer or spectrophotometer. The principle is the same for both fluorescence microscopy and spectroscopy, however, where fluorescence microscopy produces an image from the fluorescence emitted at a given wavelength range, fluorescence spectroscopy reveals the spectrum of the emitted light, normally presented on a wavelength (λ) scale, where the units of length are in nanometers [nm] (Lakowicz, 2006).

The fluorescence spectrometer is placed following the long pass filter as the detector, as demonstrated in Figure 10b. The fluorescent emission from a sample can be guided into the spectrometer through an optical fibre. Inside the spectrometer the light is collimated, dispersed and redirected into a linear image sensor which provides a spectral output, Figure 11 provides more details on components and functions of a fluorescence spectrometer. An example of the measured emission of the fluorophore calcein is shown in Figure 12.

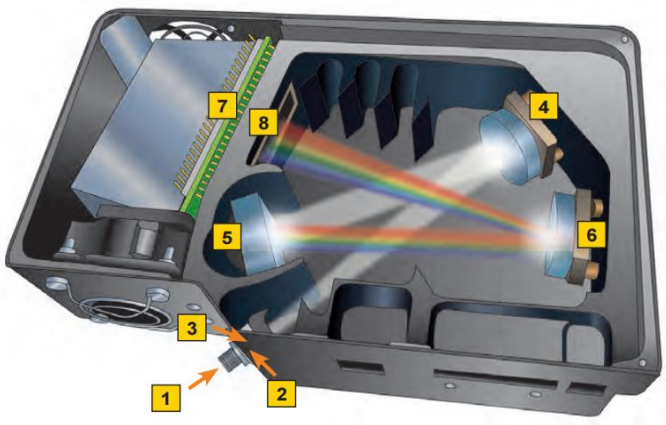

Figure 11: Diagram of fluorescence spectrometer (Ocean Optics, 2016). 1) SMA (Sub-miniature version A) connector for fibre cable attachment (entry point of fluorescence light).2) Entrance slit that acts as an aperture of the light from the fibre cable.3) In some cases, an additional optical filter is installed limiting the bandwidth of the entering light.4) Collimating mirror which redirects the collimated light to the grating mirror. 5) Grating mirror which disperses the light. The spectral range is a function of the groove density of the grating, the groove angle determines the most efficient region of the spectrum. 6) Focusing mirror for focusing of the spectra into the detector plane. 7) Detector FFT-CCD (Full frame transfer charge-coupled device) detector with high quantum efficiency designed for low-light-level detection. 8) Additional filter can be added to block second and third order light.

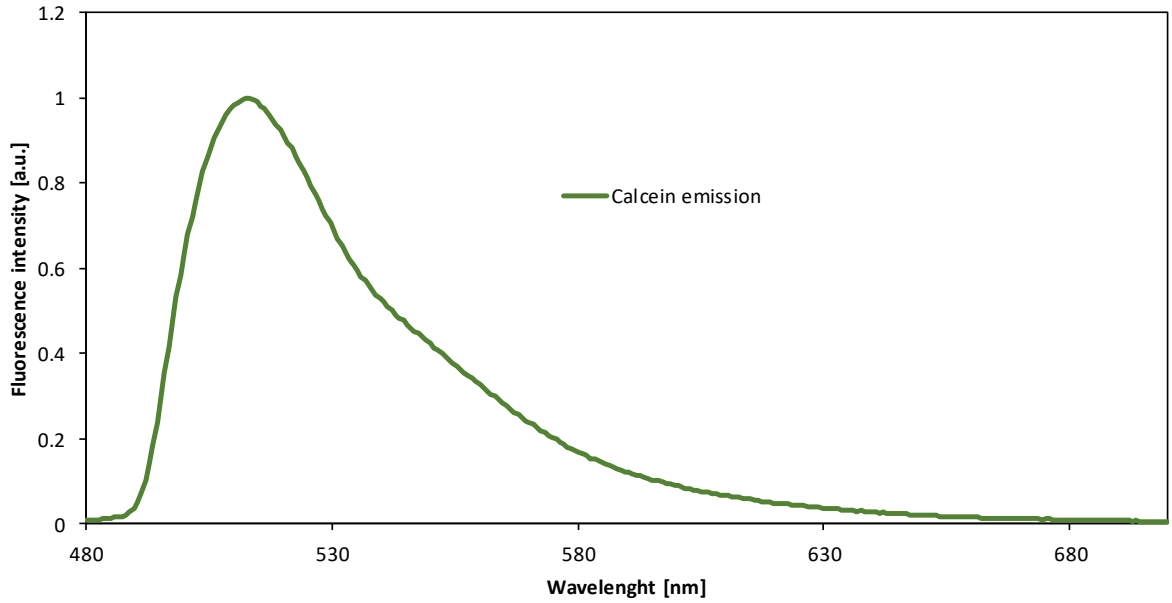

Figure 12 Emission spectra of calcein taken with an Ocean Optics QE65000 fluorescence spectrometer

The measured spectra recorded from fluorescent samples provide detailed information on the nature and intensity of the emission. However, overlapping of fluorescence spectra a is significant limitation for spectral microscopy and even spectroscopy. Ideally, fluorophores with sufficiently differentiated emission wavelengths are chosen to separate the individual fluorescent signals. Using separate filter cubes for each fluorophore, the excitation signals can be separated. The required fluorophores may not always be available with non-overlapping spectra, in addition, imaging conditions may result in overlapping autofluorescence. The same issues apply to fluorescence spectroscopy, especially when using multiple overlapping fluorophores. A solution to this issue is to apply spectral unmixing (Dickinson and Davidson, 2017).

Linear spectral unmixing determines the contribution of individual spectra to an experimental spectral recording. The spectra of the individual fluorophores or autofluorescent signals must be known before applying the spectral unmixing. These known spectra are often referred to as base or reference spectra (Garini et al., 2006). A general formula for the application of linear unmixing takes into account that the recorded spectrum ***S***, is composed of the proportion ***A*** of each base spectrum ***B*** as is shown in Equation 1. Usually, a least-square algorithm is applied, to minimise the error of the spectral unmixing. The base spectra are

normalised to their area so that only the differences in the spectral shape are tested (Garini et al., 2006).

$$S = \sum A_n \times B_n$$

Equation 1

As the name suggests, linear unmixing is reliant on the total recorded signal to be linear to the sum of the contributing of the fluorophores present (Dickinson and Davidson, 2017; Thaler and Vogel, 2006; Zimmermann, 2005). Figure 13 illustrates spectral unmixing of the recorded spectrum and shows the contribution of the base spectra with relative contributions of 2:1. This linear relationship can be affected by fluorescence quenching at high fluorophore concentrations or fluorescence saturation at high excitation power (Dickinson and Davidson, 2017).

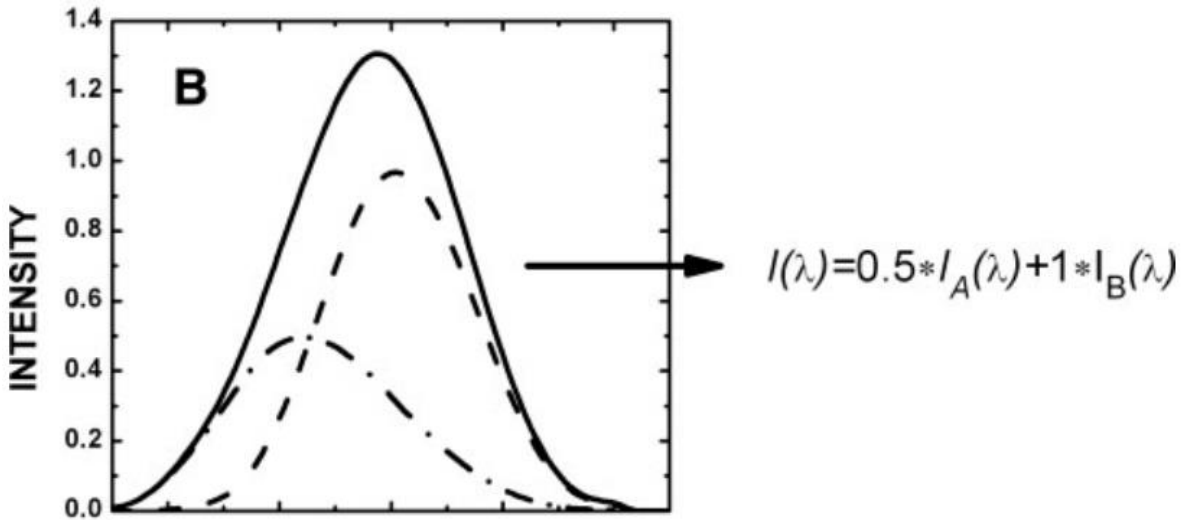

Figure 13: linear unmixing of recorded spectrum (solid line) with base spectra showed with dash and dash-dot lines . Permission of use granted by John Wiley and Sons.

Linear unmixing has been applied to fluorescence imaging to overcome the overlap of fluorescence emission when using multiple fluorophores (Thaler and Vogel, 2006; Lansford et al., 2001; Dickinson and Davidson, 2017; Zimmermann, 2005; Zimmermann et al., 2003). Lansford *et. al* used unmixing analysis with 2p microscopy to distinguish between green

fluorescent protein and fluorescein (Spectra and image shown in Figure 14) which have very strongly overlapping spectra. Further, they spectrally separated as many as four fluorophores despite substantial overlap (Lansford et al., 2001).

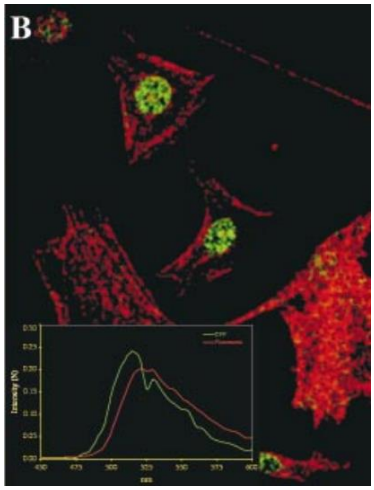

Figure 14: 2p image of cells with nuclear localised GFP (green) and actin bound fluorescein (red). The inset shows the strongly overlapping emission spectra for both fluorophores excited at 900 nm. Permission of use granted by SPIE Publications and Professor Rusty Lansford.

Since a broad fluorescence spectrum can be collected and separated into the contributing fluorophores by their individual spectra, spectral unmixing offers and increase in sensitivity (Kraus et al., 2007).

1.4.3 Fluorescent dyes

Fluorescent molecular dyes (also known as stains or probes) are fluorophores with high quantum yields. The fluorescence quantum yield is the efficiency of a fluorophore calculated by the number of photons emitted divided by the number of photons absorbed. Fluorophores can be used to stain and visualise cells or cellular components for fluorescence microscopy. The combination of various fluorescent molecular dyes provides a method of selective biofilm quantification and visualisation. In “live/dead staining”, the chosen dyes ordinarily make use of metabolic activity or compromised cell membranes, have a high affinity to cell structures such as nucleic acid and are able to contrast viable from dead cells (Tawakoli et al., 2012).

Fluorescent biofilm dyes can be broadly categorised into the following.

- Viability stains such as calcein AM or fluorescein diacetate, are permeable to cellular membranes and are able to diffuse into the cell where they are altered by endogenous enzymes producing the fluorescent form, which is retained by the cell. Lack of specific binding can lead to leaking of the dye after a given time.
- Nucleic acid stains such as Syto9, Hoechst and ethidium homodimer rely on membrane permeability or the lack thereof to contrast live from dead cells (Stewart and Franklin, 2008).
- The third type of stain applicable to biofilm visualisation is the EPS matrix stain. An example of this is Sypro Ruby which binds to positively charged amino acids in the EPS matrix (Frank and Patel, 2007).

Availability of a large number of dyes allows their selection for ideal characteristics and fluorescent properties with a suitable emission spectrum, which would be especially important when combining two or more stains. Tables 3-4 summarise and describe a selection of fluorescent stains with different staining mechanisms, chosen due to their potential for broad bacterial detection. It is to be noted, however, that the use of universal fluorescent stains is not necessarily limited to detection of bacterial cells, meaning the differentiation between different bacterial cell or even between bacterial and host cells may not be possible based on the fluorescence. Implications of this will be discussed in Chapter 5.

Table 3: Examples of fluorescent molecular dyes to be used in biofilm staining.

Type	Molecular Dye	Mechanism	Em/Ex maxima
Viability	Calcein AM	- Non-fluorescent hydrophobic molecule which is able to passively diffuse across cell membranes. - Once within a living cell the acetoxymethyl (AM) group gets cleaved by esterases revealing calcein. - Green fluorescent fluorescein derivative, owes fluorescence to a contained xanthene group. - Does not bind within the cell but is retained due to charge (once cleaved). - Its intrinsic non-fluorescent form coupled with good retention within the cell makes this a reliable viability stain.	495/515 nm
	Film Tracer Calcein red-orange	- Modified version of calcein AM, also contains an AM group which allows it to diffuse across membranes of viable cells. - Once cleaved inside the cell the charged compound is retained within the cytoplasm. - Unlike calcein AM this stain does not contain the xanthene compound but instead fluoresces in red due to a boron-dipyrromethene group. - Intrinsically fluorescent dye, thus washing procedures are of necessity.	576/590 nm
	Fluorescein diacetate (FDA)	- Non-fluorescent molecule, able to passively diffuse across cell membranes. - Conversion to fluorescein by intracellular hydrolysis. - Xanthene based dye. - Fluorescein can rapidly leak out of the cell.	494/521 nm
	Di-4-ANEPPDHQ	- Polarity/Potential sensitive fluorescent dye. - Fluorescence changes in response to electrical potential of the environment. - Fluorescence of ordered membrane (vital) shifted to the blue by 60 nm compared to disordered (non-vital)	488/560 & 620 nm

Table 4: Examples of fluorescent molecular dyes to be used in biofilm staining.

Type	Molecular Dye	Mechanism	Emission/Excitation maxima
Nucleic Acid	Syto9	- Cyanine based dye with affinity to nucleic acids. Exact binding mode unknown, correlations with both minor groove binders and intercalators. - Membrane permeable live cell dye (in combination with dead cell dye). - Increased quantum yield when bound to nucleic acid.	483/500 nm
	Propidium Iodide (PI)	- Phenanthridinium based dye, intercalation to DNA between bases with no specific base affinity at one molecule per 4-5 DNA base pairs. - Membrane Impermeable dead cell dye. - Increased quantum yield upon binding.	304/620 nm
	Ethidium homodimer	- Dye-containing two phenanthridinium rings, non-selective intercalation to 4 base pairs. - Membrane impermeable dead cell dye. - Increased quantum yield upon binding. - Narrower Stokes shift compared to PI.	528/617 nm
	Hoechst	- Minor groove binding dye with wide range of DNA affinities to A-T sequences. - Membrane permeable (Hoechst 3342 more so than Hoechst 33258) - Displaces certain intercalators.	350/460 nm
EPS Matrix	Sypro Ruby	- Intrinsically fluorescent ruthenium-based dye. - Binds non-covalently to positively charged amino acids and N-Terminal amines. - Commonly used as protein gel stain, stains proteins in EPS matrix - Requires thorough washing steps.	469/630 nm

1.4.4 Optical coherence tomography (OCT)

OCT was developed in 1991 by Huang *et al*. as a method for non-invasive cross-sectional imaging with micrometre resolution using near infrared light. Unlike fluorescence imaging, it doesn't rely on emitted light, but rather on reflected light and optical scattering, more specifically low-coherence interferometry (Huang et al., 1991; Bachmann, 2006). Figure 15a outlines the principle of OCT: Light (830 nm) emitted from a diode gets split, part to the sample and part to a reference mirror (known as the two interferometer arms). Comparison and simultaneous scanning of the reference mirror can, therefore, measure the delays from the tissue reflection. The resulting optical coherence tomography is a 2D image as shown in the retinal cross-section in Figure 15b.

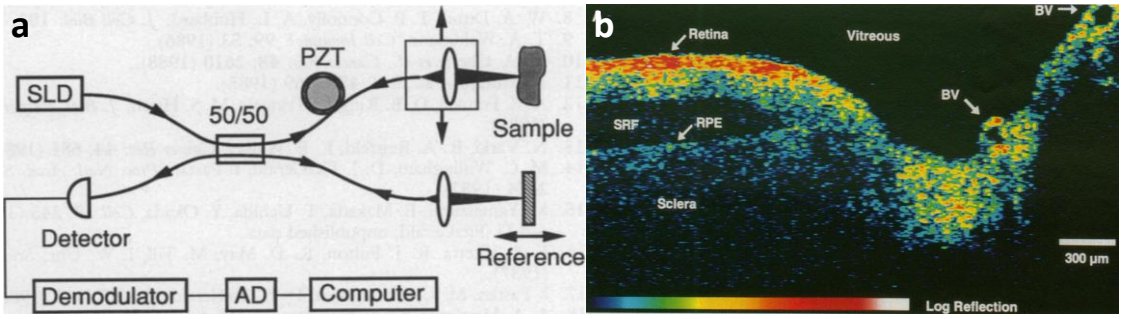

Figure 15: a) Diagram of the OCT scanner and b) an OCT cross section of a retina (Huang et al. 1991). Permission of use granted by The American Association for the Advancement of Science.

OCT has emerged as a suitable method for biofilm characterisation. Xi *et al*. make use of the non-invasive sectioning to monitor the 3D structure of a *P. aeruginosa* biofilm in real time. Penetration of the low coherence light allows monitoring the entire depth of the biofilms (Xi et al., 2006). In a more recent study determining the suitability of OCT for biofouling research, it was shown to have used in *in-situ* biofilm characterisation, enabling investigation of biofilm thickness, growth and structure over time (Dreszer et al., 2014). In a more clinical setting, OCT has been applied to create cross section images from the middle ear detected biofilm presence, directly linked to chronic otitis media (Nguyen et al., 2013).

Fluorescence imaging and OCT have a large range of applications in research. A number of fluorescence Imaging techniques have been developed, with various advantages and drawbacks, as described throughout this chapter. However, not all of these techniques are limited to just research and can therefore offer applications over a broader range, including the

use of fluorescence markers and analysis as diagnostic tools (Shah et al., 2015; Sato et al., 2012).The following chapters will examine the use of fluorescence analysis as a tool for detection of residual bacteria, with a focus on root canal treatment.

Chapter 2 *Proof of Concept Studies*

2.1 Introduction

Biofilm detection, especially in clinical situations, is very challenging. Due to the varied nature of biofilms dependent on species involved and the environment, finding general markers to determine biofilm presence remains an unresolved issue (Alavi et al., 2012). Culturing methods are still often seen as a gold standard and are frequently used for bacterial detection and assessment of disinfection in endodontic and clinical samples in general (Martinho *et al*. 2014; Huffaker *et al*. 2010; Marsh *et al*. 2014; Hassan *et al*. 2011). Molecular techniques such as PCR have been used to gain additional information on bacterial species involved in infections (Anderson et al., 2012; Bago et al., 2013; Blome et al., 2008). Both culture and molecular-based techniques are limited to research and have certain drawbacks. Culturing is very time-consuming and is limited to culturable bacteria. Molecular-based techniques such as PCR, despite being faster, still exceed clinically relevant time periods and mostly give little information on cell viability (Young et al., 2007).

Fluorescence as a method for clinical detection of RC infections has been investigated by relatively few studies. The DIAGNOdent device, currently in clinical use for caries detection was shown to differentiate between clean and infected dentine in the RC space. However, little indication of the sensitivity to small amounts of bacteria was shown, in addition, dentine autofluorescence does not give information on the presence of vital bacteria.

Using fast-acting vital cell stains on root canal pathogens, the limitations of these techniques could be overcome, enabling a clinically feasible bench side detection method. The aim of this chapter is to demonstrate the feasibility of utilising fluorescence detection of fluorophores in clinical settings: directly in the RC space (*in-situ)* and on a sampling substrate such as clinically used endodontic paper points (*ex-situ)*. Fluorescent beads were used as an experimental simulation for fluorescently stained bacteria: For the *ex-situ* approach, the fluorescent beads were sampled with endodontic paper points and a 2p microscope was used for detection. For the endoscopic *in-situ* detection of fluorescent particles directly within the RC space, RCs of extracted teeth were contaminated with fluorescent beads and scouted using a microendoscope. This allowed us to gain information on contamination pre and post a mock RCT. To highlight the need to induce fluorescence in vital cells, the autofluorescence inside a root was assessed during a RCT, using a clinically applicable device.

2.2 Materials and methods

The proof of concept studies described here involve the demonstration of how both the *ex-situ* as well as the *in-situ* approach are feasible under ideal conditions. Using fluorescent beads as a substitute for stained bacteria, the *ex-situ* approach was accomplished by visualising the fluorescent beads on an endodontic paper point, using 2p microscopy. The *in-situ* approach was demonstrated by using a prototype Storz microendoscope to detect fluorescent beads within the roots of extracted single-rooted teeth. Additionally, the need for induced fluorescence was demonstrated by the lack of detectable autofluorescence during a RCT.

2.2.1 Ex-Situ approach

For the *ex-situ* proof of concept, 2p microscopy was used to detect fluorescent beads on an endodontic paper point in order to establish the principle under ideal conditions. The fluorescent beads used were red and green 1µm carboxylate fluorospheres (FluoSpheres® Carboxylate-Modified Microspheres, Life Technologies, UK) with excitation and emission peaks of 580/605 nm and 505/515 nm. They were diluted in ethanol at a ratio of 20 µl fluorosphere solution to 1.4 ml of ethanol to be distributed over the endodontic paper points (ProTaper universal paper points F2, Dentsply, UK).

The laser used for the 2p excitation was a Chameleon Vision, widely tunable (680 - 1080 nm), single box precompensation, hands-free modelocked Ti:S pulse laser (Coherent, USA, California). The laser was used in combination with a fluorescence microscope (Eclipse Ti, Nikon, UK) and a photomultiplier tube (HPM-100-40, Becker & Hickl, Germany) for photon detection. All Images were taken with a 20x / 0.75 NA air immersion objective (CFI Plan Apo Lambda 20X, Nikon, Japan). Despite being shorter than expected, excitation wavelengths of 720 nm were found to be ideal for the excitation of the red beads and 920 nm for the green beads, with emission filters of 650/40 nm and 510/41 nm, respectively. The fibres of the paper points were visualised using second harmonic generation (SHG) at 940 nm with an emission filter of 470/10 nm (Figure 16).

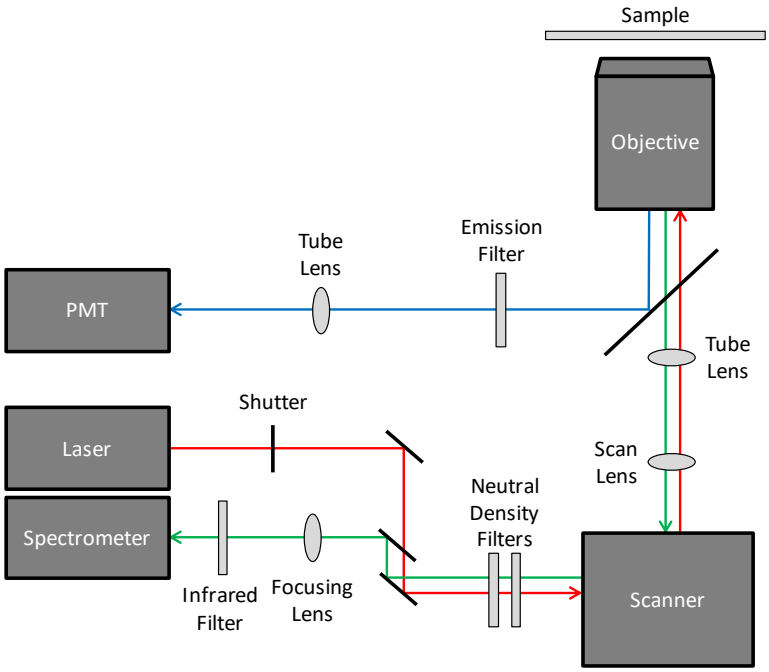

Figure 16: 2p setup for detection of fluorescent particles on an endodontic paper point.

2.2.2 In-situ approach

For the *in-situ* proof of concept, the presence of fluorescent beads in the RC spaces of extracted teeth was recorded using the Storz microendoscope of 0.5 mm diameter (Miniature Straight-forward Microendoscope (prototype), Storz, Germany) with a 3 CCD progressive scan RGB colour camera (AT-140 GE, 20.8fps, jAi, Japan) and blue light excitation (Cold Light Fountain Xenon source, Storz, Germany). The endoscope was inserted as far as possible into the RC space; recordings were then taken whilst removing the endoscope from the apex out towards the crown.

Eleven single single-rooted extracted human incisors, which had been obtained following signed informed consent (Research Ethics Committee Reference Number 10/H0804/056) were used for this study. Teeth were stored in an airtight container with de-ionised water, which was exchanged every 3 days. The canals were initially prepared by removing the pulp where necessary and using path finder files (K-File, KFS00625, Lexicon, UK). In addition, irrigation with 1%NaOCl was carried out before rinsing with sterile water. The fluorescent beads were then pipetted into the canal space for imaging (Corning™ Universal Fit Pipet Tips 200 µl, UK). 40 µl of 3 µm green fluorescent beads (Fluoresbrite® YG Carboxylate Microspheres 441/486 nm, 3 µm, Polysciences, Germany) diluted in 400 µl of ethanol were inserted into the RC space and distributed with a paper point (ProTaper universal paper points

F2, Dentsply, UK). After initial imaging, the RCT was carried out by a postgraduate endodontist using the ProTaper Universal method and the canals were re-imaged to detect remaining fluorescence using a green emission filter (500/70 nm).

Clinical detection of autofluorescence

In order to test if relevant autofluorescence could be detected *in-situ* during a RCT (approved by the Ethics Committee of the King's College London University (05/Q0705/051)) by a clinically applicable device during a RCT, a number of setups were tested with the Storz microendoscope. The RC was scouted, as previoiusly, with the Storz microendoscope post removal of the pulp, testing a number of different excitation and emission conditions.

Table 5: Setups used to test detection of autofluorescence in an in-situ RC treatment using the Storz micro endoscope.

Excitation	Expected Detection	Emission/Camera	Results/Comments
Cold Light Fountain Xenon source; white light (Storz, Germany)	-	No filters	Showing RC morphology after accessing canal
Cold Light Fountain Xenon source; blue light (Storz, Germany)	Bacteria – red channel Dentine – green channel	3 CCD RGB camera, red channel separated from blue excitation, no filters	No autofluorescence detection
Cold Light Fountain Xenon source; blue light	Dentine	3 CCD RGB camera, green emission filter (500/70 nm)	No autofluorescence detection
Xenon Nova; red light (650/75 nm) (Storz, Germany)	Bacteria	Monochrome camera, far/infrared emission filters (750/40 nm and 800/40 nm)	No autofluorescence detection
Xenon Nova; green light (550/100 nm) (Storz, Germany)	Bacteria	Monochrome camera, red/far-red emission filters (650/40nm and 700/40 nm)	No autofluorescence detection

Detection of individual beads

The sensitivity, in respect to the size of fluorescent particles detectable, of the Storz microendoscope device was determined by detecting single 6 µm and 3 µm fluorescent beads (Fluoresbrite® YG Carboxylate Microspheres 441/486 nm, Polysciences, Germany). Additionally, a ProFlex microprobe with a Cellvizio micro-endoscopy imaging system was used; the setups used are described in Table 6. Separation of single beads was achieved by diluting the initial bead mixture at a ratio of 1.25 µl to 1.5 ml of ethanol, the beads were then pipetted onto a glass coverslip and making use of wide-field fluorescence microscopy, single beads were picked up using a dental probe and then re-suspended on a dentine surface. For detection, the endoscopic probes were mounted on a translation stage over the beads.

Table 6: Setup for detection of single 3 µm and 6 µm beads.

Imaging Fibre	Excitation	Detection	Specs
ProFlex microprobe (ProFlex S300 1B, Mauna Kea Technologies, France)	Cellvizio GI Laser Scanning Unit (LSU) with 488 nm wavelength (Mauna Kea Technologies, France)	Cellvizio GI Laser Scanning Unit (Mauna Kea Technologies, France)	Lateral resolution: 5 µm. Axial resolution: 15 µm. Field of view: 300 x 300 µm. Working distance: 0 µm.
Storz microendoscope (Storz, Germany)	Cold Light Fountain Xenon source; blue light (Storz, Germany)	ORCA-03G Digital CCD camera (Hamamatsu, Japan)	Endoscope resolution specs unknown (prototype). Camera pixels: 1344 x 1024.

2.3 Results and discussion

2.3.1 Ex-situ approach

Using suitable excitation wavelengths and emission filters, we were able to distinguish red and green fluorescent beads from each other and show the structure of the paper point fibres using second harmonic generation (SHG) (Figure 17). Optical sectioning of the paper point was achievable to a depth of about 40 µm, this was most likely limited by light scattering caused by the paper point fibres. Analysis of the image stack was carried out by thresholding and using the ImageJ plugin '3D object counter'. The number of green and red beads corresponded largely to manual counting as shown in Table 7. As a measure to increase the speed and be more adapted to biofilm detection, final detection of biofilms attached to paper points could be carried out using fluorescence spectroscopy rather than the counting of fluorescent particles. However, as a proof of concept, this example shows that it is possible to detect different fluorescent beads on a paper point substrate to a high sensitivity.

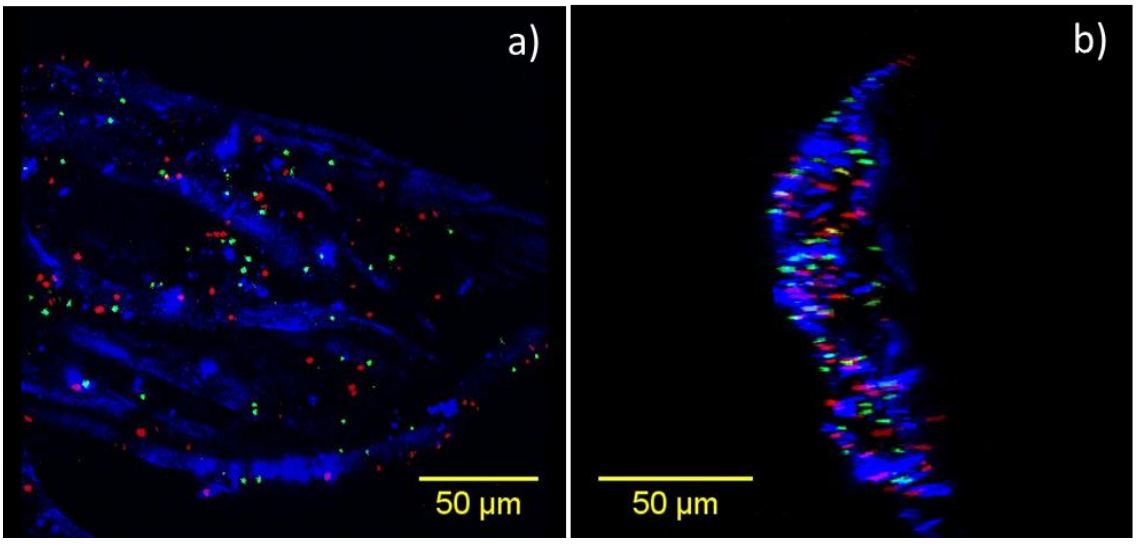

Figure 17: 2p microscopy images of an endodontic paper point tip immersed in green and red fluorescent 1 µm beads. Paper point fibres were visualised using SHG (blue). a) Front view and b) side view of a rendered 3D stack with images taken at 2 µm intervals.

Table 7: Red and green 1 µm bead numbers and ratios as determined by ImageJ and manual counting.

Beads	Automated Analysis	Manual Count
Red	55	57
Green	42	45
Ratio Red/Green	1.31	1.26

The positive result of this initial fluorescent bead simulation validates the basic analytical principles of the *ex-situ* approach; the detection of fluorophores on and within the outer layers of the paper point can be seen as a simulation of live/dead stained bacteria. By validating this principle, further steps can be taken in the direction of visualising live bacteria on paper points.

There is currently no application for optically quantifying or detecting bacteria sampled in use in an endodontic clinical setting. Means to achieve this are mostly limited to research. Predominantly, these include techniques such as cell culturing and polymerase chain reaction (PCR) (Sathorn et al., 2007; Anderson et al., 2012; Giana et al., 2003). For a method to be clinically feasible in determining an end point to the RC debridement previous to obturation, reliable detection must be produced in an order of minutes. In addition, due to the variety of possible root canal pathogens, it must allow for broad bacterial detection. These criteria eliminate a number of methods: cell culturing, for example, is unfeasible due to its time consuming off-site procedure and inability to grow viable-but-non-culturable biofilms (Sathorn et al., 2007; Shen et al., 2010). PCR and related DNA detection methods such as loop-mediated isothermal amplification methods can be a powerful tool in detection of bacterial species; they improve the speed of detection and can have high sensitivity. However, PCR has shown to fail to produce detection of species cultured from the same endodontic lesions and can falsify results by amplifying DNA of dead bacteria (Anderson et al., 2012). Loop-mediated isothermal amplification has been suggested as a method of rapidly detecting *E. faecalis* with high sensitivity after sampling the RC with a paper point. This method further improves detection speed. However, the time frame remains in the magnitude of an hour and is specific only to bacterial DNA of a species determined by primers used, which is unfavourable in detecting highly versatile RC pathogens (Kato, A. Yoshida, et al., 2007). A recent approach by Tan *et al*. utilises the detection of vital bacteria by ATP activity. Although the ATP assay is rapid (~5 min) and sensitive, the technique described requires numerous sampling steps and RC preparation before application of the ATP assay, increasing the overall time for treatment.

Optical analysis of fluorescently stained bacteria adherent to a paper point may offer the required characteristics for fast, broad detection of residual bacteria in the RC space in a manner that could be implemented in a clinical setting.

2.3.2 *In-situ* approach

For the *in-situ* detection of fluorescent beads with the Storz microendoscope, blue excitation allowed differentiation of the bead fluorescence from reflected blue light. This method proved to be applicable to RCs of extracted teeth; blue excitation allowed to detect and differentiate the fluorescent beads from the dentine background (Figure 18a, b). Additional use of green emission filters allowed visualising only the fluorescent beads (Figure 18c). The yellow arrows indicate the areas of detected bead fluorescence with the red arrows indicating areas without beads. Viewing only the green channel for Figure 18b) and measuring the intensity for the indicated areas showed a 1.82-fold increase in mean intensity for the fluorescent beads. Measuring the areas indicated in Figure 18c) produced a 1.45-fold increase, suggesting the need for more specific emission filters. By contrast Figure 18d) shows white light excitation of the contaminated RC where the detection of beads is not possible.

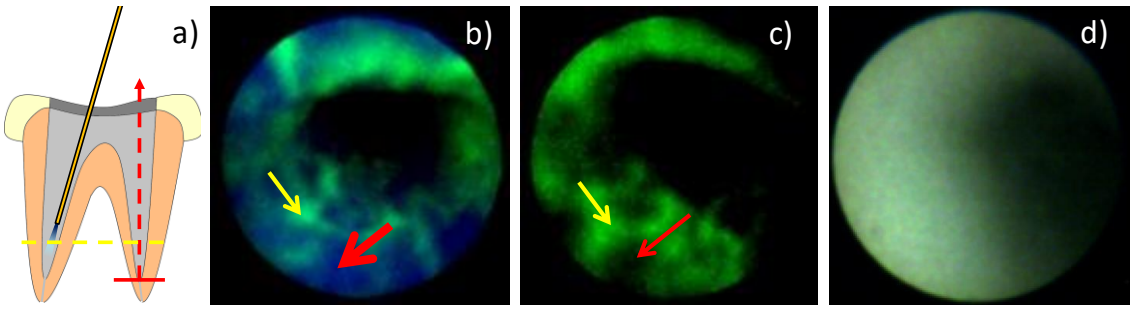

Figure 18: Representative images of the scouting of a RC containing fluorescent beads. a) Diagram illustrating how images were recorded, by inserting the Storz endoscope down to the apex and capturing images whilst retracting (red). Example images were taken from the apical third of he tooth (indicated in yellow). b) Using blue excitation light without filters, green fluorescent beads (yellow arrow) are visible on reflected blue background (red arrow). c) Blue excitation of the root canal with green emission filter showing only the fluorescence of the beads (yellow arrow) with absence of reflection (red arrow) and d) white light illumination of a RC without filters.

With regards to applying this simulation of induced fluorescence to a clinical situation, eleven single rooted teeth were prepared and imaged as above, using green emission filters. Following this, a RCT was performed on each tooth after which the teeth were re-imaged. Figure 19 illustrates a comparison of the mean fluorescence emission at 500/70 nm for every frame acquired whilst recording the microendoscope scouting the length of the canal (Figure 19a). The initial teeth contaminated with the beads are shown in green, the remaining fluorescence post treatment in red and the negative control, lacking beads, in black. Figure 19b-c) show a thorough removal of the beads and thus low fluorescence emission. This was the

case for the majority of the treated teeth. However, in Figure 19d-e), as indicated by the arrows, fluorescence was detected post treatment, indicating that the beads had not been thoroughly removed and the debridement of the canal was insufficient to remove the beads.

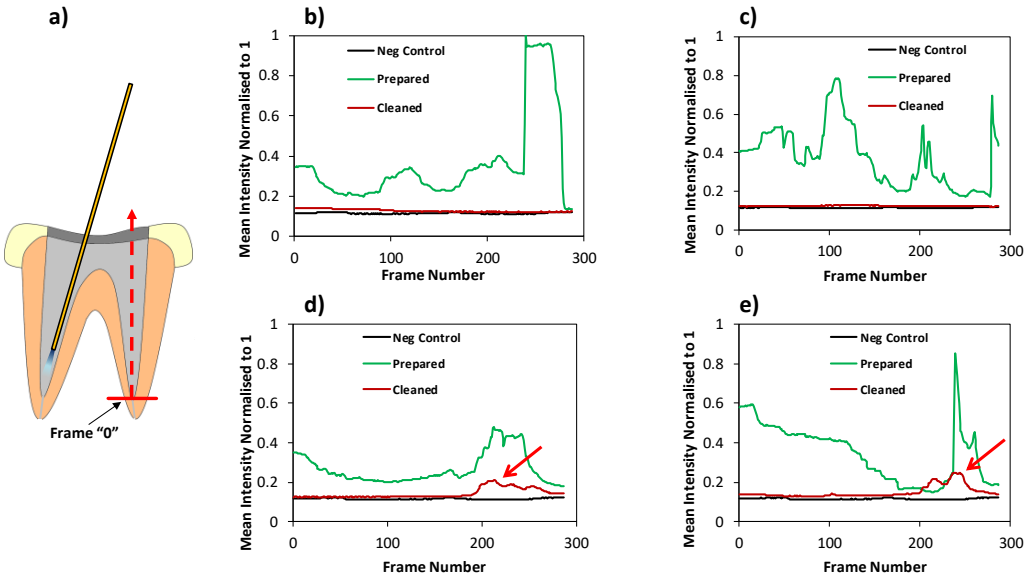

Figure 19: Representative diagrams showing mean fluorescence intensity at 500 ± 35nm for prepared (green) and cleaned (red) root canals with the negative control lacking beads (black). a) Images were aquired starting from the root apex, moving towards the crown of the tooth. Diagrams b) and c) indicate complete removal of the debris, whereas the fluorescent peaks indicated by the arrows in d) and e) suggest incomplete removal of the beads.

These results imply the practical applications for the RC endoscope to detect the presence of fluorescent particles and evaluate the quality of disinfection, in order to determine when a thorough removal of the fluorescent particles and subsequent endpoint to a root treatment has been achieved. Application of such a system could also have an application in endodontic training.

Clinical detection of autofluorescence

Investigation of autofluorescence using a clinical setup *in-situ* during a RCT did not allow for detection of any dentine or biofilm autofluorescence. As outlined in Table 5, none of the used excitation or emission combinations led to the detection of any discernible autofluorescence. Figure 20 shows an example of the lack of autofluorescence in the separated red green blue (RGB) channels, when using blue excitation light without any emission filters. The comparison to Figure 18 b, where fluorescent beads are detected using the same setup, highlights the need for induced fluorescence.

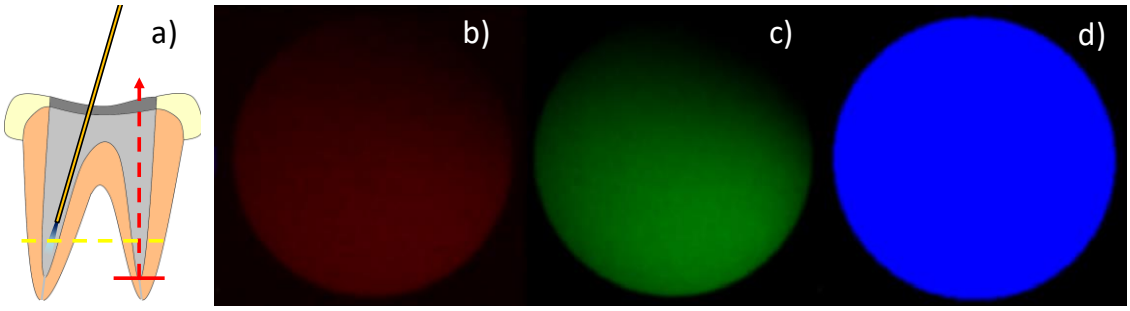

Figure 20: Representative images of the scouting of the RC space for autofluorescence: a) as in Figure 17, Storz endoscope was inserted down to the apex followed by capturing images whilst retracting (red). Example images were taken from the apical third of he tooth (indicated in yellow). b-d) Using blue excitation without filters in-situ scouting of a RC showed a lack of a distinguishable autofluorescent signal in each of the seperated RGB channel (images enhanced to show lack of visible structures).

Detection of individual beads

The limitations of the Storz microendoscope in regards to the smallest detectable particles were determined by resolving single fluorescent beads of 6 µm and 3 µm diameter. Figure 21 shows the successful detection of both 3 µm and 6 µm beads; interference by background fluorescence, especially in Figure 21a may be improved by narrower emission filters. Figure 22 shows the detection of the same beads using a Cellvizio endomicroscopy imaging system with a ProFlex microprobe, both beads are distinguishable from the background. The beads are not to scale as the ProFlex microprobe has a working distance of 0 and direct contact with the beads was avoided. Detecting fluorescent particles of 3 µm should be efficient in detecting remnant biofilms. Single cells of typical RC colonisers such as *E. faecalis* are only of about 1.4 µm in diameter (Signoretto et al., 2000). However, planktonic cells are susceptible to antimicrobial agents: the resistance to treatment stems from biofilm formation (Distel et al., 2002). The shown limitations should allow for the detection of small accumulations of bacteria. The quantum yield of the fluorescent beads is high, resulting in the intensity of the fluorescence measured likely being close to tenfold of the intensity produced by fluorescently stained biofilms, as will be discussed in section 3.3.1. The research carried out here is, therefore, to be seen as an indication of the limitation of the detection method in regards to the detection systems. For the Storz microendoscope (Figure 21) the bead size is likely below the resolution limit and detection will therefore depend on number of fluorophores per pixel. Ideal excitation wavelengths and emission filters and sensitive detectors may improve the detection of fluorescent particles with lower quantum yields.

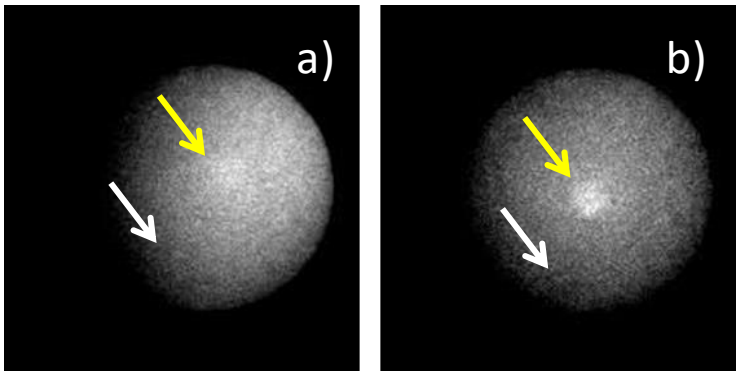

Figure 21: Using the Storz microendoscope coupled to a monochrome CCD camera, single fluorescent beads were detected on a dentine background: a) 3 µm beads, b) 6 µm beads. Yellow arrows show where the higher intensity indicates the presence of a fluorescent bead, white arrows indicate areas where beads are absent.

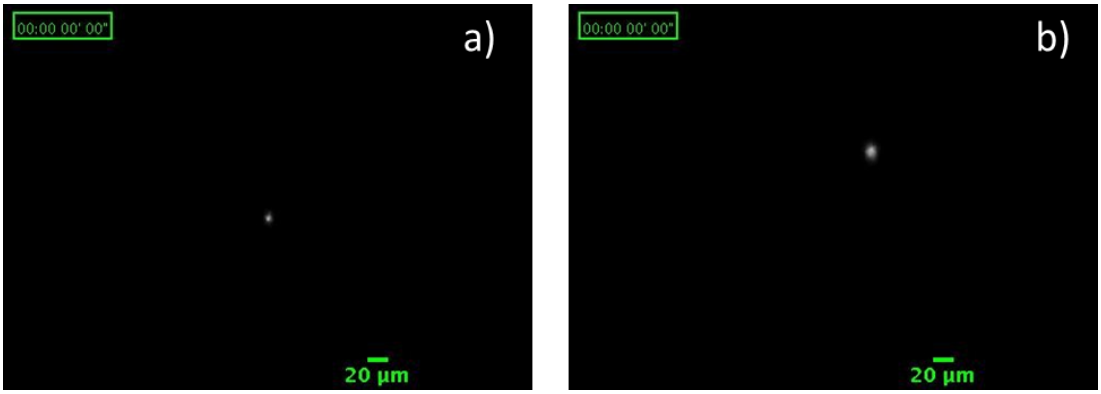

Figure 22: Detection of single fluorescent beads using a ProFlex microprobe and Cellvizio endomicroscopy imaging system on dentine background: a) 3 µm beads, b) 6 µm beads.

The use of fluorescence microendoscopy for the detection of bacterial residues in RCs is currently limited to research. A study exploring the suitability for the DIAGNOdent Classic which is currently in clinical use found positive results in detecting bacteria in the coronal third of the RC. The DIAGNOdent method uses red light laser excitation at 655 nm and measures near-infrared fluorescence from bacterial fluorophores. Using a thin sapphire probe designed for detecting subgingival calculus, both *in-vitro* grown monocultures and extracted infected teeth were analysed and high specificity was reported. However, due to size limitations, only the coronal part of the canal was investigated with little reference to sensitivity in the case of small localised remnants within the canal. For this method to be applicable, it would need assessment in the apical areas of the RC which would prove to be more challenging for bacterial removal and detection (Sainsbury et al., 2009b). The study was followed up by combining 300 - 400 µm diameter germanium-doped silica fibres with the 655 nm laser system. Differentiation between clean and infected dentine was shown, achieved by purposefully leaving the apical area

untreated. However, this study does not demonstrate sensitivity to small amounts of bacteria (Ho et al., 2010). Using laser-induced red excitation in the detection of infected dentine suggests that this may be a fast method for the detection of general infection. However, the limitations of this approach are yet to be described and the detection of bacteria related autofluorescence is not an indication of vital bacteria.

Other than the detection, the diameter and flexibility of the probe must be taken into consideration. Figure 23 shows a scale comparison of the RC space after initial shaping (Ruddle, 2005) (red) to various probes: a) a single core fibre (diameter 105 µm) (M15L01, Thorlabs, USA, New Jersey) b) the ProFlex fibre (diameter 300 µm) and c) the microendoscope (diameter 500 µm). The diameter of the single core fibre is small enough to reach the apex, whereas the ProFlex microprobe and microendoscope have diameters which do not allow access to the lower apex. The microendoscope could overcome this by having a long optical working distance, however, curvatures in the apex would block detection. A study comparing curvatures of maxillary molars found the greatest curvatures to be in the apical third of the roots with a mean radius of 4.5 ± 2.5 mm and a maximum of 1.7 ± 0.8 mm (Lee et al., 2006). It must be taken into consideration, that these root curvatures were established by µCT on unshaped roots. Initial shaping by rotatory instruments and files enlarges the cavity and will reduce these high curvatures. Despite a treatment-induced reduction in curvature, a high flexibility in the chosen probes is necessary, the low curvature of single core fibre and ProFlex microprobe (curvature radius of 10-15 mm) and the large diameter of the microendoscope restrict such probes to moderately curved canals. Further attention must be paid to fibre probes with narrower curvatures such as plastic optical fibres or graded index fibres.

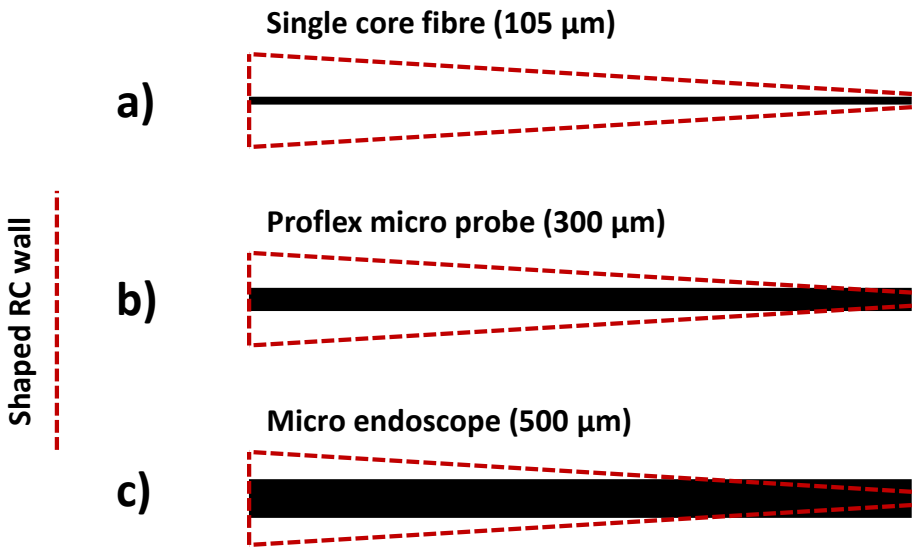

Figure 23: Scale comparison of probes to a shaped root canal (red): a) single core fibre as could be used for spectroscopy b) ProFlex micro probe, as used by the Cellvizio imaging system and c) the Storz micro endoscope (Prototype for RC imaging)

Making use of induced fluorescence provides the possibility of using clinically available wide-field excitation rather than being dependent on a laser. Endoscopic detection of stained bacteria may allow for a more sensitive technique and more importantly, allow for detection of vital bacteria only.

Residual vital bacteria in the RC space can lead to persistent or reoccurring infections, resulting in the need for complicated re-treatments. The current methods used to clinically assess the cleanliness of RCs are imprecise, subjective and rely largely on factors such as clear irrigant solution from the RC space, or clean and odourless dentine on the rotary instruments. Current means for bacterial detection are limited to laboratory research and are predominantly techniques based on culturing or PCR (Anderson et al., 2012; Sathorn et al., 2007; Kato, a Yoshida, et al., 2007). Both of which are valuable for research purposes but have limitations when applied clinically.

In order to be clinically applicable and relevant, detection must be achieved within minutes. The solution to this could be applying fast-acting fluorescent stains, either directly to the RC space or to bacterial samples taken from the RC space before the completion of the treatment.

2.4 Conclusion

This chapter has highlighted the potential to detect small fluorophores under ideal conditions. Fluorescent beads sampled with an endodontic paper point and analysed with a 2p fluorescence microscope, demonstrated that the fluorescent particles could easily be seen and differentiated from each other as well as from the paper point. *In-situ* experiments with RCs of extracted teeth directly contaminated with fluorophores and analysed using endoscopic techniques established the *in-situ* method to be suitable for detection of fluorescent material in a RC space. Further, using mock RCTs showed how the detection of residual fluorescence within the RC could potentially be used following treatment.

Autofluorescence measurements taken throughout a RCT demonstrated the benefits of using fluorescent markers to highlight residual vital bacteria: The autofluorescence recorded during the treatment did not result in any recognisable signals, whereas the small fluorescent beads were easily detected, indicating that autofluorescence measurements would require far more sensitive instruments and/or integration times.

Following the proof of concept for detecting fluorescent particles for both the *in-situ* and *ex-situ* approach, the next step requires characterisation of appropriate fluorescent stains to rapidly detect vital bacteria in mature endodontic biofilms.

Chapter 3 *In-vitro Studies*

3.1 Introduction

Fluorescent staining has become a popular method for visualisation of cells and cellular structures. A large variety of fluorescent dyes exist with differing excitation and emission spectra, they also vary in staining mechanisms and can differentiate live from dead cells and have an affinity to cell components such as DNA or amino acids.

Fluorescent dyes have been applied to oral biofilm research in a wide range of studies, in order to:

- Highlight the link between the EPS structures and biofilm virulence (Xiao et al., 2012).
- Detect individual species using fluorescence *in-situ* hybridisation (FISH) (Chávez de Paz, 2012; Shah et al., 2015).
- Assess early oral biofilm adherence (Tawakoli et al., 2012).
- Determine penetration of antiseptic mouth rinses into biofilms (Wakamatsu et al., 2014).
- Evaluate antimicrobial agents in peri-implantitis (Gosau et al., 2010).

Model biofilms, which attempt to mimic specific environments for biofilm maturation, can be used to study biofilm characteristics *in-vitro* and are often applied to assess antimicrobial agents (Takenaka et al., 2008; Guggenheim et al., 2001). The biofilm model chosen for the studies in this chapter is a mature, nutritionally starved, multispecies biofilm, which simulates the environment expected within the RC space, as described by Niazi *et al* (Niazi et al., 2014).

Analysis of the stained biofilms is typically carried out by fluorescence microscopy, with confocal microscopy being a very popular method, due to the rejection of out of focus fluorescence and the ability to create z-stacks (optical sectioning). However, with the goal of detecting fluorescence from vital cells (high-resolution images not being necessary), wide-field fluorescence microscopy may allow for a cheaper and more appropriate method. Furthermore, instead of using filter cubes with emission filter bandpasses at predetermined wavelengths, fluorescence spectroscopy can provide a rapid method to evaluate the presence and intensity of specific fluorescence spectra (Zimmermann et al., 2003).

The *in-vitro* studies outlined in this chapter include the characterisation of fluorescent stains for staining a mature endodontic biofilm within a fixed time-frame, as well as rapid

fluorescence spectroscopic detection of vital cells in endodontic biofilms: Following the establishment of a suitable fluorescent dye, simultaneous image localisation and spectroscopic detection were carried out on nutritionally stressed biofilms sampled using an endodontic paper point, applying spectral unmixing for rapid analysis. In addition, optical glass fibre cables were applied to record spectra and demonstrate the possibility of remote, *in-situ* detection.

3.2 Materials and methods

The *in-vitro* studies described here involve the characterisation of fluorescent dyes on a nutritionally starved endodontic biofilm model, using conventional confocal microscopy. Following establishment of a suitable fluorescence dye (calcein AM), the use of a rapid detection method, which combines wide-field fluorescence microscopy with spectral analysis was demonstrated. The detection method was then applied to detect residual vital cells in toxicity stressed biofilms.

3.2.1 Establishment and confirmation of an endodontic *in-vitro* biofilm

Replication of a multispecies biofilm typically found in the RC required *in-vitro* culturing of a model biofilm system as described by Niazi *et al* (Niazi et al., 2014, 2015). The strains used for the formation of the biofilm were *Propionibacterium acnes, Staphylococcus epidermidis, Actinomyces radicidentis* and *Streptococcus mitis,* which have been shown to be the predominant taxa from refractory endodontic lesions and were cultivated in-house (Niazi et al., 2010). In addition, *Enterococcus faecalis* OMGS 3202, known to be involved in RCT failures, was added to the biofilm (Dahlen et al., 2000). The bacterial isolates were revived from storage at - 80˚ C and cultured at 37˚ C in a MACS-MG-1000-anaerobic workstation (80% N, 10% H, 10% $C0_2$) on fastidious anaerobe agar (FAA) supplemented with 5% defibrinated horse blood (FAA, 8045, Southern Group Laboratory, UK). Following 3 days of growth the bacterial colonies from each strain were transferred to 9 ml of modified fluid universal medium (mFUM), as described in Table 8, before being incubated anaerobically for 3 h at 37˚ C (Niazi et al., 2014). The inoculum was adjusted with fresh mFUM to obtain an optical density of 0.5 at a wavelength of 600 nm (OD_{600}), corresponding to 10^7 cells/ml, confirmed using a plate reader (Labsystems iEMS Reader MF, UK), based on preliminary studies developed in the department. The biofilms were then grown on autoclaved hydroxyapatite (HA) discs with dimensions of 9.5 mm x 2 mm (Clarkson Chromatography Products Inc. USA, Pennsylvania) which were previously pre-

reduced for 3 h in 1 ml of mFUM. The HA discs were then placed in petri dishes (10 discs per dish) and seeded with 2 ml of the starter culture of each strain. Biofilms were grown anaerobically with a medium change every 24 hours for 7 days followed by anaerobic incubation for another 7 days without medium change, to simulate nutritionally poor conditions similar to those found in the RC space (Niazi et al., 2014). Before further use, biofilms were then rinsed in phosphate buffered saline (PBS) (BR0014, Thermo Scientific, UK) to discard any non-adherent bacteria.

Table 8: recipe for mFUM as used by by Niazi *et al*. (Niazi et al., 2014)

Item	Quantity
Cysteine hydrochloride	0.5 grams
Distilled water	1 litre
Dithiothreitol	0.1 gram
Glucose	3 grams
NaCl	2.9 grams
Na2CO3	0.5 grams
(NH4)SO4	0.9 grams
MgSO4.7H2O	0.188 grams
K2HPO4	0.45 grams
KH2PO4	0.45 grams
KNO3	1 gram
Stock hemin (5mg/ml) solution	0.4 millilitres
Stock menadione (2mg/ml) solution	0.5 millilitres
Tryptone	10 grams
Yeast extract	5 grams
Heat inactivated horse serum	100 ml

After growing the biofilms, the presence of the selected bacteria was confirmed using culturing and 16S rRNA gene sequence analysis. The discs containing the biofilms were transferred into 1 ml BHI medium for vortexing before serial dilution. Aliquots of 10 µl of the BHI containing

bacteria were cultured on FAA plates and grown anaerobically for 24 h. Bacterial genomic DNA from the CFUs grown on the FAA was extracted by boiling 100 µl of cultured cell suspension prepared in sterile distilled H_2O for 10 min, followed by cooling on ice for 10 min and centrifugation at 13,000 rcf for 2 min (McDowell et al., 2005). The supernatant containing the genomic DNA was stored at −20°C. DNA amplification of a partial fragment of the 16S rRNA gene of the isolates was performed using universal primers; 9F (5'-3' GAGTTTGATCCTGGCTCA) and 907R (5'-3' CGTCAATTCCTTTGAGTT)(Lane, 1991). The amplification was carried out with the following reaction mixture: 0.5 µl of 9F forward primers (concentration 10 pmol/µl; MWG, UK), 0.5 µl of 907R reverse primer (concentration 10 pmol/µl; MWG), 23 µl of Readymix buffer (AB-057/LD/A, Thermo Scientific, UK) and 1 µl DNA extract. The thermal cycling conditions included initial denaturation at 94°C for 10 min, denaturation at 94°C for 30 sec, annealing at 49°C for 30 sec and extension at 72°C for 90 sec, repeated for 34 cycles and a final extension at 72°C for 5 min. The amplified products were run on a 0.5% agarose gel (A9414, Sigma, United Kingdom) and visualised under UV transillumination. PCR products were cleaned for the sequence reaction with illustra ExoProStar 1-Step (US77705, GE Healthcare Life Sciences, UK) according to the manufacturer instructions. Amplicon sequencing was performed by using the BigDye Terminator v3.1 sequencing kit (4336917, Applied Biosystems, UK) with 30 cycles of denaturation at 96°C for 10 sec, annealing at 50°C for 5 sec, and extension at 60°C for 2 min. Sequencing reaction products were run on an ABI 3730xl sequencer (Applied Biosystems, UK). All DNA sequences were analysed, trimmed, and aligned using BioEdit software (version 7.0.0; http://www.mbio.ncsu.edu/BioEdit/bioedit.html). The partial gene sequences were identified by a BLAST search of the NCBI database (http://0-www.ncbi.nlm.nih.gov.ilsprod.ilb.neu.edu/BLAST/), the Human Oral Microbiome database (http://www.homd.org/), or the Ribosome Database Project database http://rdp.cme.msu.edu/). Precise results of the gene sequencing are shown in the appendix. In addition to gene sequencing, the biofilms were plated out anaerobically on FAA plates after 14 days in order to ensure the presence the CFUs of all the individual strains, as shown in Table 9 .

Table 9: The CFU counts of individual species from the endodontic biofilms grown in duplicates on HA discs. CFU counts were taken after 14 days of growth (the last 7 days without media exchange).

Species	Average [CFU / ml]	Standard deviation	Range
P. acnes	3.38×10^7	8.75×10^6	1.75×10^7
E. faecalis	4.56×10^7	9.82×10^6	1.96×10^7
S. mitis	2.03×10^6	5.03×10^5	1×10^6
S. epidermidis	1.23×10^6	2.08×10^5	4×10^5
A. radicidentis	1.35×10^7	1.82×10^6	3.5×10^6

3.2.2 Fluorescent dye characterisation

Fluorescent dyes were broadly categorised into their proposed use of staining either live or dead cells. All the dyes were tested on the endodontic biofilm model for a range of concentrations. Where this showed a favourable result, the dyes were also evaluated on substrates of HA and paper points to ensure that fluorescence was only induced in the biofilm/cells within the biofilm. Statistics were performed using a one-way ANOVA test with the Holm-Sidak method.

The vast selection of fluorescent dyes was narrowed to the selection shown in Table 10. Stock solutions of all the fluorescent stains were created as specified by manufacturers, generally in dimethyl sulfoxide 99.9% (DMSO) (Sigma-Aldrich, UK). Final working solutions are also outlined in Table 10. The endodontic biofilms grown on HA discs were rinsed by immersing the disc into 1 ml of PBS in a 24 well plate (CLS3527, cell culture plates, flat bottom, Corning Costar, UK), in order to remove planktonic bacteria before being incubated in the fluorescent dyes. Manufacturing guidelines recommended incubation times between 15-60 min, depending on the type of fluorescent stain. However, our incubation time was limited to 5 minutes to comply with a clinically relevant treatment time. Before imaging, the stained biofilms were rinsed twice again with PBS in a 24 well plate, then transferred to a borosilicate coverslip (thickness no. 1.5) and imaged with an inverted confocal microscope (DM IRE2, Leica, Germany) and a 20× / 0.7 NA HC-PL-APO water immersion objective (Leica, Germany). Excitation (Ex) and emission (Em) wavelengths for each dye are also outlined in Table 10. For each dye and

concentration, 9 images were acquired on the HA disc. The image locations were chosen to be evenly distributed across the disc.

Background autofluorescence measurements of the sterile HA disc, sterile paper point in PBS (ProTaper universal paper points, Dentsply, UK) and biofilms were taken. PBS was added as in an endodontic situation the canals would be rinsed with saline before sampling, the presence or absence of PBS could affect the autofluorescence of the paper point. Further controls included fluorescently stained sterile HA discs, stained sterile endodontic paper points and stained non-vital biofilms (fixed in formalin for 24 hours, in order for the biofilm structure to remain, before rinsing in PBS). These controls were carried out to ensure the fluorescent dyes chosen did not produce unwanted fluorescence in non-vital cells, endodontic paper points or HA substrates: Staining of the sterile paper points would indicate the fluorescent dye to be unsuitable for the *ex-situ* approach where staining of the HA would pose issues for the *in-situ* approach. The above imaging protocol was repeated for these samples on HA, whereas for the endodontic paper points, the 9 images were taken along the length starting from the tip.

Images were analysed by measuring the mean fluorescence intensity. Biofilms have irregular 3D structures, leading to variation in depth, which needs to be taken into account during analysis. Confocal microscopy was used to discard out of focus fluorescence, allowing multiple surface locations to be compared on the same disc without the influence of biofilm thickness. Images were analysed by measuring the fluorescence intensity using Image J 1.47v (Schneider et al., 2012) and the auto-threshold MinError(I) plugin. Application of the plugin automatically thresholds the image after which measurements can be carried out in the areas of in-focus fluorescence emission. MinError(I) plugin was chosen as it effectively differentiated from out of focus background and biofilms, even at lower fluorescence intensities (Figure 24)

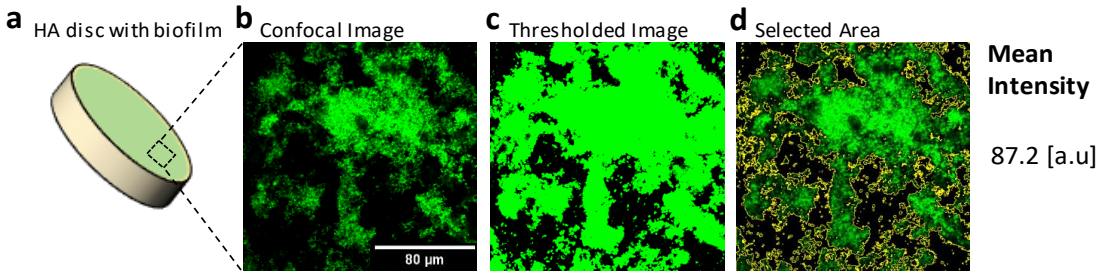

Figure 24: Representative diagram of fluorescence intensity analysis of stained biofilms. a) HA disc with stained biofilm b) Confocal image of biofilm. c) Thresholded image to create a selection for Intensity measurement. d) Selected area for intensity measurement in the confocal image is outlined in yellow.

Table 10: A selection of fluorescent dyes and concentrations evaluated for rapid biofilm staining.

Fluorescent stain	**Concentrations [ug/ml]**	**Wavelength [nm]**	
		Ex	**Em**
Calcein AM (sc-203865, Santa Cruz Biotechnology, inc. USA, Texas)	10, 15, 20 and 50	488	510 – 580
Filmtracer Calcein Red-Orange (F10319, Lifetechnologies, UK)	6.66, 10, 13.33 and 33.33	488	585 – 700
Syto 9 (L10316 Filmtracer Live/Dead, Lifetechnologies, UK)	10, 15, 20 and 50	488	495 – 510
Sypro Ruby (Biofilm Matrix Stain, Lifetechnologies, UK)	One concentration	488	590 – 710
Propidium Iodide (L10316 Filmtracer Live/Dead, Lifetechnologies, UK)	60,90,120 and 300	488	600 – 644
Ethidium Homodimer (sc-211428 Santa Cruz Biotechnology, inc. USA, Texas)	5,10,20 and 40	488	585 – 670
Di-4-ANEPPDHQ (D36802, Thermo Fisher, UK)	1.66, 3.33, 6.66 and 10	488	540 – 590 & 630 – 680
FilmTracer FM 1-43 Green (F103147, Thermo Fisher, UK)	1,2.5, 5 and 10	488	530 – 611

Correlation between fluorescence and presence of vital bacteria

To investigate the correlation between amount of bacteria and fluorescence, serial dilutions of fluorescently stained bacteria were analysed. Planktonic cells of *Enterococcus faecalis* OMGS 3202 were suspended in PBS following anaerobic growth on FAA with 5% horse blood to an optical density of 1.5 and serially diluted by a factor of 5. Aliquots of each dilution were simultaneously plated out for CFU counting and stained by adding 15 µg/ml of CAM for 5 minutes at 37˚ in a dark environment. For the CFU counting, each initial serial dilution was again serially diluted by a factor of 10, 100 µl of each serial dilution was then plated on FAA plates and again incubated anaerobically for 3 days. CFUs were counted to calculate the concentration of CFU/ml. Analysis of the fluorescence intensity was carried using a microplate fluorometer (Fluoroskan Ascent™ FL Microplate Fluorometer and Luminometer, Labsystems, UK) taking readings from duplicate samples with excitation/emission wavelengths of 485/510 nm and an integration time of 500 ms.

3.2.3 Spectroscopic detection: Ex-situ approach

Ex-situ biofilm detection involved constructing an optical setup combining fluorescence spectroscopy and microscopy, allowing for rapid spectral analysis of bacterial fluorescence spectra whilst using the fluorescent image to determine the position on a sample.

A wide-field fluorescence microscope (Axiovert 200, Zeiss, Germany) was coupled to a fluorescence spectrometer (QE 65000, Ocean Optics, The Netherlands) using a fibre patch cable (Ø 400 µm, 0.48NA SMA step-index multimode Fiber Patch Cable, M40L02, Thorlabs, UK). Combining a 10× objective (Fluar 10× / 0.5 NA Infinity/0.17, Zeiss, Germany) and 80/20 beam splitter (spectrometer port/camera) enabled simultaneous acquisition of fluorescent images and spectral data from the same field of view. Samples were excited using a high power LED (M470L3 Blue, 470 nm, Thorlabs, UK) and a customised filter cube was used to remove the excitation light while collecting a broad spectrum emission: Ex 440/40 nm (FF01-440/40-25, Semrock, USA), Em 473 nm LP (BLP01-473R-25, Semrock, USA), and a dichroic mirror: 488 nm (Di02-R488-25x36, Semrock, USA) (Figure 25). Figure 26 shows a diagram illustrating this setup: unless stated otherwise, the power output from the objective was set at 200 µW, leading to an optical intensity of 2.07 mW/cm^2.

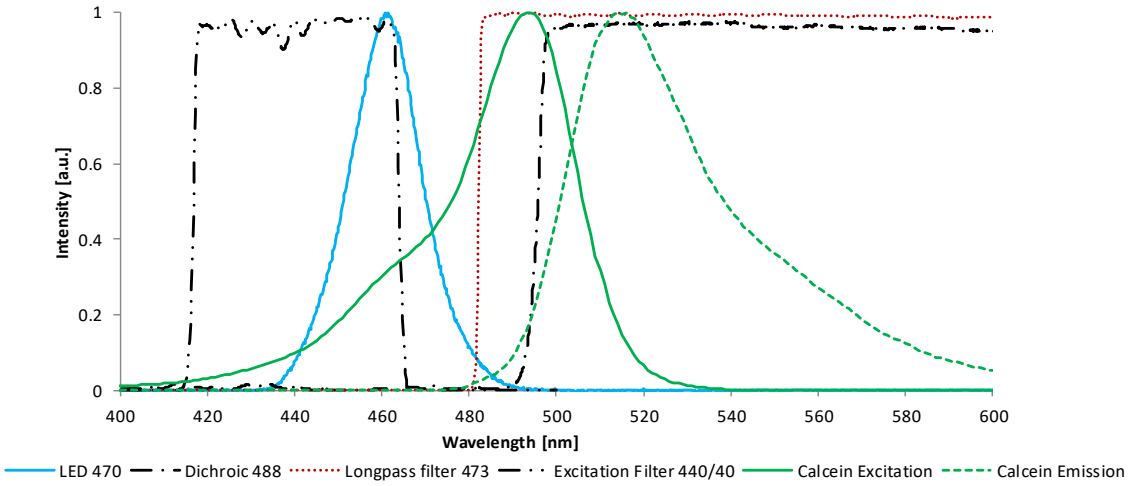

Figure 25: Diagram of filter cube used: Spectra of filter cube components as well as excitation light and calcein excitation and emission.

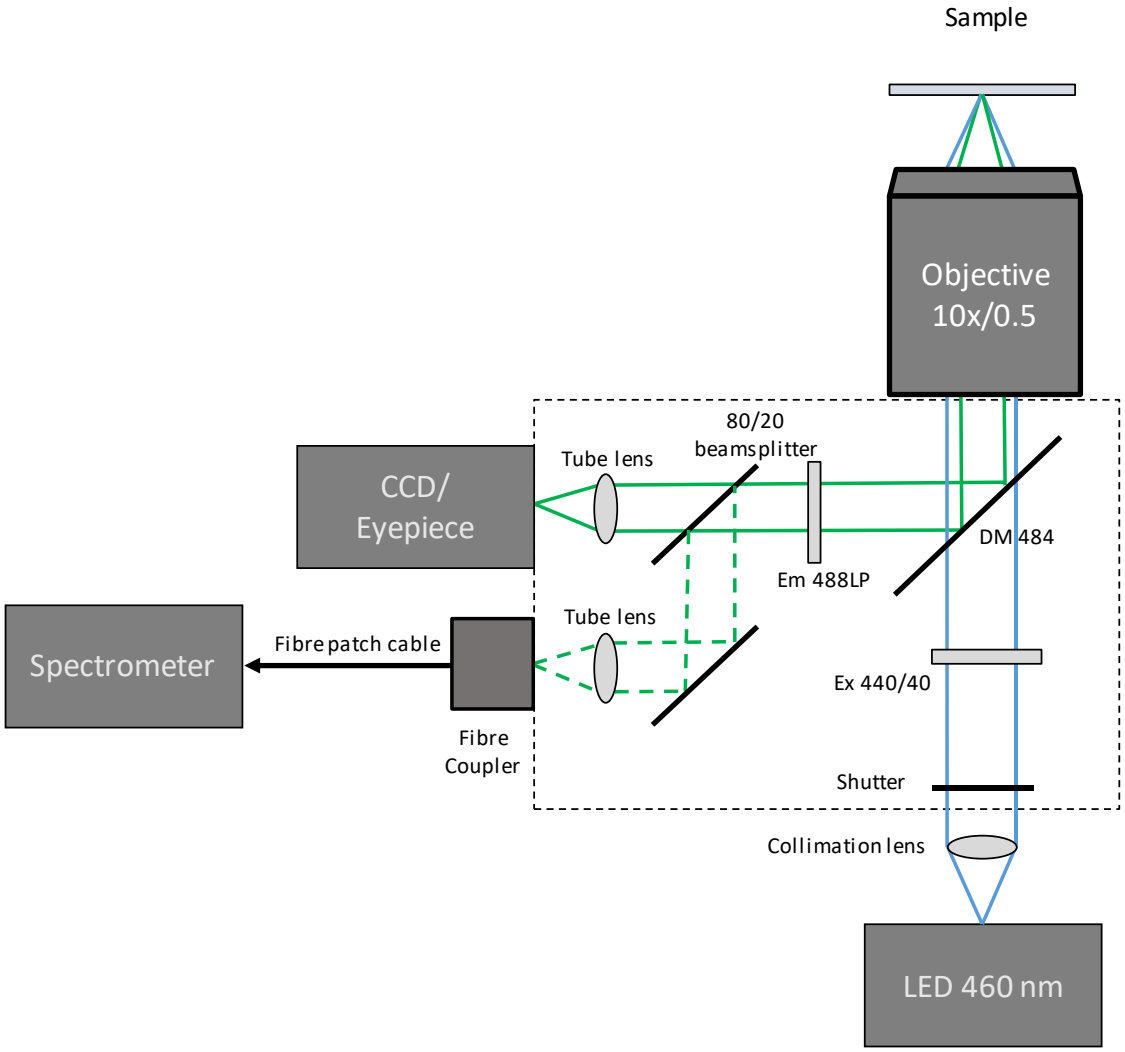

Figure 26: Optical setup allowing for sample excitation with a blue LED and simultaneous detection of the fluorescence image and spectrum. This was achieved by modifying an infinity corrected Zeiss Axiovert 200 microscope with a blue LED excitation light and fluorescence spectrometer. The fibre coupler used contains a 0.4x lens, resulting in a field of view of 500 µm for the spectral analysis.

When illuminated by the 470 nm excitation light, a non-negligible autofluorescence signal was found to be emitted by the substrates (paper points and HA) and this background signal became problematic when the fluorescence from the calcein was very low. Spectral unmixing was used to separate the signal from the substrate, precisely determining the proportion of calcein fluorescence contributing to the recorded spectrum. Control spectra of calcein and substrate autofluorescence were recorded, intensity normalised and used as base spectra for an in-house Levenberg–Marquardt curve-fitting algorithm. The base spectra were described as either signal or background spectra: Signal spectra (S_S) refers to the calcein spectrum, indicating the presence of vital bacteria. Background spectra (S_B) consist of Biofilm/HA autofluorescence, CAM stained non-vital biofilms treated with NaOCl for 15 min and CAM stained non-vital biofilms fixed in formalin for 24 hours (Figure 27a). The addition of the formalin fixed non-vital biofilm was chosen as incubation in NaOCl removed the majority of the biofilm. Figure 27b shows an example fit output of analysed experimental data, with the proportional signals of the base spectra

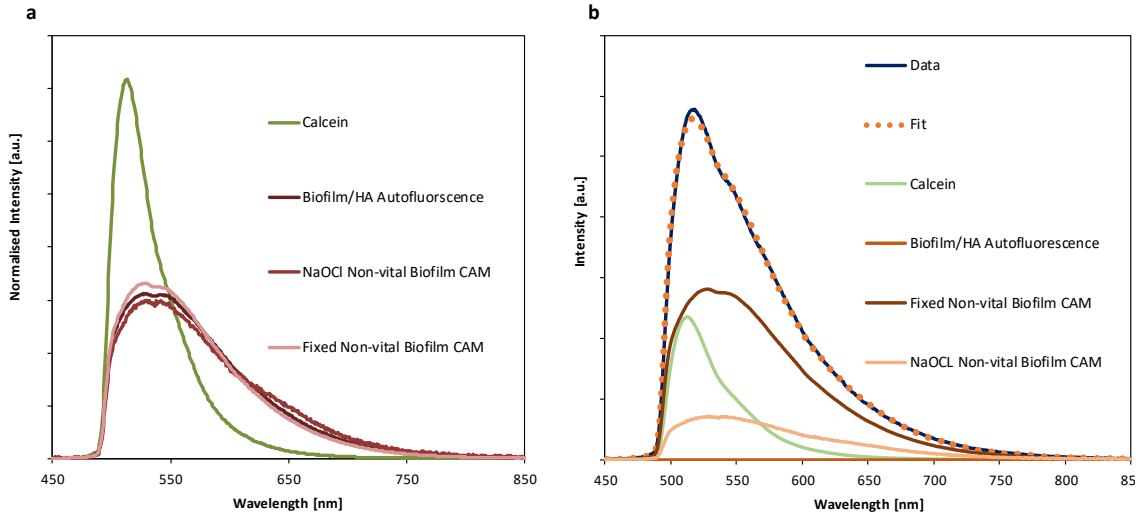

Figure 27: a) Base spectra normalised to the area under the curve, with signal spectra in green and background spectra in red. b) Example of experimental spectra with fitted data.

Detection of vital cells in stressed biofilms

To evaluate the detection sensitivity in comparison to gold-standard CFU counting, endodontic biofilms grown on HA discs were exposed to 1% NaOCl (as clinically used during RCT disinfection). For each disc, increasing exposure (from 1 to 200 sec) to NaOCl was performed at 10 exposure points (5 discs per NaOCl exposure duration). Positive controls (vital

biofilm) consisted of biofilms exposed to PBS for 200 s and negative controls (non-vital biofilm) were biofilms fixed with formalin for 24 h. Controls were also repeated for n = 5. Biofilms were rinsed with 1 ml PBS, transferred to 1 ml of 1% NaOCl and then rinsed in PBS twice before staining. All biofilms were stained in a 500 µl CAM solution (15 µg/ml for 5 min taken from results of characterisation in section 3.3.1) and rinsed with 1 ml PBS, before placing them into glass bottom well plates for imaging (662892 24-SensoPlate, Greiner Bio-One, Austria). Spectra were taken for each disc (20 locations per disc). Locations were programmed for the motorised x-y stage of the microscope, ensuring them to be the same for each disc. This experiment was repeated by sampling the HA discs with endodontic paper points (F2 ProTaper, Dentsply, UK), sampling was carried out by rubbing the paper point parallel over the entire surface of the HA disc, ensuring the tip of the paper point was in line with the edge of the HA disc. Spectra were then taken from 10 locations along the paper point at 500 µm intervals from the tip.

Prior to staining, half of a biofilm sample was taken from an HA disc from each NaOCl exposure point and transferred to Eppendorf tubes containing 1 ml brain heart infusion broth (BHI CM1135, Oxoid, UK) for serial dilution. Biofilms were transferred using a sterile scalpel. 100 µl of the serial dilutions were plated on FAA plates and incubated anaerobically for 4 days before CFU counting for comparison with the calcein signal.

3.2.4 Remote spectroscopic detection: In-situ approach

In-situ detection applied the same general setup as was used as for the *ex-situ* approach (section 3.2.3). In addition, a single core glass fibre cable (Ø 200 µm, 0.22NA SMA step-index multimode Fiber Patch Cable, Thorlabs, UK) was coupled to the 10× microscope objective. The other side of the SMA connector was removed and the cable declad in order to reveal the naked Ø 200 µm fibre core, which was used as a probe, allowing for remote detection of a fluorescence signal (Figure 28).

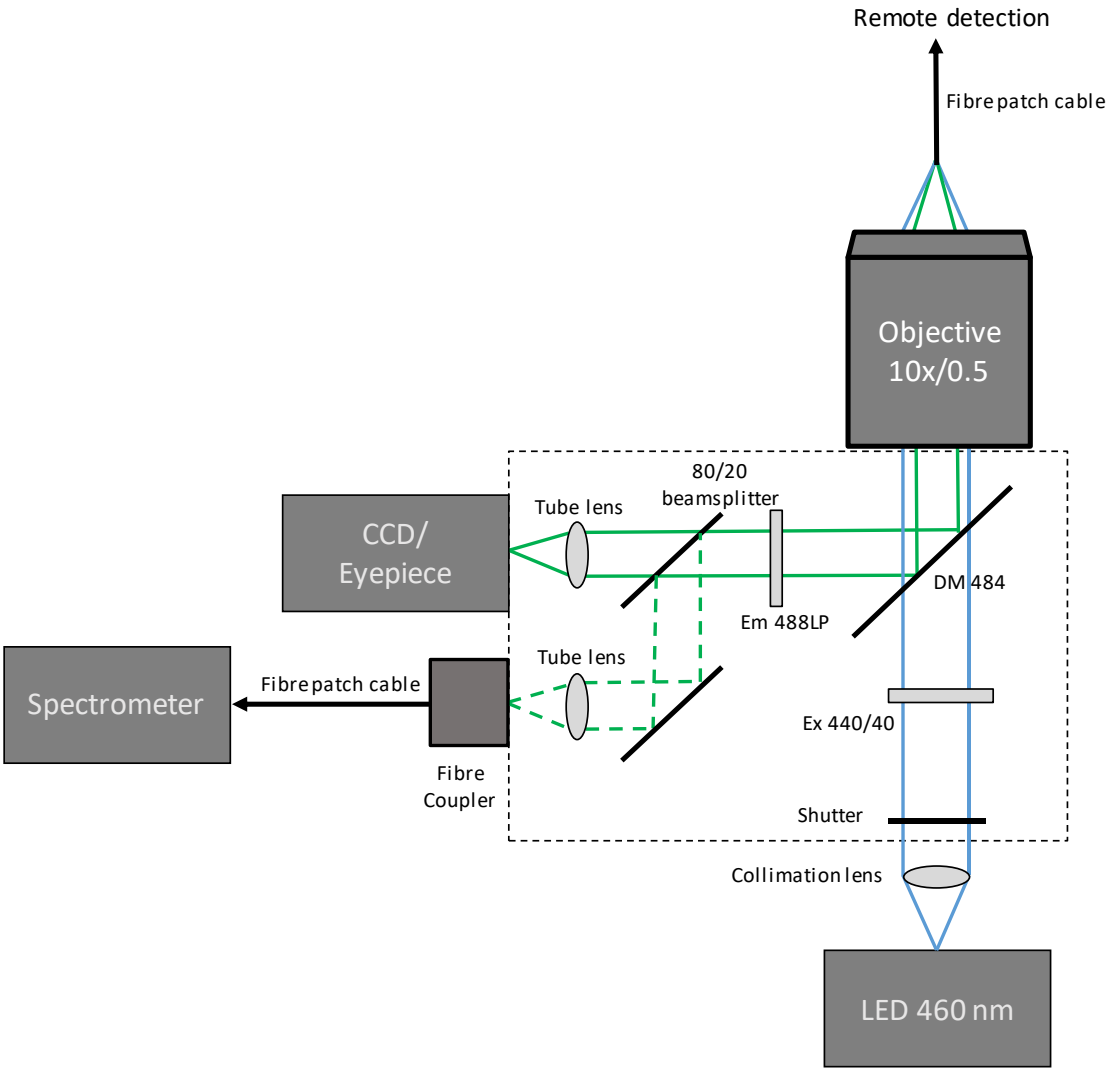

Figure 28: Adapted *ex-situ* setup (Figure 26) for the *in-situ* concept of spectral analysis, including declad optical fibre cable for remote detection.

In order to demonstrate the potential use of remote spectral detection *in-situ, endodontic* biofilms (as described in section 3.2.1) were grown on HA discs and nutritionally starved for 0, 4, 7 and 11 days (one disc per period of nutritional starvation). Following this, they were stained with 1 ml of 15 µl/ml CAM and 4.5 µl/ml Propidium Iodide in the dark for 5 minutes before rinsing by placing the discs into 1 ml PBS in a 24-well plate. CAM and propidium iodide were chosen as these were established to be most suitable for live/dead staining as shown in section 3.3.1. Using the described setup, both fluorescent stains were excited at the same wavelength (460 nm) and due to the long pass emission filter, both emission spectra were recorded (See Figure 29 for a simplified version of the filter cube including both excitation and emission spectra). For each disc, 10 spectral readings were recorded by contacting the surface of the biofilm with the tip of the fibre probe. The fibre was cleaned with hydrogen peroxide

between each reading, as used in commercial systems (Mauna Kea Technologies, France). The autofluorescence of the HA and dentine were measured to ensure these wouldn't interfere with the fluorescence staining (dentine autofluorescence was measured for future reference in order to foresee potential autofluorescence issues when probing the root canal. Finally, spectral unmixing was carried out using the calcein and propidium iodide, as well as HA and dentine autofluorescence spectra as the base spectra, to calculate the ratio of the proportion live/dead stained cells.

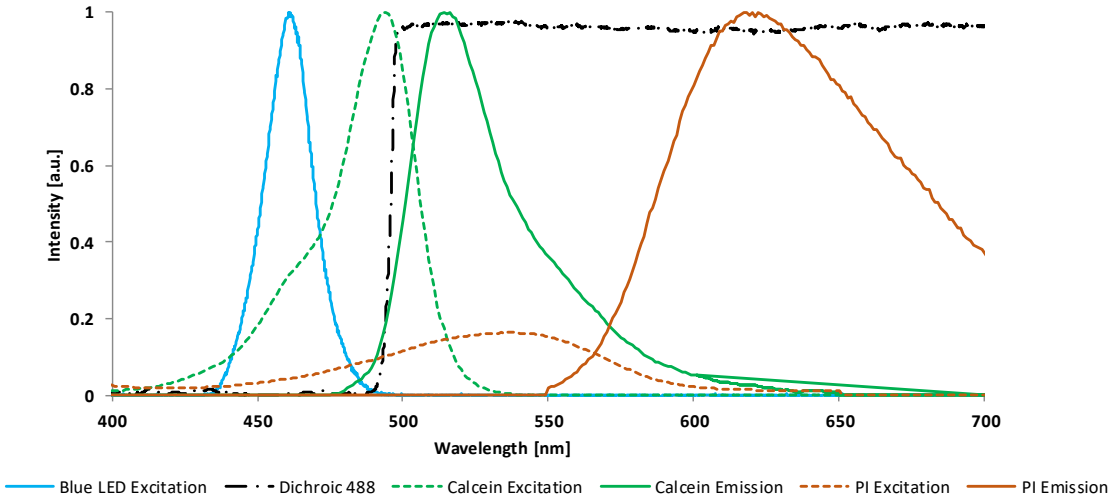

Figure 29: Excitation and Emission spectra of Calcein and PI, as well as excitation light and dichroic filter used in the filter cube.

3.3 Results and Discussion

3.3.1 Fluorescent dye characterisation

The aim of the bacterial staining both *in-situ* and *ex-situ* is to induce fluorescence in vital bacteria with suitable fluorophores, therefore allowing the detection of fluorescence specific to the live stained bacteria. This can be achieved by using fluorescent dyes which have a non-fluorescent state until exposed to vital cells. Alternatively, the additional use of fluorescent counter-dyes for dead cells, emitting at alternate wavelengths, may enhance the detection by contrasting the vital to the dead cells (live/dead staining). Using a mixed species biofilm of RC pathogens (described in section 3.2.1.), stains were evaluated for incubation time, fluorescence intensity and ability to stain only the viable biofilm, as opposed to substrates or non-vital biofilms (described in section 3.2.2.)

Live fluorescent dyes

Initial staining of the biofilm with CAM was performed at increasing incubation times as well as increasing concentrations. The results showed the dye being taken up by the cells of the mixed species biofilm (Figure 30) and producing increased fluorescence intensity as the concentration increased. This was especially noticeable at the highest incubation time of 30 mins (Figure 30& 30). The most favourable fluorescence intensities from the vital stained biofilm were achieved at 30 min incubation time with 10 µg/ml. However, to comply with clinical relevance the incubation time was then limited to a maximum of 5 mins for all the following experiments, deemed to be a feasible timeframe to be incorporated into a clinical endodontic workflow.

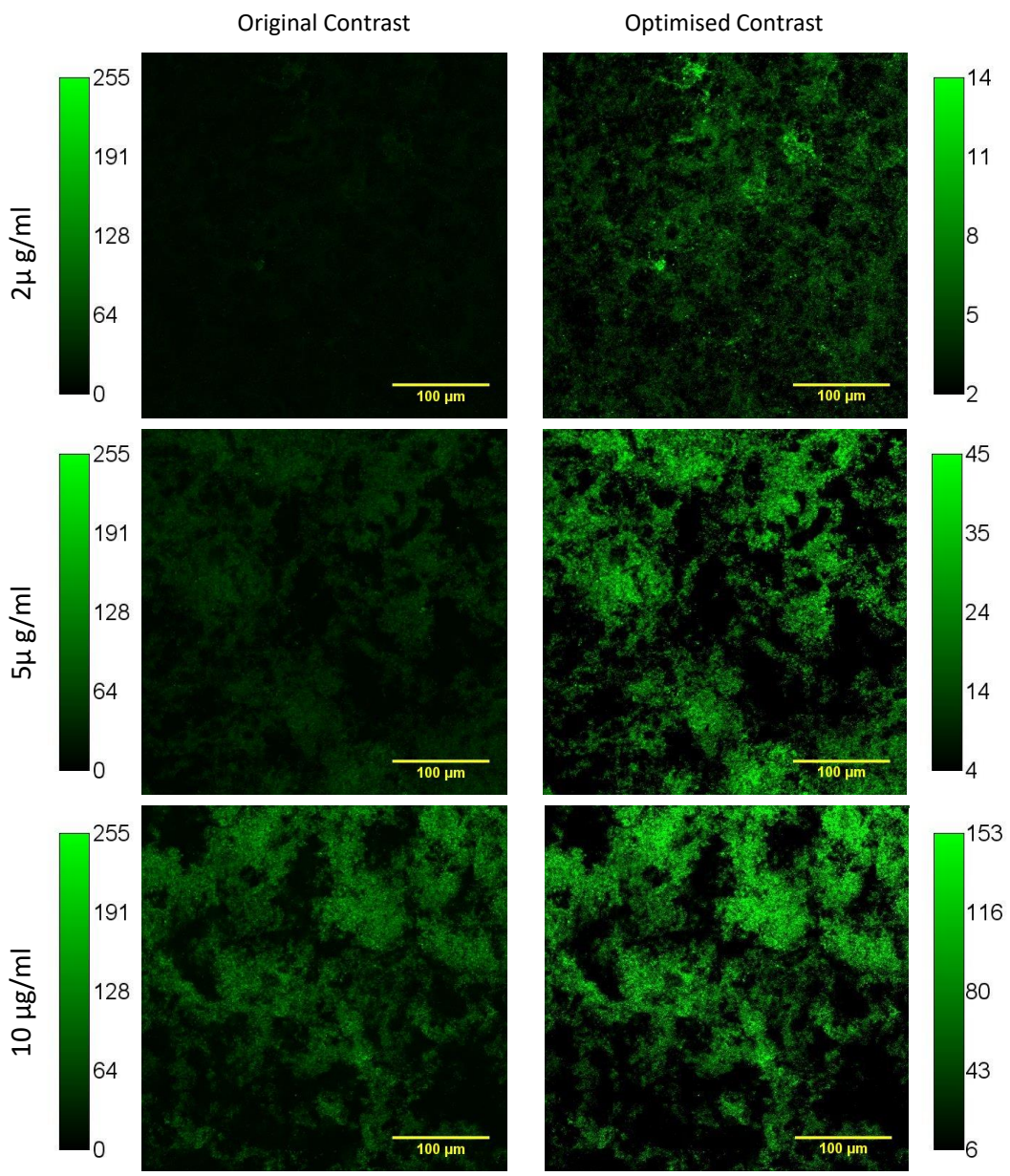

Figure 30**:** Representative confocal images of CAM staining at 30 min incubation time at given concentrations. Original images in the left column, adjusted contrast for visualisation in the right column. Increasing intensity at higher concentrations is evident.

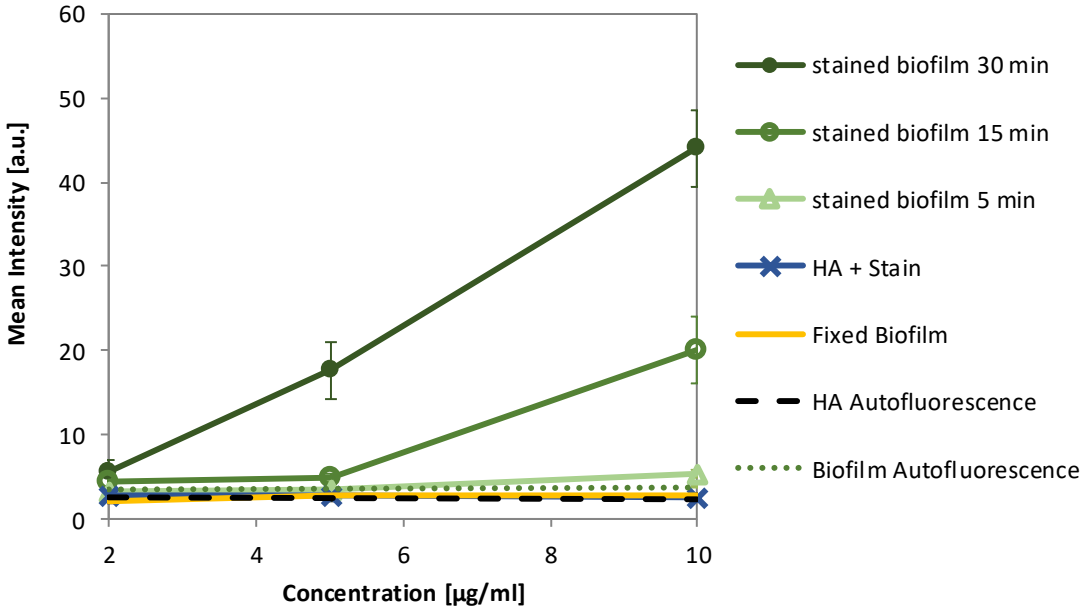

Figure 31: CAM mean intensity against concentration at 5, 15 and 30 min incubation time.

Increasing the concentrations at a set incubation time of 5 minutes led to increased fluorescence intensity from the stained vital biofilm (Figure 32), when comparing the concentrations of 15 µg/ml to 10 µg/ml. At 15 µg/ml, the highest ratio of fluorescence from the vital biofilm to the non-vital biofilm was achieved (11.7). When further increasing the concentration, the mean intensity remained within the standard deviation of 15 µg/ml (Figure 32). CAM staining resulted in a higher fluorescence intensity for the stained vital biofilm at all concentrations, when compared to stained non-vital biofilms and stained substrates (HA and paper points). These results indicate that CAM could be suitable for detection of vital cells even on absorbent substrates such as paper points.

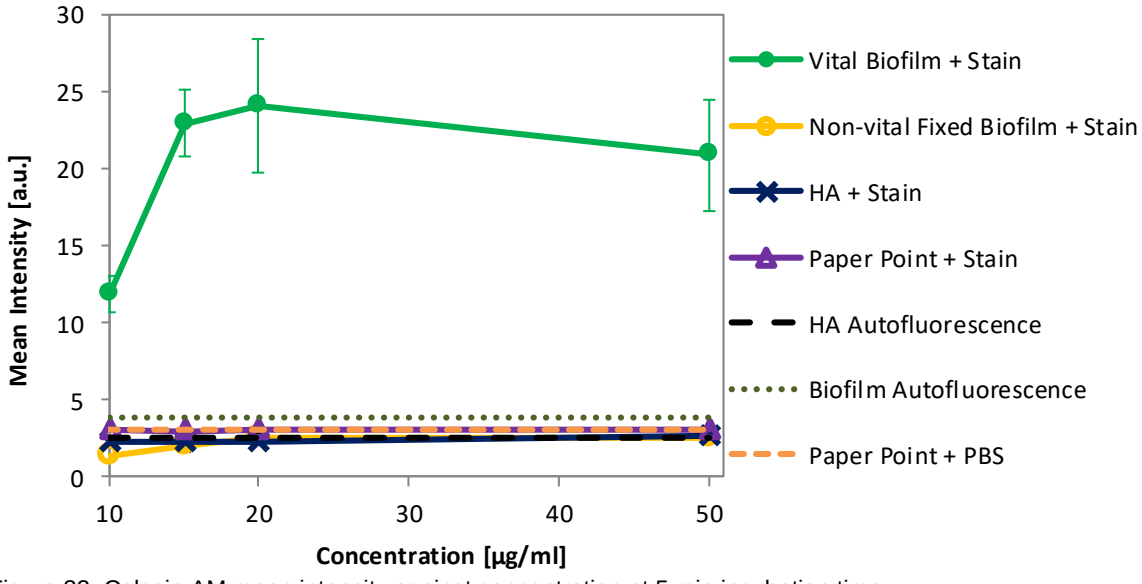

Figure 32: Calcein AM mean intensity against concentration at 5 min incubation time.

FilmTracer Calcein Red-Orange showed uptake into the biofilm. Similarly to CAM, basic visualisation of the biofilm was possible after 5 minutes of incubation time. The change in concentration of the dye had little effect on the intensity (Figure 33). Staining of the non-vital fixed biofilm control showed higher fluorescence intensity than the viable biofilm at concentrations over 13.3 µg/ml, possibly indicating that only small amounts of the dye were able to penetrate the membrane of viable bacteria within the short incubation time. The comparatively high intensity of the stained HA disc (control) showed the stain being retained on the surface of the HA disc without cells being present (Figure 33). The high background staining is due to the stain's intrinsically fluorescent nature and resulted in unsatisfactory characteristics for rapid detection of vital cells in this model biofilm.

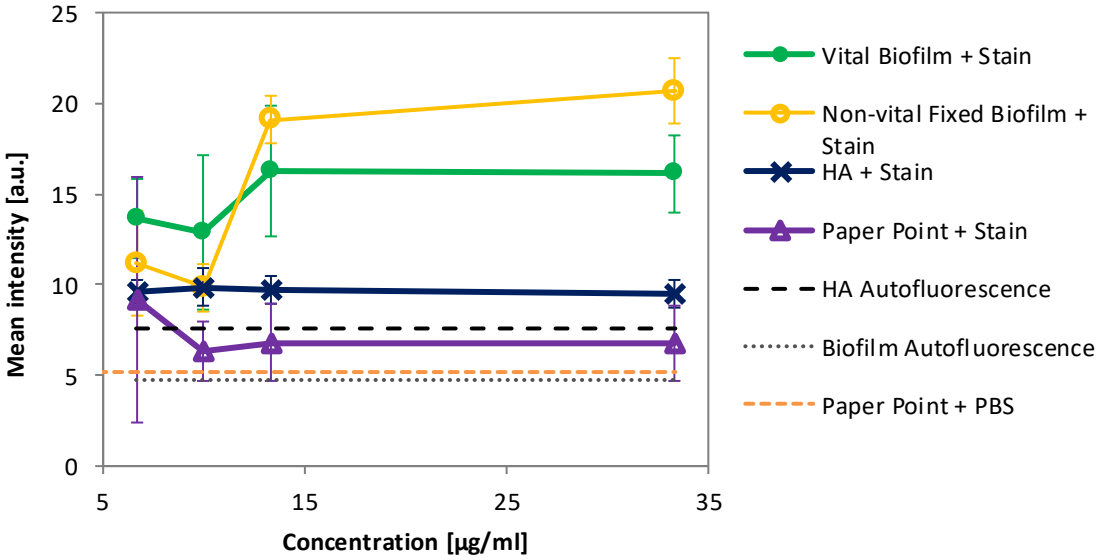

Figure 33: FilmTracer Calcein Red-Orange mean fluorescence intensities against concentration at 5 min incubation time.

FM-143 is a lipophilic dye and therefore reacts with cell membranes. It has shown an increase in fluorescence when inserted into surface membranes. Basic visualisation of the biofilm was possible, however, strong fluorescence intensity of stained non-vital biofilms as well as paper points was recorded. The short incubation time, resulting in the need for high concentration most likely resulted in high background staining. Fixing of the non-vital biofilms may have led to increased staining of non-vital cells, as the membrane may still be intact enough for accumulation of the dye (Figure 34).

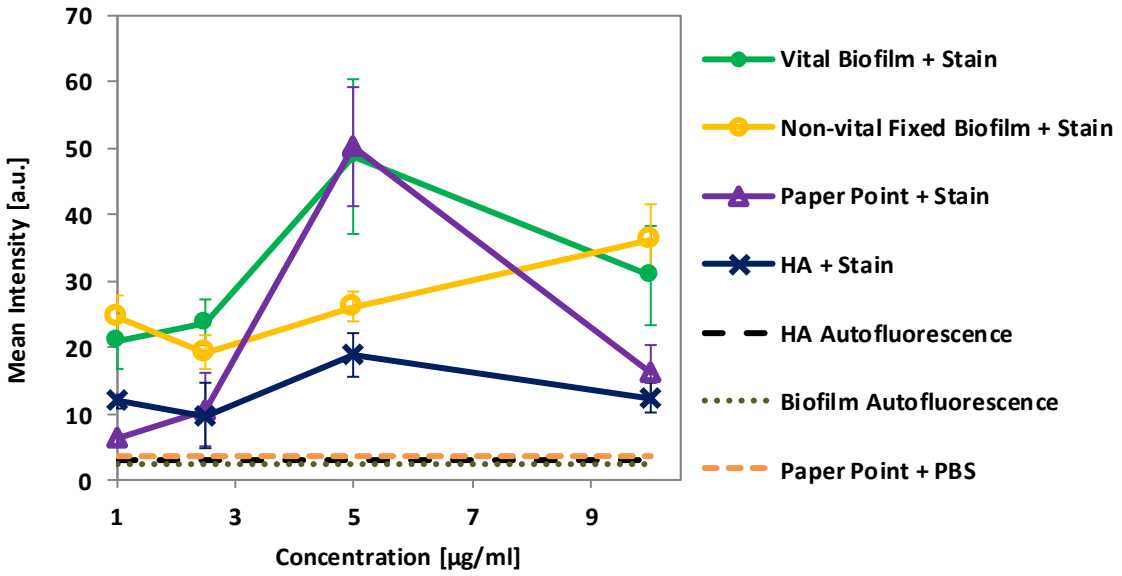

Figure 34: FM-143 mean fluorescence intensities against concentration at 5 min incubation time.

Di-4-ANEPPDHQ fluorescence is dependent on the electrical potential charges of the environment, thus having a fluorescence shift when in a liquid-ordered state in an intact membrane of a vital cell compared to a disordered state of compromised membrane or even the absence of a membrane. Visualisation of the biofilm was possible, however, analysis between 540 – 590 nm (for live cells) showed no difference between the vital and the non-vital fixed biofilms (

Figure 35). The lack of differentiation between vital and non-vital cells could be attributed to the fixation of the biofilm, as this leads to the biofilm and the membrane of the cells maintaining structure (Chao and Zhang, 2011). Characterisation of this fluorescent stain may require an alternate method to create a non-vital biofilm, as the in-tact membrane structure may not allow for the fluorescence shift, which would occur in a compromised or absent membrane.

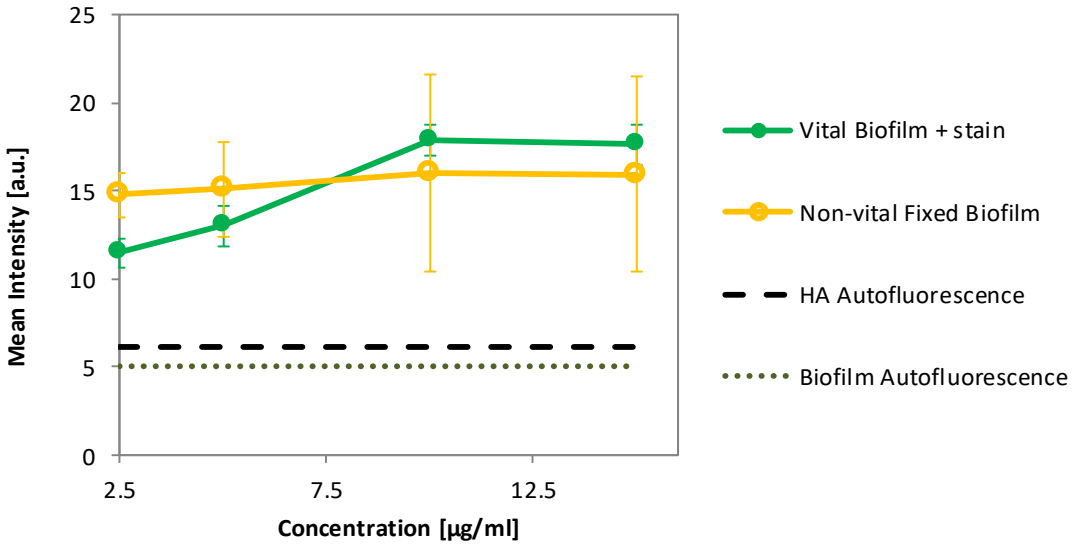

Figure 35: Di-4-ANEPPDHQ mean fluorescence intensities against concentration at 5 min incubation time.

Vital nucleic acid stain Syto9 was used in combination with propidium iodide (PI) and was taken up by the biofilm allowing for visualisation. At concentrations of 15 µg/ml and 50 µg/ml the fluorescence intensity emitted was higher for the vital biofilm compared to the non-vital one. Most noticeably, the fluorescence intensity of the stained sterile paper point was highest at all concentrations. The intrinsically fluorescent nature of the stain is likely to be the reason for the staining of the paper point. Once bound to DNA the fluorescence of Syto 9 increases. However, at only 5 min incubation, the fluorescence of a large amount of stain accumulated in the paper point led to higher fluorescence intensity, demonstrating Syto 9 not to be suitable for detection of bacteria sampled with paper points (Figure 36).

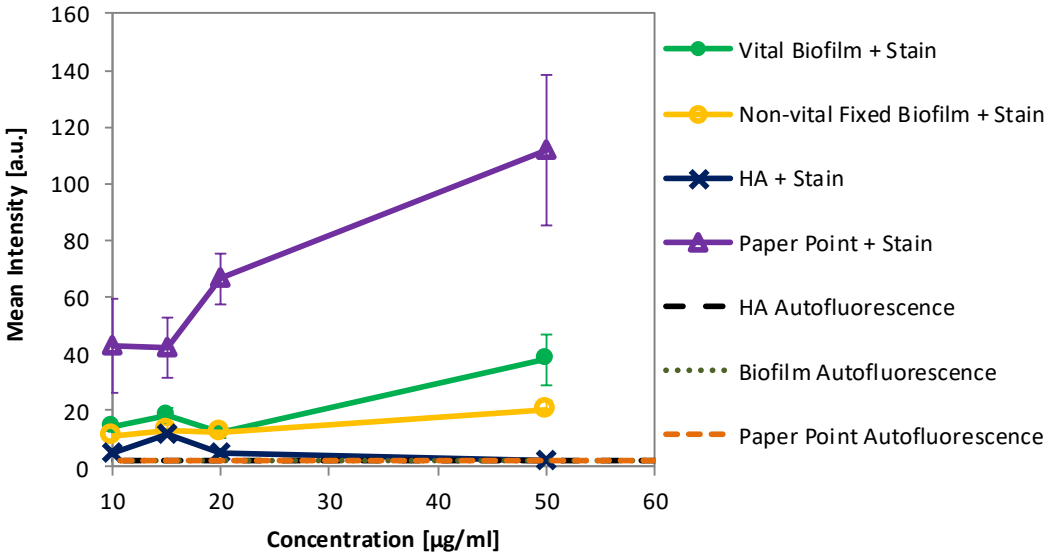

Figure 36: Syto 9 mean fluorescence intensities against concentration at 5 min incubation time.

Dead fluorescent dyes

PI, being the nucleic acid stain for dead cells used in combination with Syto 9, showed higher fluorescence intensity for non-vital fixed biofilms, with the most favourable outcome at concentrations of 90 and 120 µg/ml. Despite the contrast between the vital and non-vital biofilm generally not being high, the increased fluorescence intensity at 120 µg/ml for the dead cells indicates the potential for PI to be used in combination with a vital cell stain to identify dead cells in a population, which is a common application of this stain. An unexpected intensity peak for the stained HA was observed at 90 µg/ml, which could potentially be attributed to irregularities on the disc retaining the fluorescent dye. (Figure 37).

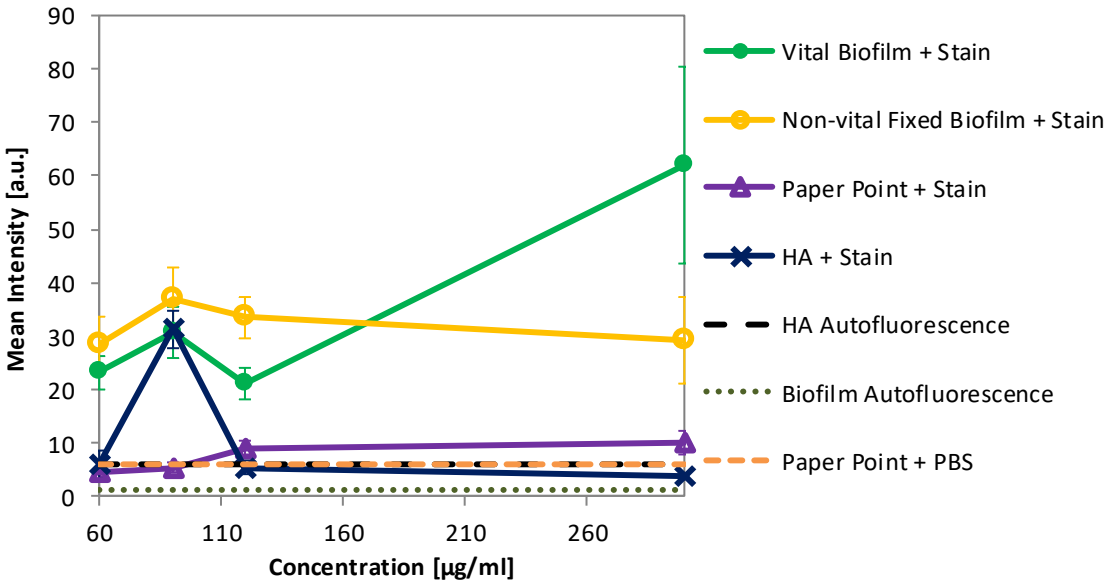

Figure 37: Propidium Iodide mean fluorescence intensities against concentration at 5 min incubation time.

Ethidium homodimer was taken up by the biofilm and allowed for biofilm visualisation. However, the vital biofilm exhibited either the same or higher fluorescence intensity at all concentrations, showing that this stain is not suitable for dead cell staining in biofilms at a short incubation time. The absence of stronger fluorescence intensity in the non-vital biofilms is likely to be due to the short incubation time. Ethidium homodimer penetrates cells with compromised membranes and binds to the DNA, therefore, 5 minutes incubation time may not be sufficiently long (Figure 38).

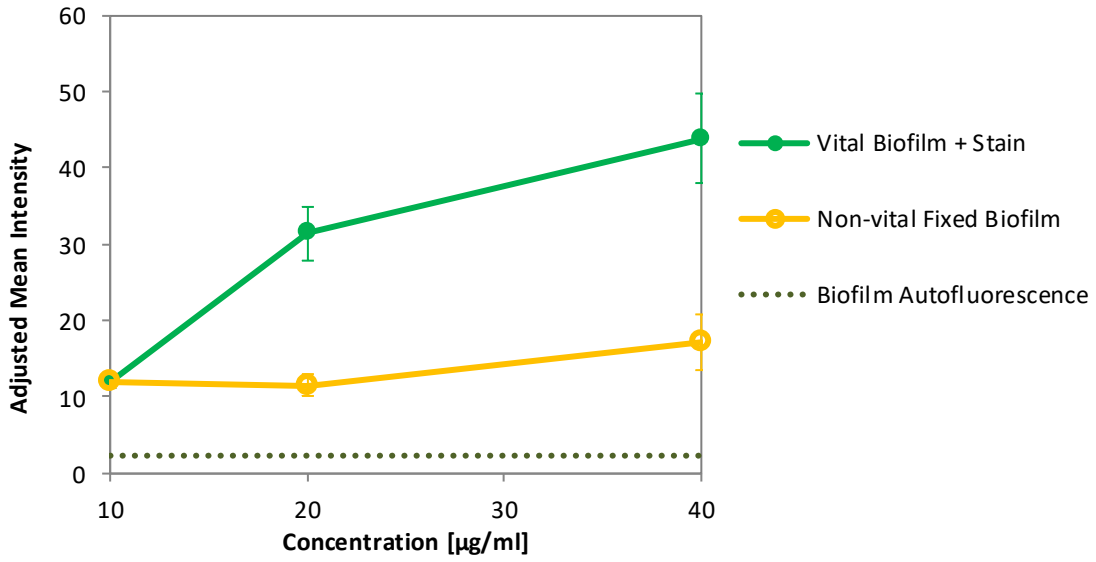

Figure 38: Ethidium homodimer mean fluorescence intensities against concentration at 5 min incubation time.

Characterisation for biofilm detection

To compare the ability of each fluorescent dye and concentration to specifically detect vital biofilms, as opposed to non-vital biofilms, the ratio (R_v) between the fluorescence of vital and non-vital biofilms was measured. For the dead cell dyes, the fluorescence ratio (R_d) was inverted (non-vital/vital) to evaluate the dyes ability to stain non-vital cells in the biofilm. Similarly, the ratio (R_s) between the fluorescence of vital biofilm and the endodontic paper point (substrate) was used to compare their ability to not stain the substrate.

Characterisation of this selection of fluorescent dyes highlighted CAM to be the most suitable fluorescent dye to detect vital cells within the endodontic biofilm model: it showed the highest ratios at all concentrations for all the dyes (Figure 39a). Maximum ratio R_v = 11.7 was observed at a concentration of 15 µg/ml and is significantly higher than all other dyes characterised ($p<0.001$) (Figure 39b). Above this concentration, the ratio dropped slightly due to an increased staining of the non-vital cells at high concentrations. By comparison, only minimal changes were observed in the maximum R_v for the other dyes.

Characterisation of the nucleic acid binding dead cell dyes ethidium homodimer and PI revealed PI to be more appropriate to stain non-vital cells in a mature endodontic biofilm at a 5-minute incubation time. Ethidium homodimer staining even resulted in an equal or higher

fluorescence intensity for the live biofilm. PI produced higher R_d at all concentrations with the maximum signal at 1.59 (Figure 39c) being significantly higher than for ethidium homodimer (P<0.001) (Figure 39d).

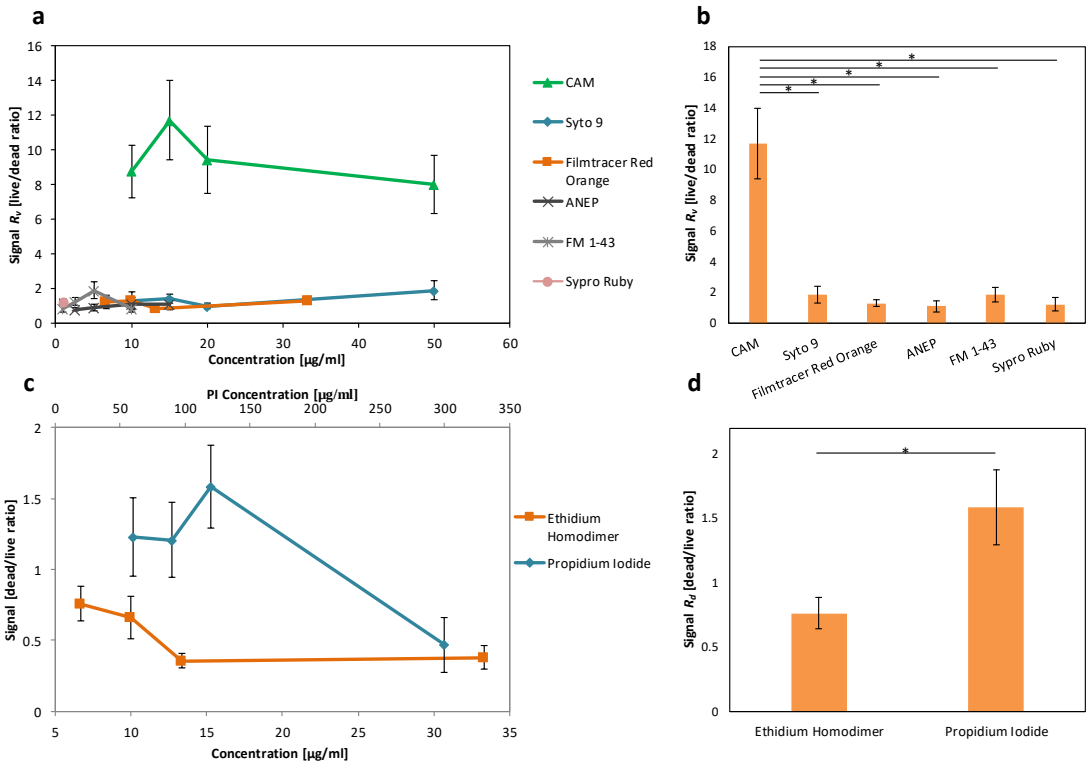

Figure 39: Characterisation of fluorescent stains. a) Comparison of fluorescence ratio of stained vital biofilms to stained dead fixed biofilms for live staining at different concentrations. b) The ratio of stained vital biofilms to stained non-vital fixed biofilms at each stain's optimal concentration. c) Comparison of fluorescence ratio of non-vital to vital biofilms for dead stains at different concentrations. d) The ratio of stained non-vital biofilms to vital biofilms at each stain's optimal concentrations. Error bars show the standard deviation and statistics were performed using a one-way ANOVA test with the Holm-Sidak method n = 9, *p< 0.001).

Comparing the ratio R_s of stained biofilms to stained endodontic paper points, the same high signal for CAM compared to the other live dyes was observed at all concentrations (Figure 40a, b). PI produced its highest R_s of 6.8 at 90 µg/ml concentration. Using the ideal concentrations determined by the R_v, calcein showed the highest R_s of 7.6, significantly higher than the other dyes tested (P<0.001). PI (R_s of 3.8) was significantly higher than the remaining dyes tested (P<0.001).

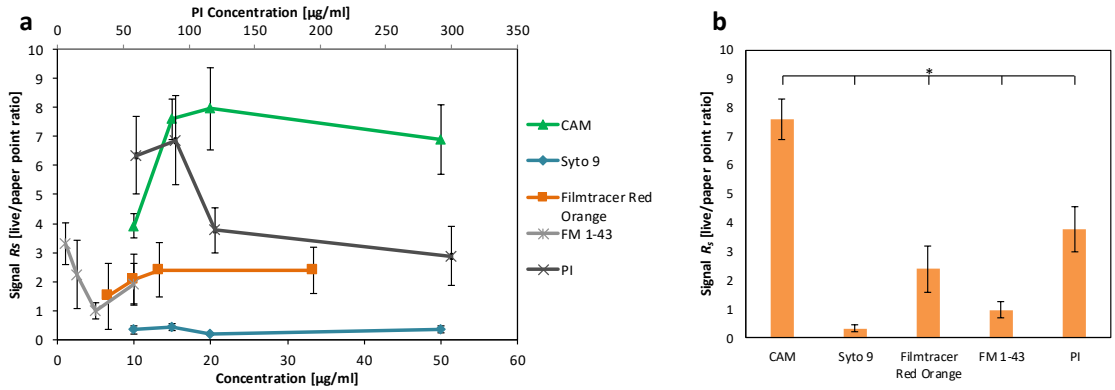

Figure 40: Characterisation of fluorescent stains. a) Comparison of fluorescence ratio of stained biofilms to stained endodontic paper points at different concentrations. b) The ratio of stained biofilms to stained endodontic paper points at each stains optimal concentration. Error bars show the standard deviation (*p< 0.001).

The short incubation time, as well as the requirement that the dyes must not stain substrates, ruled out most of the dyes tested. 5 min incubation time, which was counteracted by increasing concentrations for CAM, was not enough reaction time for the other dyes. Most dyes do not switch from non-fluorescent to fluorescent as CAM does, but rely on being washed off and/or increasing in fluorescence once bound to targets in the cells. Attempting short incubation times and increasing concentrations can lead to unwanted background staining.

Characterisation of the nucleic-acid-binding dead cell dyes ethidium homodimer and PI revealed PI to be more appropriate to stain non-vital cells in a mature endodontic biofilm at a 5-minute incubation time. Ethidium homodimer staining resulted in an equal or higher fluorescence intensity for the live biofilm, whereas PI, at the right concentrations led to a significantly higher fluorescence intensity in the dead biofilm ($p<0.001$) (Figure 39d). Aside from the low staining ratio of the dead cell stains characterised here, the nature of the chemo-mechanical treatment must be kept in mind. The treatment includes the use of NaOCl, which has been shown to degrade nucleic acid and therefore the results of nucleic-acid-binding stains cannot necessarily be relied on (Young et al., 2007). For the purpose of detecting residual endodontic biofilm bacteria after a short incubation time, these results have established CAM to be the most suitable fluorescent dye with optimal live staining at 15µg/ml. Indeed, due to being intrinsically non-fluorescent, it can be used in the absence of a dead counterstain, in contrast to a more time-consuming approach for bacterial detection post-RCT suggested by Sato *et al.,* where live/dead staining was carried out using DAPI and propidium Iodide (Sato et al., 2012). DAPI, being a cell permeable nucleic acid stain, is not an indicator of vitality, therefore requiring the additional counterstain of impermeable propidium iodide.

Correlation between fluorescence and presence of vital bacteria

Comparing the number of CFUs to the fluorescence intensity of a stained dilution series of planktonic *E. faecalis*, which is a common RC coloniser (Stuart et al., 2006), allows us to demonstrate the connection between a number of vital cells and fluorescence intensity. As shown in Figure 41, there is a correlation between the amount of CFUs present and the fluorescence intensity, caused by the varying amount of vital cells converting the CAM to fluorescent calcein. At lower cell concentrations, the fluorescence signal decreases to a level plateau, due to the autofluorescence signal of the PBS, in which the cells are suspended, as well as the bacteria themselves. The presence of a background signal caused by autofluorescence demonstrates the need for further differentiation between the potentially overlapping autofluorescence and calcein fluorescence.

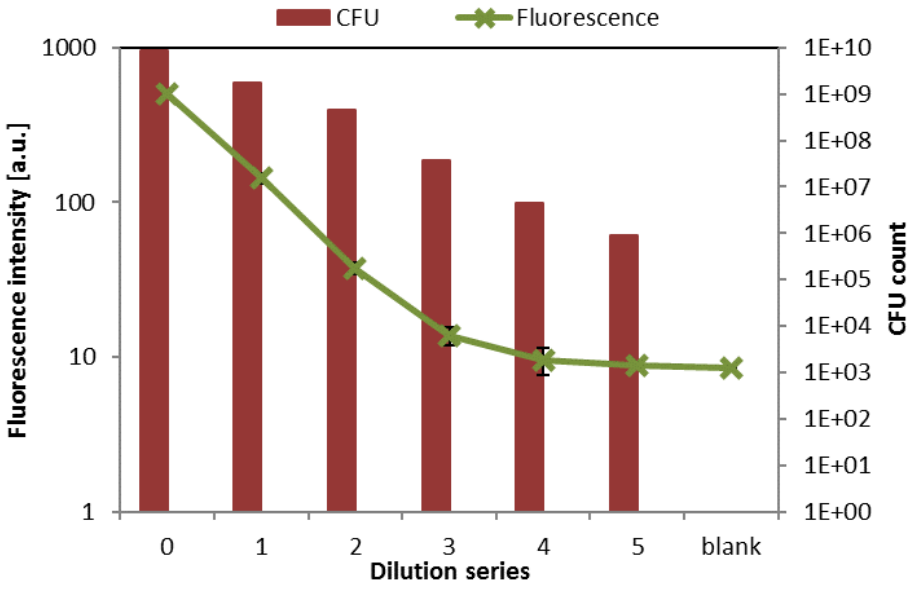

Figure 41: Comparison of fluorescence intensity and CFUs, showing a correlation between CFUs and fluorescence intensity on a log10 scale.

3.3.2 Spectroscopic detection: *Ex-situ* approach

The *ex-situ* approach relies on the sampling of bacteria, using an endodontic paper point, followed by fluorescence staining and spectral analysis. The *ex-situ* approach has the benefits of the staining and analysis occurring in a controlled environment rather than in the RC space of a patient. Additionally, this avoids any issues of biocompatibility of the fluorescent dye being used with patients. Following the characterisation of suitable stains, staining was carried out using CAM at 15 µg/ml for 5 minutes, immediately followed by spectral analysis.
Sensitivity of this detection method was evaluated by exposing mature endodontic biofilms to NaOCl for varying durations and comparing detection to the gold standard of CFU counting.

NaOCl is a commonly used irrigant solution in endodontics, classified as a chlorine-releasing agent, which has oxidising properties and has been shown to penetrate bacterial cell walls, destroy protein activity and degrade bacterial DNA (Donnell, 1999; Young et al., 2007).

Detection of vital cells in stressed biofilm

The optical biofilm sampling/detection method was compared to the gold standard of CFU counting by using nutritionally stressed biofilms, which were exposed to NaOCl for increasing durations from 0 – 200 sec. An immediate 3.4-fold drop in the calcein signal was observed after 2 sec of NaOCl exposure. As expected, increased exposure duration resulted in a further decrease of the calcein signal. However, detection of this signal remained possible for up to 40 sec of exposure with NaOCl. After being exposed for 200 sec, it dropped below to the non-vital positive control, indicating a complete loss of vitality (Figure 42a). The protocol used here was established with future clinical trials in mind. Therefore, NaOCl was chosen to be thoroughly rinsed with sterile PBS rather than neutralisation with sodium thiosulfate, as sterile saline would be readily available in clinical settings. Rinsing with sterile PBS removed a sufficient amount of NaOCl for the sensitivity of the CAM staining still to be substantially higher than that of CFU counting.

In comparison to the calcein signal, the CFU counts showed a far stronger drop (861 fold) after 2 sec of NaOCl exposure and the stressed biofilms completely lost the ability to form colonies after 15 sec of NaOCl exposure (Figure 42a). These results indicate that the bacteria within the biofilm are losing the ability to form CFUs but remain in a detectable vital state for up to 40 sec of exposure, in agreement with findings of bacteria in biofilms being vital but dormant in a non-culturable state (Shen et al., 2010, 2011).

These measurements were repeated by sampling the same biofilms with endodontic paper points and interestingly, detection of remnant vital cells was improved at low levels of detection (Figure 42b-c). These results suggest that condensing the biomass into a small surface area maximises the concentration of stained cells and increases the sensitivity of calcein detection, an advantage which would be replicated during clinical sampling of the RC.

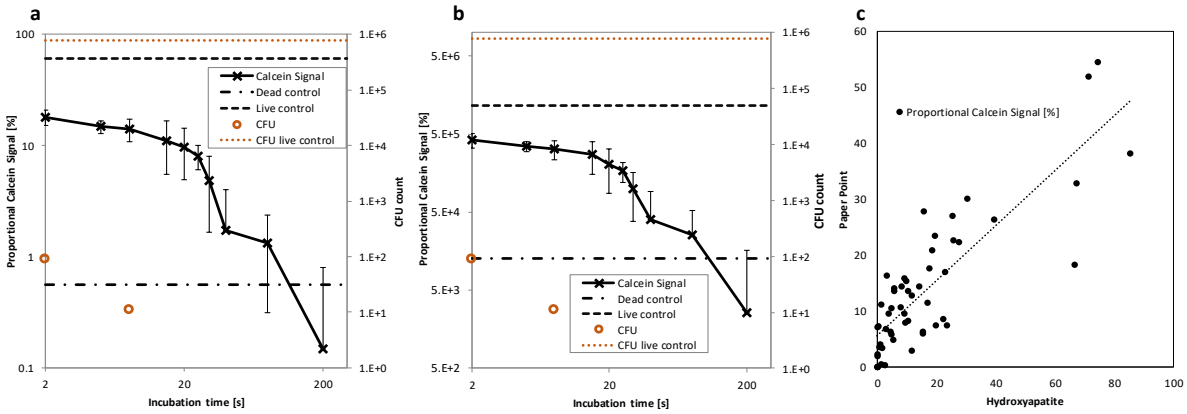

Figure 42**:** Spectral analysis of biofilms exposed to NaOCl at various incubation times. a) Direct detection in biofilms grown on HA and b) detection on endodontic paper points. Error bars represent the standard error of the mean. c) Correlation of fluorescence detection on paper points compared to direct detection on HA discs.

3.3.3 Remote spectroscopic detection: *In-situ* approach

The *in-situ* approach involves direct fluorescent staining, followed by scouting with an endoscope or fibre probe. The disadvantages are that the fluorescent dyes would need to be biocompatible due to being inserted and incubated directly in the RC space of patients. In addition, the complex morphologies of RCs pose challenges to scouting with an endoscope or probe. Remote detection, would however have the advantage of eliminating a sampling step and gaining information on the location of the detected fluorescence. Evaluated as most suitable, CAM and propidium iodide were used as a live and dead stain, respectively, for analysis with a 200 µm optical fibre cable as a probe (shown in Figure 43, setup described in section 3.2.4). The subsequently recorded spectra give information on the vitality of the biofilms. Both stains were excited simultaneously and the long pass filter allowed to capture both emission spectra to compare the ratios.

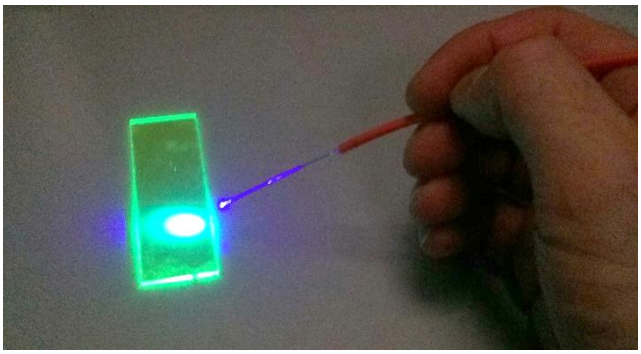

Figure 43: Optical fibre cable used for *in-situ*/remote detection, inducing fluorescence in reference material.

The autofluorescence of unstained biofilm, and HA, as well as a stained non-vital biofilm, were recorded as control spectra, to ensure the autofluorescence peaks didn't overlap/interfere with the staining. Staining of the non-vital biofilm with CAM and PI as a control demonstrated that the calcein fluorescence only occurs in vital biofilms. In addition, dentine autofluorescence was also recorded with *in-situ* application in RCs in mind. As shown in Figure 44a, the peaks of the control spectra of the HA, dentine and biofilm autofluorescence did not overlap with the CAM or PI staining of the biofilm. In the non-vital biofilm, no calcein fluorescence was detected, with only the red PI spectrum showing with a peak at around 620 nm. Figure 44b shows the ratio of the proportional calcein/PI spectra contribution, demonstrating a decrease as the duration of nutritional stress increased. In addition, the calcein intensity was shown follow a similar trend (Figure 44 c). The proportional calcein signal decrease can be attributed to the number of vital cells diminishing, due to the nutritional stress. Figure 44d-g shows the individual spectra at each time point. After 11 days of starvation, the live dead ratio stops decreasing and even showed some reversing. An explanation for this is provided by the biofilm adapting to the nutritionally starved environment: as shown previously, in reaction to poor availability of nutrition, biofilms can enter a dormant, non-growing state, which increases resistance to antimicrobial treatment (Poole, 2012). Maturity of the biofilms grown for longer periods compared to "young" ones and oxygen depletion are additional factors in biofilm resistance to antibiotic treatment (Borriello et al., 2004). These results show that CAM can detect vital cells in a nutritionally stressed and anaerobically grown endodontic biofilm model and when used in combination with a dead stain such as PI, can give ratio-metric information on the proportion of live and dead cells. Calcein detection, as used in the *ex-situ* approach, could be applied to detect remnant cells directly in the RC space. The combination of live/dead

staining and spectral analysis could lead to a faster and more flexible and user-friendly method to evaluate bacterial killing by various antimicrobial agents.

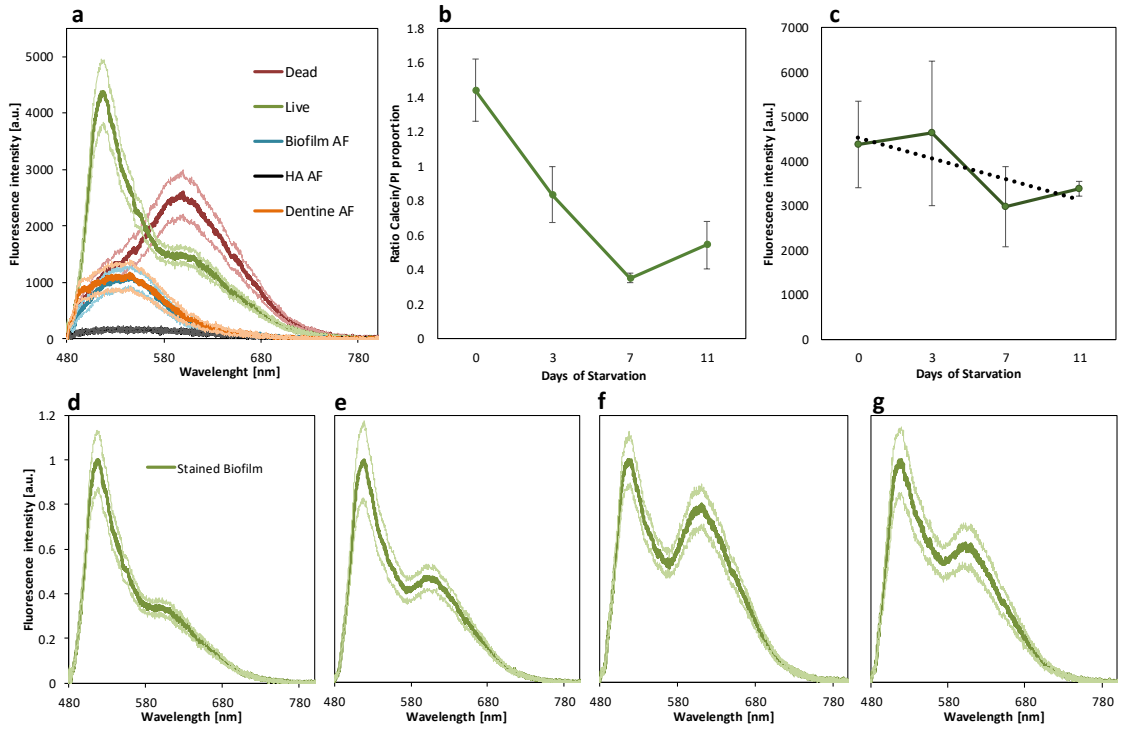

Figure 44: Remote fluorescence spectroscopy showing a) the spectra for a live and dead biofilm stained with CAM and propidium iodide, as well as the autofluorescence of the biofilm, the HA substrate and root canal dentine. b) The ratio of the CAM/PI contribution (error bars representing standard deviation). c) CAM fluorescence intensity (error bars representing standard deviation) and d) – g) the recorded spectrum (normalised to 1) as it changes over time.

Overall, CAM has been shown to be a fluorescent dye suitable for rapid biofilm staining. In addition to this, fluorescence only occurs in the presence of vital cells, avoiding false positive readings from dead cells or substrate reading, as well as negating the need for a dead cell counterstain. The use of spectroscopic analysis and curve fitting allows a more distinct detection of the calcein signal compared to fluorescence microscopy (Zimmermann, 2005; Zimmermann et al., 2003; Kraus et al., 2007; Thaler and Vogel, 2006). Characterisation of CAM on a starved endodontic biofilm combined with the successful rapid detection of vital cells using spectral analysis suggest that this method could offer a viable technique for use in clinical settings. Compared to current and proposed methods, it does not have the drawbacks of being too time consuming or lacking in an indication of the vitality of residual material in the RC space (Tan et al. 2015; Sato et al. 2012; Sainsbury et al. 2009c).

3.4 Conclusion

The *in-vitro* studies carried out in this section aimed to evaluate suitable fluorescent dyes and detection systems on a mature, nutritionally starved, endodontic biofilm, to imitate conditions in the RC space. The model biofilm chosen contained 5 bacterial strains, typically involved in reoccurring endodontic infections (Niazi et al., 2014).

Various fluorescent dyes were characterised by staining the biofilm for 5 minutes, a time chosen to be clinically relevant, to not disrupt the clinical workflow. CAM was shown be a suitable live stain, as it successfully induced fluorescence only when vital bacteria were present and showed very little to no background staining: it produced a significantly higher fluorescence ratio for both R_v and R_s. PI was the most suitable non-vital stain demonstrating a significantly higher R_d than ethidium homodimer and higher R_v than the others dyes, apart from CAM. In general, the use of stains which do not have a non-fluorescent state before being converted by cell components was shown to be challenging at such a short incubation time: higher concentrations are required and this often led to staining of unwanted non-vital cells or substrates.

The *in-situ* approach demonstrated the possibility of remote spectral analysis of rapid live/dead staining. Ratiometric analysis of the CAM and PI showed how spectral analysis could be used as a simple alternative to conventional live/dead staining, resulting in a fast and simple analysis, which could be automated. CAM was also shown to be able to detect vital bacteria in biofilms exposed to a nutritionally stressed environment for prolonged periods, which would contain dormant, anaerobic bacteria, known to be more resistant to antimicrobial treatment (Borriello et al., 2004; Poole, 2012). Furthermore, as no image is required, thin single core fibres can be used for remote measurements. In the future, with appropriate dyes, this could be a valuable tool for general *in-situ* detection of infections.

The *ex-situ* approach was also shown to be a feasible method to detect vital bacteria. Applying spectral unmixing enabled accurate quantification of both the stained biofilm and the substrate (endodontic paper point or HA disc) autofluorescence. Subjecting biofilms to 1% NaOCl with increasing durations showed that our method proved to be more sensitive to very low quantities of vital cells, compared to CFU counting. Bacterial biofilms have numerous mechanisms of reacting to environmental stress, including downregulating metabolism and entering a viable but non-culturable state not detectable by CFU counting (Shen et al., 2011;

Stewart and Costerton, 2001; Mah and O'Toole, 2001). However, as shown in Figure 3c, the bacterial metabolism was sufficient to hydrolyse CAM into the fluorescent calcein, enabling fluorescent detection, even when the cells had lost the ability to form CFUs. Detection of bacteria in stressed conditions is of great importance when aiming to detect bacteria deep within the nutrient poor RC space, where surviving biofilms may enter a non-culturable state, whilst still causing inflammation (Shen et al., 2010). *Ex-situ* staining of the samples avoids complications concerning the biocompatibility of the agents used for the fluorescent staining, further using paper points, which are part of regular RC treatments, results in a patient-friendly method, which can directly be applied in clinical settings.

Chapter 4 *Assessment of Disinfection Techniques in Peri-implantitis*

Following the previous chapters, which established the fundamentals and demonstrated the feasibility of fluorescence staining and spectral analysis in endodontic settings, we explored the possibility of expanding the range to which this methodology could be applied. Alternate uses were demonstrated by applying the methodology to the detection of vital bacteria in an implant related biofilm, following disinfection by techniques suggested for peri-implantitis treatments.

Similar to RC infections, the presence of biofilms on implants can lead to persisting infection, bone loss and ultimately treatment failure. Failure can also occur as a result of factors such as trauma, insufficient bone support, unsuitable implant design or poor oral hygiene. However, bacterial infections are considered the most important factor in implant failures (Mahato et al., 2016). Reported success rates vary, depending on definition of the treatment success and duration of the follow-up, a study by Simonis *et al.* indicated an 82.94 % success rate, however, they also reported a 48.03% complication rate, meaning patients required additional treatment, following the placement of the implant (Simonis et al. 2010).

Microbial contamination can occur either at the time of placement of the implant or by bacterial colonisation at a later stage. Peri-implantitis is defined as an inflammatory reaction leading to loss of both hard and soft tissue around the dental implant. If the bone loss around the implant is not too severe when assessed, disinfection of the infected implant and surroundings may be attempted either surgically or non-surgically, often involving a combination of mechanical and chemical disinfection (Lang et al., 2015).

This chapter aims to evaluate the potential application of the developed optical methodology to rapidly assess the antimicrobial nature of a number of disinfection methods which are used, or have been suggested to be used, in the clinical removal of biofilm formation on implants. The disinfection methods include air abrasion with bioactive glass, photo-activated disinfection, cold plasma and 1% NaoCl, which were applied to an *in-vitro* grown single species *P.gingivalis* biofilm grown on titanium discs. The treated biofilms were then analysed using spectral unmixing applied to an *ex-situ* approach using paper point sampling, an *in-situ* approach using a glass fibre cable for remote detection, as well as directly on the microscope stage, without a fibre probe. The results were then further compared to the gold standard of CFU counting, standard wide-field microscopy and OCT.

4.1 Materials and methods

Optical methods for the detection of residual vital biofilm bacteria were compared by analysing a number of disinfection techniques. Each disinfection technique was repeated for n = 5 for each optical detection method. *P. gingivalis* biofilms were grown on titanium discs for 8 days. The titanium discs containing the biofilms were then removed from the growth media and placed in 1 ml PBS in a 24 well plate (CLS3527, cell culture plates, flat bottom, Corning Costar, UK) to remove planktonic bacteria, before carrying out the disinfection treatments. Following disinfection, the discs were again rinsed with 1 ml of PBS prior to staining. Statistics were performed using a one-way ANOVA test with the Holm-Sidak method. An overview of the used detection and disinfection methods is illustrated in Table 11.

Table 11: Experimental overview: Detection methods in grey boxes and disinfection treatments in white (Abbreviations: Sodium hypochlorite (NaOCl), Photoactivated disinfection (PAD), Phosphate buffered saline (PBS)).

Disinfection methods	NaOCl	Air Abrasion	Cold Plasma	PAD	PBS
Detection methods	Fluorescence imaging (on disc and paper point)				
	Spectroscopy (on disc and paper point)				
	Remote Spectroscopy				
	Optical Coherence topography				
	CFU counting				

4.1.1 Establishment of *in-vitro* implant biofilm

For the *in-vitro* studies involving biofilm removal in peri-implantitis, a monospecies biofilm consisting of *Porphyromonas gingivalis* was chosen, due to its association with implant infections (Persson and Renvert, 2014; Portillo et al., 2013). *P. gingivalis* monospecies biofilms have been used in previous implant related studies (Di Giulio et al., 2015; Amoroso et al., 2006; Papaioannou et al., 2012). *P. gingivalis* (ATCC 33277) isolates were revived from - 80˚ C and cultured at 37˚ C in a MACS-MG-1000-anaerobic workstation (80% N, 10% H, 10% $C0_2$) on FAA plates. Following 8 days of growth, the bacterial colonies from each strain were transferred to 9 ml of mFUM using 3 µl culture loops (one loop per 3 ml). Following 3 h of anaerobic incubation the bacterial inoculum was adjusted to a standard concentration by measurement of

the optical density (OD_{600} = 0.5). The HA discs were replaced with grade 5 Ti-6Al-4V Titanium discs (9 x9 mm), which were sandblasted to an average surface roughness of Ra = 2 µm, confirmed by confocal microscopy. Sandblasting was carried out using aluminium oxide (Al_2O_3) particles of 93 µm size (Medivance Instruments Ltd, UK) as has been used for the roughening of commercial implants, where Ra values in the range of 0.5 µm to 6 µm are achieved. (Alla et al., 2011). An Aquacut Quattro unit (Velopex International, UK) was set up with the nozzle at 3 cm distance from the titanium discs, which were held in place using forceps, during abrasion for 10 sec. Following this, discs were rinsed and sonicated in acetone for 10 mins before autoclaving at 121°C for 30 minutes, after which the surface roughness was confirmed again. The sterile titanium discs were then anaerobically incubated with 5 ml of saliva in petri dishes, for preconditioning with a salivary pellicle. Saliva was collected from 3 healthy volunteers without any carious lesions. Following consent (REC Reference Number: BDM/12/13-54) and collection, the saliva was centrifuged at 6000 rpm for 20 minutes and filter sterilised (0.2µm, 190-2520, Nalgene Syringe Filter, Thermo Scientific, UK). Following the preconditioning, excess saliva was removed and the bacterial inoculum was seeded for anaerobic growth. mFUM growth media was exchanged every 48 hours for 8 days. The longer 48-hour interval between the exchange of growth medium was chosen to avoid disruption of the biofilm. Being a late coloniser, it was found that even in the presence of a pellicle the biofilm took more time to adhere to the discs (Kolenbrander et al., 2006).

Confirmation of vital biofilm presence

Following the growth of the *P.gingivalis* biofilm on the titanium disc, using sterile forceps, the discs were placed into 1 ml PBS in 24 well plates (CLS3527, cell culture plates, flat bottom, Corning Costar, UK) to remove planktonic bacteria, before being placed in 0.5 ml of 15 µg/ml of CAM for 5 min in the dark, for vital staining. After a final rinse in PBS, discs were inverted and placed into a glass bottom well plate (662892 24-SensoPlate, Greiner Bio-One, Austria). Confocal microscopy was carried out, taking Z-stacks at 1 µm intervals, to visualise the presence of the biofilm. CAM staining confirmed the cells in the biofilm to be vital. An inverted confocal microscope (DM IRE2, Leica, Germany) and a 20× / 0.7 NA HC-PL-APO water immersion objective (Leica, Germany) were used. Excitation (Ex) and emission (Em) wavelengths were Ex 488 nm and Em 500 – 580 nm, repeated for n = 5 biofilms.

Confocal microscopy images confirmed the presence of a vital biofilm adherent to the discs following rinsing in PBS, as shown in Figure 45a. In addition to this, use of optical sectioning allowed us to gain information regarding the biofilm thickness, however, this must be interpreted with caution: Due to using an inverted microscope, the weight of the titanium disc is likely to affect the thickness of structures such as biofilms, which have a very high water content. Figure 45b shows the mean intensity of such an optical section including CAM fluorescence and reflection of the titanium disc. The thickness of the biofilm (32 µm σ = 25.4 µm) was established by measuring the distance from the initial reflection peak (biofilm surface) to the second more intense peak (surface of titanium disc). In addition, the fluorescence of the biofilm is shown to be highest directly under the surface, reducing towards the disc. The reduction in fluorescence intensity could be either attributed to scattering deeper in the biofilm, or, may indicate the biofilm being dislodged by physically inverting the disc and placing it into the glass bottom well plate. In order to aid biofilm adherence and formation following this, pellicles were formed on the discs before seeding the planktonic bacteria for biofilm formation.

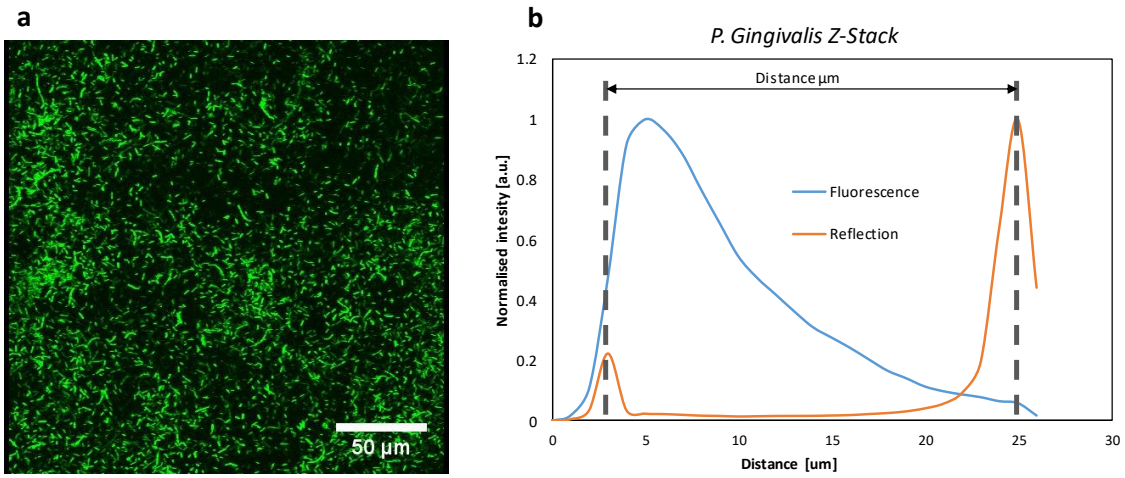

Figure 45: a) Front view of rendered 3D image confirming the presence of the vital *P. gingivalis* biofilm. b) Mean intensity of CAM fluorescence and reflection in representative optical section. For this, the offset in the PMT signal for the fluorescence and reflection was subtracted and both peaks were normalised to 1. The fluorescence peak appears to be below the surface of the biofilm (shifted to the right on the diagram), when compared to the reflection peak. This was assumed to be due to the reflection peak occurring at the surface of the biofilm, whereas a higher density of fluorescent bacteria slightly below the surface led the fluorescence peak to be shifted to the right.

4.1.2 Disinfection techniques

1) Cold plasma brush

Disinfection by cold plasma occurs predominantly by UV light and generation of reactive oxygen/nitrogen species as well as very high electric fields (Reylon Plasma GmbH, n.d.). Biofilm-covered titanium discs were removed from the anaerobic cabinet and planktonic cells were discarded by gently placing the disc in 1 ml of PBS in a 24 well plate. Discs were placed in a sterile petri dish for disinfection. Using a clamp stand, a PZ2 cold plasma brush (piezo brush® PZ2, Reylon Plasma, Germany) was adjusted for the nozzle to be set up to be at a 7 mm distance from the titanium disc containing the vital biofilm and activated for 120 seconds. As shown by Ziuzina *et al.* 120 seconds of direct exposure to cold plasma significantly reduces the amount of vital cells in a range of biofilms (Ziuzina et al., 2015). Following disinfection, the discs were transferred back into the 24 well plate for rinsing.

2) Air abrasion

Disinfection during air abrasion occurs predominantly from physical removal by air and abrasive bioactive glass particles being fired at the surface of the biofilm. Following rinsing, the discs were again placed in individual petri dishes. Using the same clamp stand, the nozzle of the air abrasion was set up to be at a 20 mm distance from the titanium disc containing the biofilm. Each disc was air abraded for 10 seconds with 53 µm bioactive glass particles (45S5,Sylc for Aquacut, Velopex International, UK). 10 seconds were chosen as this has been shown to be sufficient for plaque removal (Petersilka, 2011). The air abrasion system (Aquacut Quattro Complete, Velopex, UK) used added water flow to rinse away the expelled abrasive sylc powder.

3) Photo-activated Disinfection

Disinfection primarily occurs through production of highly reactive free radicals, which have a cytotoxic effect. Discs were placed in an empty 24 well plate in which a syringe was used to cover the biofilms with tolonium chloride (100 µg/ml), which was left to incubate for 60 seconds. Discs were exposed to red light (635 nm) for another 60 seconds, chosen in accordance with the implant disinfection settings of the device as well as the literature (Eick et

al., 2013). The light activation was delivered through the handpiece of a PAD system (Denfotex Research Ltd, UK), at a distance of 10 mm from the titanium disc. Residual tolonium chloride was again gently rinsed off with PBS.

4) Controls

As a negative control, the biofilms were removed from the petri dishes, rinsed in PBS followed by immersion in PBS for 15 mins, before rinsing again in order to simulate the conditions used in the disinfection techniques. Exposure to 1% NaOCl for 15 minutes, a commonly used disinfectant in dentistry, was used as a positive control. The use of NaOCl was chosen due to its well established anti-microbial properties, commonly used in clinics (Bürgers et al., 2012; Niazi et al., 2014).

4.1.3 Detection techniques

1) Fluorescence Intensity

Fluorescence intensity measurements were carried out on a wide-field fluorescence microscope (Zeiss Axiovert 200, Zeiss, Germany) with a FITC filter cube: Em 467 - 498 nm and Ex 513 - 556 nm, and a 506 nm dichroic mirror. Using a 10× objective (Fluar 10× / 0.5 NA Infinity/0.17, Zeiss, Germany), the intensity was calculated to be 19.24 mW/cm^2. 10 Images were taken with an integration time of 100 ms, chosen to avoid oversaturation of the camera. For each paper point, the images were taken at 500 µm intervals starting at the tip whereas on the titanium discs the 10 images were evenly distributed. Using Image J, the Images were analysed and the mean intensity was measured. Images of the paper points were thresholded before measuring the mean intensity, as the paper point did not cover the whole field of view. The threshold was set to discard the background (absence of paper point). Using the same principle outlined in section 3.2.2 and Figure 24, a selection was created to measure only the fluorescence intensity of the area where the paper point was present.

2) Spectral Analysis (on disc and paper point)

Spectral analysis and unmixing on the discs and paper points was carried out as using the *ex-situ* spectroscopic approach as previously described in section 3.2.3. The base spectra used for detection on the discs directly are shown in Figure 46, whereas base spectra applied to detection on paper points are shown in Figure 47. The fluorescence spectra recorded from the paper points vary slightly, hence multiple paper point spectra were used as base spectra for the

unmixing. The base spectra for the porphyrin autofluorescence was measured directly from the biofilms which exhibited it. Measurements were again taken from 10 different areas, as done for the fluorescence intensity analysis. Where paper points were used, the biofilms were sampled from the disc by rubbing the paper point parallel over the entire surface of the titanium disc, ensuring the tip of the paper point was in line with the edge of the disc

3) Spectral Analysis (remote)

Remote detection was accomplished using the same setup as above, with addition of a single core glass fibre cable (Ø 200 µm, 0.22NA SMA step-index multimode Fibre Patch Cable, Thorlabs, UK), which was coupled to the 10× microscope objective on one side On the other side the SMA connector was removed and the cable was declad, revealing a Ø 200 µm fibre core (as described in section 3.2.4). The base spectra shown in Figure 46 were used for the curve-fitting. In all cases 10 spectra from different areas of the titanium disc were taken, by probing the biofilm with the tip of the fibre core at a 45° angle (a 90° angle was avoided, so as not to displace the contacted biofilm when lowering the fibre down onto the disc).

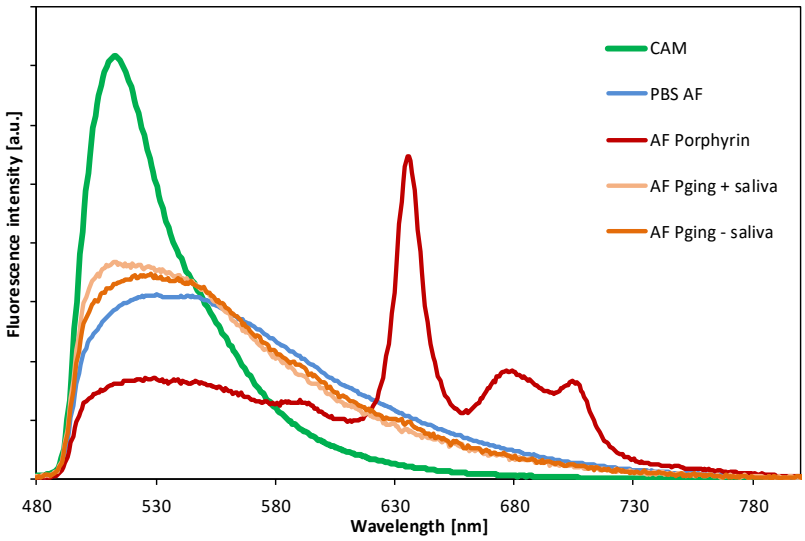

Figure 46: Base spectra used for spectral un-mixing of spectra recorded from analysis on the disc directly as well as remotely. Containing spectra recorded from *P. gingivalis (Pging)* biofilm autofluorescence (AF), porphyrin-like autofluorescence, PBS autofluorescence and converted Calcein AM (CAM).

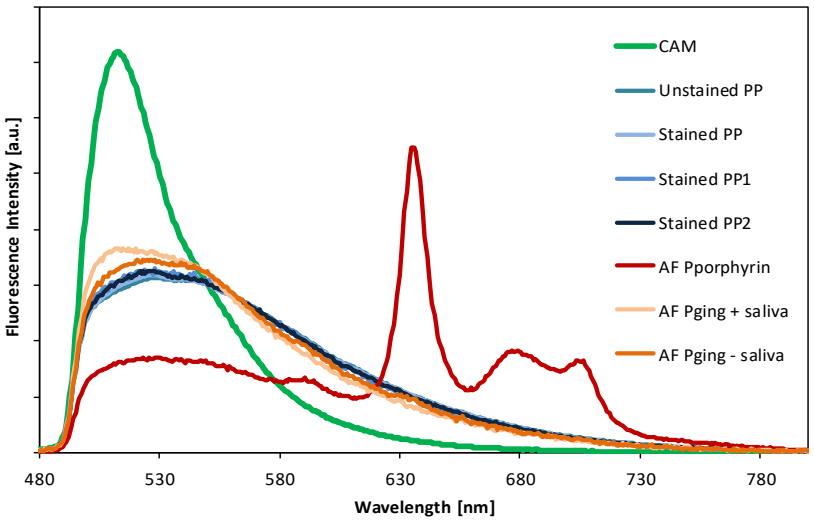

Figure 47: Base spectra for paper point analysis. Spectra recorded from paper points (PP) samples, biofilm autofluorescence (AF), porphyrin-like autofluorescence and converted Calcein AM (CAM)

4) CFU counting

CFU counting was achieved by placing the entire disc or paper point into a bijou tube (03440, Greiner Bio-One, UK) with 1 ml of BHI (CM1135, Oxoid, UK), followed by vortexing for 30 seconds. Dilution series were carried out and 100 µl aliquots were plated on FAA plates for anaerobic growth. After 10 days the FAA plates were removed from the anaerobic cabinet, CFUs were checked for typical black *P. gingivalis* morphology and counted.

5) Coherence Tomography (OCT)

OCT measurements were carried out using a VivoSight multi-beam system (VivoSight, Kent, UK) operating at 1305 nm, 10 kHz rate and 15 mW on a 6 x 6 mm field. The y-axis was adjusted to 4.06 µm steps, chosen to match the pixel size of the x-axis. The vertical (z) pixel of the system is dependent on the refractive index of the material examined; 4.06 microns in tissue with n = 1.35, and 5.48 microns in air with n = 1.0. Given that the biofilms were immersed in PBS, which has a similar refractive index to tissue, it can be assumed to be close to 4.06 microns (Diéguez et al., 2009).

The biofilm thickness was calculated by taking measurements from 5 different areas for each disc. Thickness from each area was measured using the straight line tool in Image J (Schneider et al., 2012). Each measurement area was added to the ImageJ ROI (region of interest) manager and was applied to all the samples, to ensure unbiased measurements,

resulting in an average for each disc (5 discs per disinfection treatment) which was used to calculate the overall average thickness for each treatment.

4.1.4 Vital Staining

Following disinfection of the discs, they were rinsed twice in 1 ml PBS in a 24 well plate. For both the fluorescence imaging and the micro-spectroscopy (including remote detection) the discs were then stained in 24 well plates with 0.5 ml CAM staining solution of 15 µg/ml for 5 mins in a dark environment at 37.5˚ C, they were then rinsed in PBS a final time. Fluorescence intensity measurements and spectral detection required the discs to be transferred directly onto a glass bottom well plate (662892 24-SensoPlate, Greiner Bio-One, Austria) for analysis. For the spectral analysis on the paper point the treated biofilms were sampled from the discs with endodontic paper points (F2 ProTaper, Dentsply, UK) which were then stained in Eppendorf tubes with 0.5 ml of the CAM staining solution for 5 mins in a dark environment and then transferred to the glass bottom well plate for analysis. The samples for the remote spectral analysis were stained in the same manner as the other discs and placed into a petri dish to be analysed using the fibre probe.

The one-way ANOVA test with the Holm-Sidak method was performed to compare results for each method and determine significance. Averages and standard deviations are given of all the measurements, with addition of the range for the CFU counts.

4.2 Results and Discussion

4.2.1 Culturing/CFU counting

Treatment methods were compared by anaerobically culturing biofilms, immediately following treatment. After 14 days, *P. gingivalis* colonies were counted. Figure 48 shows the typical black morphology of *P. gingivalis* CFUs on a FAA plate.

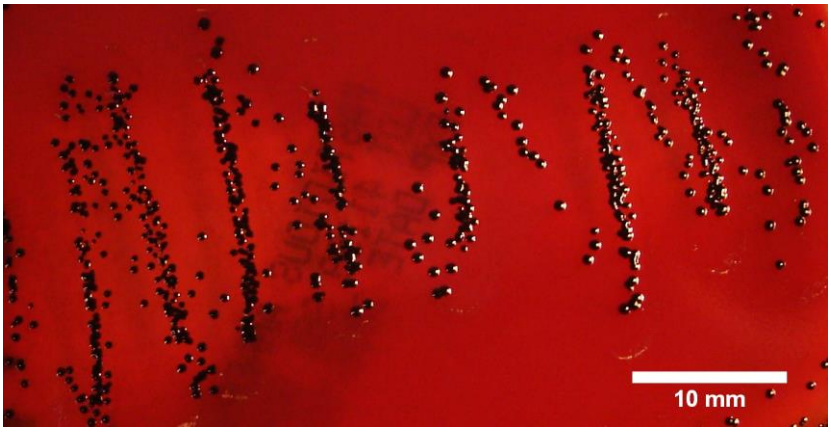

Figure 48: *P. gingivalis* CFUs, recognisable by distinct black morphology.

Compared to the negative control (treatment with only PBS), there was a significant decrease in the number of CFUs in all the treatment methods ($p<0.001$). Treatment with air abrasion resulted in lower CFU counts compared to both the negative control and the other treatment methods, however, not to a statistically significant difference ($p = 0.206$). The positive control, treatment with NaOCl for 15 minutes, resulted in a complete absence of CFUs, as was expected (Figure 49a, b). The choice of NaOCl as a positive control was based on its broad bactericidal effectiveness (Bürgers et al., 2012). Culture methods are established techniques to evaluate the effect of antimicrobial treatments (Bago et al., 2013; Eick et al., 2013; Kim et al., 2009). However, culturing and plate counting does come with the disadvantage of lengthy growth periods (up to weeks) and results must be seen with caution: there is a potential of false positive disinfection results, due to non-culturable cells which remain in a vital state (Sathorn et al., 2007; Li et al., 2014).

a

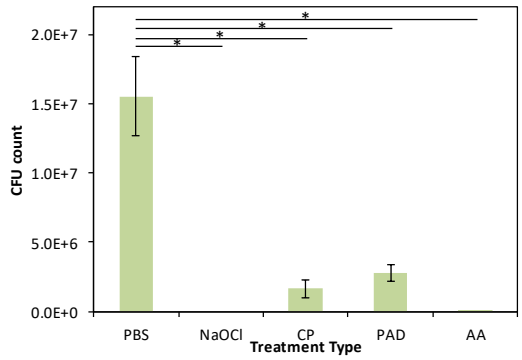

b

Treatment	Average [CFU/ml]	Standard deviation	Range
PBS	1.55×10^7	6.4×10^6	1.63×10^7
NaOCl	0	0	0
CP	1.65×10^6	1.46×10^6	3.73×10^6
PAD	2.76×10^6	1.31×10^6	30.9×10^6
AA	19	10	23

Figure 49: CFU count following treatment with disinfection techniques a) Bar graph with the average and standard error of the mean b) Average counts with the standard deviation (*p<0.001). Abbreviations: Phosphate buffered saline (PBS), sodium hypochlorite (NaOCl), cold plasma (CP), photo-activated disinfection (PAD), air abrasion (AA)

4.2.2 Fluorescence microscopy and spectroscopy

Using an inverted wide-field fluorescence microscope with a coupled spectrometer, fluorescence intensity measurements and fluorescence spectroscopy with unmixing were carried out on paper points, after sampling and staining residual biofilms from the discs. A wide-field fluorescence image of a stained paper point sample is depicted in Figure 50.

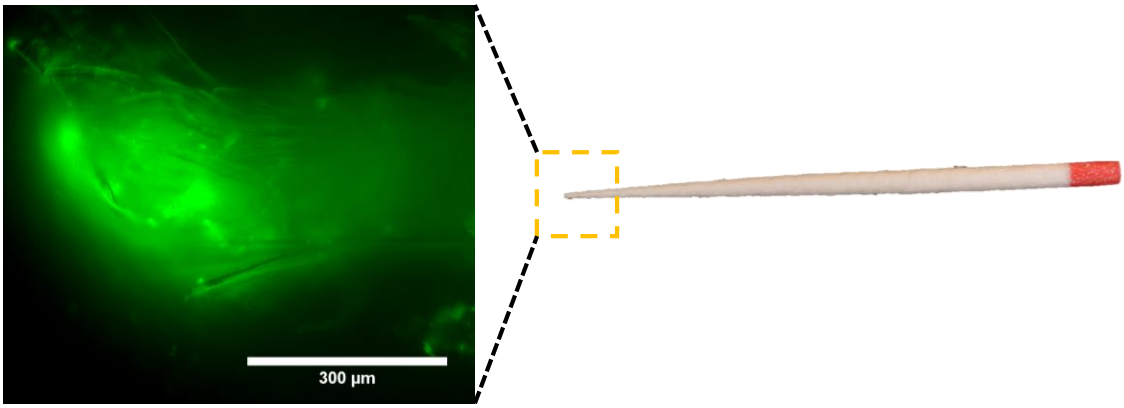

Figure 50: Representative fluorescence wide-field image of stained paper point tip from a control PBS sample, taken with a Zeiss Axiovert 2000.

Figure 51a shows the calcein signal following spectral unmixing. Interestingly, compared to the CFU counting results, the signal following PAD was a lot closer to the negative control. Cold plasma treatment, however, resulted in a significantly lower signal than both the PAD and negative control ($p<0.001$). The air abrasion treatment again resulted in the lowest calcein signal, significantly lower than both the negative control and the other treatment methods ($p<0.001$), but produced a slightly higher signal than the positive control (NaOCl) (Figure 51a, b).

Calcein fluorescence intensity measurement from images taken using the FITC filter cube produced similar results: a significantly lower signal after all disinfection treatments ($p<0.001$), comparatively high fluorescence intensity signal for the sampled treated with PAD, decreased fluorescence intensity for the cold plasma treatment and significantly lower fluorescence signal for the air abrasion treatment compared to the other treatments ($p<0.001$) (Figure 51c, d). A higher signal was detected in the positive control, when compared to the spectral analysis, which can be attributed to autofluorescence or bleed-through. The intensity measurements rely on the green light allowed through the filter set of the FITC filter cube, whereas the spectral analysis can identify the specific calcein spectrum. Both the fluorescence intensity measurements and the spectral analysis of the sampled bacteria result in signals much higher for both the cold plasma and especially the photo-activated disinfection when compared to the CFU counting. The sampling technique may offer an explanation for this: all the biomass of the remaining biofilms, including all the vital cells and fluorescent calcein are accumulated in one area on the surface of the paper point, thus resulting in a dense accumulation of the fluorescent material leading to higher fluorescence intensity.

a

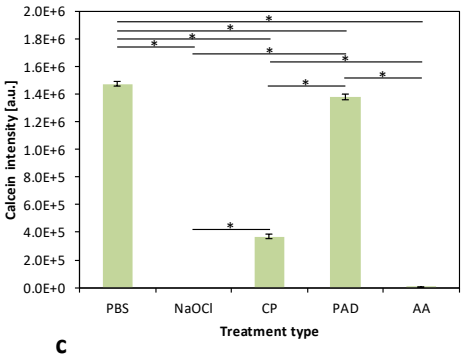

b

Treatment	Average signal	Stdev
PBS	1.48×10^6	3.24×10^4
NaOCl	0	0
CP	3.68×10^5	4.01×10^4
PAD	1.38×10^6	4.31×10^4
AA	1.19×10^3	1.56×10^6

c

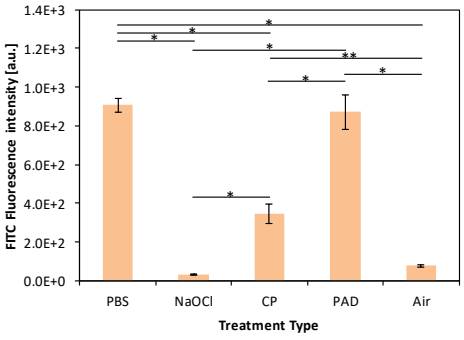

d

Treatment	Average fluorescence	Stdev
PBS	908.03	79.87
NaOCl	32.30	9.08
CP	346.96	115.26
PAD	870.31	201.78
AA	76.20	10.62

Figure 51: Spectral and imaging results from paper point sampling a) CAM average signal intensity results from spectral un-mixing with the standard error of the mean, b) Average signal with the standard deviation. c) Average calcein fluorescence intensity measured using FITC filter set with the standard error of the mean and d) Average calcein fluorescence intensity measured using FITC filter set with the standard deviation (*$p<0.001$, **$p<0.005$).

The same procedure was repeated by analysing discs placed face-down in an imaging well plate directly (Figure 52 shows the fluorescent image of a biofilm on the titanium disc). Spectroscopic analysis showed a significantly lower calcein signal intensity for all the tested treatments, compared to the negative control ($p<0.001$). Treatment with air abrasion again resulted in a significantly lower signal than all the other treatment methods ($p<0.001$) (Figure 53a, b). The fluorescence intensity measurements (image shown in Figure 52) of the same samples resulted in similar results, with all the treatments resulting in significantly lower intensity than the negative control and air abrasion lower than the other treatments ($p<0.001$) (Figure 53c, d). Interestingly, the spectral detection of the calcein signal post cold plasma treatment was lower than for the photo-activated disinfection (Figure 53a) whereas for the calcein fluorescence intensity measured with the FITC filter cube, this was the other way around (Figure 53c). Given that the readings were taken from the same samples, this is an unexpected result. Spectral analysis of unstained biofilms of the same batch revealed an autofluorescence spectrum with a strong, narrow peak at 635 nm (labelled as AF Porphyrin in Figure 46): the strong red fluorescence peak led to the assumption of this being porphyrin fluorescence. Porphyrin fluorescence has been researched, amongst other fields, in the context of tumour diagnosis (Ebenezar et al., 2015; Ando et al., 2011) where Protoporphyrin XI is one of the markers. Indeed, the spectrum shows the same intense peak at 635 nm as was recorded in this study (Ando et al., 2011; Ehrhardt et al., 1998). Bacteria have long been known to possess enzymes able to produce Protoporphyrin XI (Masataka & Seiyo 1971; Jacobs et al. 1970). Protoporphyrin is the last intermediate in the production of heme and as shown by Dietel *et al.,* bacteria in the oral cavity and digestive tract readily produce fluorescent protoporphyrin, especially in the presence of aminolaevulinic acid (Dietel et al., 2007). Figure 53a shows the intensity of this porphyrin fluorescence to be, in the case of the cold plasma treated sample, stronger than that of calcein. The porphyrin signal emits at its strongest in the red, however, it does also emit in the green, leading to the increased signal for the calcein fluorescence intensity measured when using the FITC filter cube.

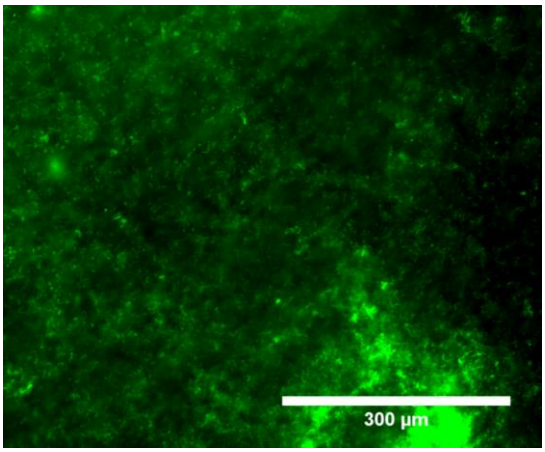

Figure 52: Representative fluorescence wide-field image of stained biofilm on titanium disc from PBS sample, taken with a Zeiss Axiovert 2000.

The strong presence of this autofluorescent signal after the cold plasma treatment could be as a result of the treatment heating up and drying out the biofilm – in effect condensing the material, resulting in less of it being removed during the rinsing steps. Another question to be addressed is why does this protoporphyrin autofluorescent spectrum appear in this batch of biofilms, where it is absent in others. *P. gingivalis* has not been shown to produce red autofluorescence and initial autofluorescence measurements showed a weak broad green spectrum (Figure 46). Research conducted by Van Der Veen et.al demonstrated that *P. gingivalis* indeed does not produce any red autofluorescence on its own, yet when in contact with other species of bacteria it can induce red autofluorescence (Van Der Veen et al., 2006). Reverting to the research protocol showed that the 0.2 µm filters used for the sterilisation of the saliva were purchased from a different manufacturer for this experiment (Pall Life sciences instead of Thermofisher). Follow up culturing of *P. gingivalis* biofilms using salivary pellicles incubated with saliva filtered with these filters resulted in the presence of the distinct black *P. gingivalis* CFUs, but also the addition of white morphologies, indicating the presence of other species introduced through the saliva. The discrepancy between the calcein fluorescence intensity measurements using the FITC filter cube and the spectral detection of the calcein signal demonstrates one of the advantages of spectral analysis when detecting a specific fluorescent dye/signal. The calcein intensity measurements, taken using the FITC filter cube, are affected by any fluorescence present, the bandwidth of which is limited by the emission filter. Within this bandwidth, however, there is no differentiation. In this case, it resulted in an increase in the green fluorescence intensity of the samples analysed after cold plasma

treatment. Using standard fluorescence microscopy, this signal would be interpreted as a stronger green fluorescence intensity produced by the CAM staining, thus skewing the results, whereas using spectral unmixing, we can determine that the fluorescence increase is in fact due to an occurrence of an overlapping autofluorescence signal.

a

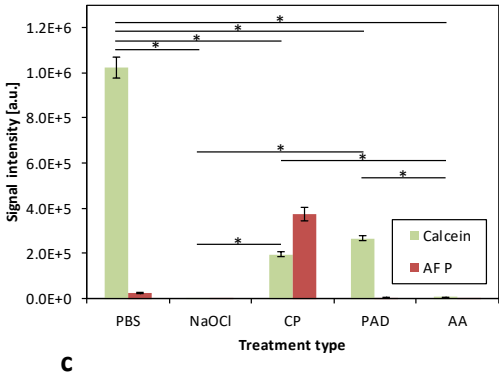

b

Treatment	Average signal	Stdev
PBS	1.02×10^{6}	1.04×10^{5}
NaOCl	6.45×10^{1}	1.1×10^{2}
CP	1.96×10^{5}	2.44×10^{4}
PAD	2.67×10^{5}	2.12×10^{4}
AA	6.6×10^{3}	4.7×10^{3}

c

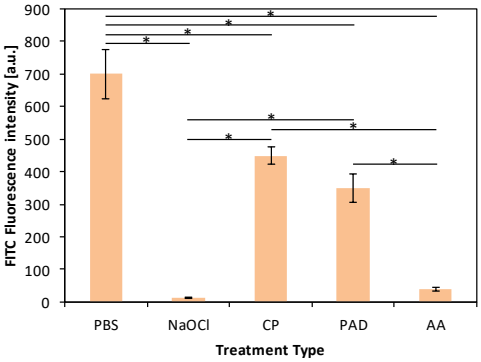

d

Treatment	Average fluorescence	Stdev
PBS	700.09	169.39
NaOCl	11.87	3.71
CP	449.08	56.89
PAD	350.08	98.35
AA	38.94	12.01

Figure 53: Spectral and imaging results from the discs directly a) CAM average and porphyrin autofluorescence (AF P) signal intensity results from spectral un-mixing with the standard error of the mean, b) Average signal with the standard deviation. c) Average calcein fluorescence intensity measured using FITC filter set with the standard error of the mean, d) Average calcein fluorescence intensity measured using FITC filter set with standard deviation (*p<0.001).

Remote spectroscopic analysis also showed a significantly lower fluorescent signal ($p<0.001$) for all of the treatments compared to the negative control. Treatment with air abrasion also led to a significantly lower signal when compared to the other treatment methods ($p<0.001$) (Figure 54). Unlike the other fluorescence detection methods, the remote method detected a higher calcein signal in the biofilms that were treated with cold plasma than those treated with photo-activated disinfection. High signal following cold plasma treatment could be explained due to the manner in which the probe was used to collect the signal on the titanium discs: the fibre probe physically contacted and penetrated the biofilm on the disc at a 45^{o} angle in 10 different areas. The single species biofilm itself is not very structurally strong, as in a natural biofilm formation *P. gingivalis* is a late coloniser, involved in multispecies biofilms (Kolenbrander et al.,

2006). The nature of the cold plasma treatment dries the biofilm and appears to make it more compact and adherent to the titanium disc. Stronger adherence to the disc is relevant in this case as, in addition to the physical probing, discs incubated in PBS had transported to the testing setup (for other methods the biofilms were directly placed into the imaging well plates following staining and rinsing). The potential physical strain by transportation and probing would therefore be less likely to affect the biofilm following cold plasma treatment.

a

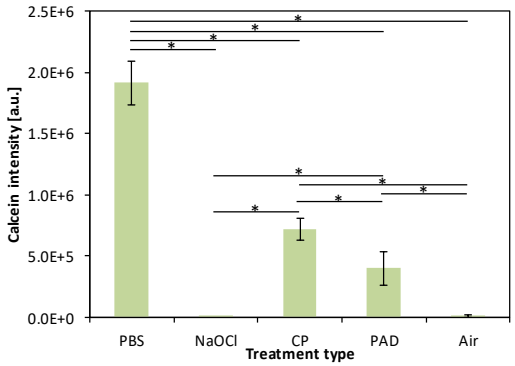

b

Treatment	Average signal	Stdev
PBS	1.91×10^{6}	1.78×10^{5}
NaOCl	3.14×10^{1}	1.77×10^{2}
CP	7.2×10^{5}	9.35×10^{4}
PAD	3.99×10^{5}	1.35×10^{5}
AA	6.36×10^{3}	9.84×10^{3}

Figure 54: Spectral results from remote fibre detection a) CAM average signal intensity results from spectral un-mixing with the standard error of the mean, b) Average signal with the standard deviation (*p<0.001).

Using the culturing as well as all of the fluorescence based methods described here, remnant vital bacteria were detected following treatment with PBS as the negative control, as well as after all of the other treatments. The positive control of the NaOCl treatment resulted in a complete lack of CFU counts and in general very low signal from the fluorescence-based techniques. Calcein fluorescence intensity measurements using the FITC filter generally showed similar results to the spectral analysis. However, for the positive control which had an absence of calcein signal, despite the post recording removal of the general background noise, a false fluorescence signal was detected, potentially due to the bleed-through of the excitation light after reflection from the titanium disc. A further drawback when just measuring the fluorescence intensity was shown where a significant autofluorescence signal was present (Figure 53), leading to an artificial increase in green fluorescence, which would be interpreted as calcein fluorescence, thus giving false results. Using spectral analysis, a much more precise detection of the fluorescent signal is possible(Zimmermann, 2005; Thaler and Vogel, 2006; Kraus et al., 2007). By adding the autofluorescent signal to the base spectra before spectral unmixing, this error was identified (Figure 53a). Any potential presence of unexpected spectra can easily be identified by monitoring the fitting residuals. Detection after applying the

disinfection techniques using the fluorescence-based methods was generally higher when compared to CFU counting, possibly as a result of some bacteria having entered a non-culturable state as well as an effect of the imaging and sampling techniques.

The spectral analysis techniques were able to show detection of bacteria after all of the disinfection techniques after a 5-minute incubation period in CAM, providing a much more immediate method for detection, which was more sensitive in detecting the source of a fluorescent signal than conventional fluorescence imaging/intensity measurements. The use of such a method in a regulated *in-vitro* study could be highly automated, negating the need for a trained microscopist to evaluate images. Other *in-vitro* studies investigating the efficacy of various antimicrobial treatments frequently rely on CFU counting or conventional live/dead staining and imaging techniques, or a combination thereof (Bürgers et al., 2012; Eick et al., 2013; Gosau et al., 2010; Rupf et al., 2011). Whilst these are very effective methods, especially when used in combination, they do have downsides: CFU counting, as previously mentioned, is very time-consuming and can be misleading for non-culturable bacteria. Live/dead staining and fluorescence microscopy requires experience in both acquisition and analysis of images. Using simple wide-field illumination and software analysis of recorded spectra could present a simple time-saving alternative. Bypassing the need for an image also means simple single core glass fibre cables can be used for remote detection of fluorescence, resulting in a simple and versatile technique, which could lead to the development of a handheld device.

4.2.3 Optical coherence tomography (OCT)

As previously demonstrated (Xi et al., 2006; Haisch and Niessner, 2007), OCT analysis of samples allows for rapid and label-free 3D visualisation of the remnant biofilm, shown in Figure 55. The *in-vitro* monoculture biofilm grown here, resulted in a smooth structure, unlike mixed species biofilms grown in environments with potential flow creating sheer stress (Haisch and Niessner, 2007; Dreszer et al., 2014) (Figure 55a). Following treatment with both NaOCl and air abrasion, the biofilm was completely absent for most of the OCT images as shown in Figure 55b. Treatment with PAD resulted in a biofilm with a similar appearance to the negative control, however, with more signs of detachment and some disruption Figure 55c. Cold plasma treatment led to a very condensed biomass of the biofilm as well as some folds along the surface, this drastically different phenotype is likely due to the biofilm structure becoming dehydrated during the treatment Figure 55d.

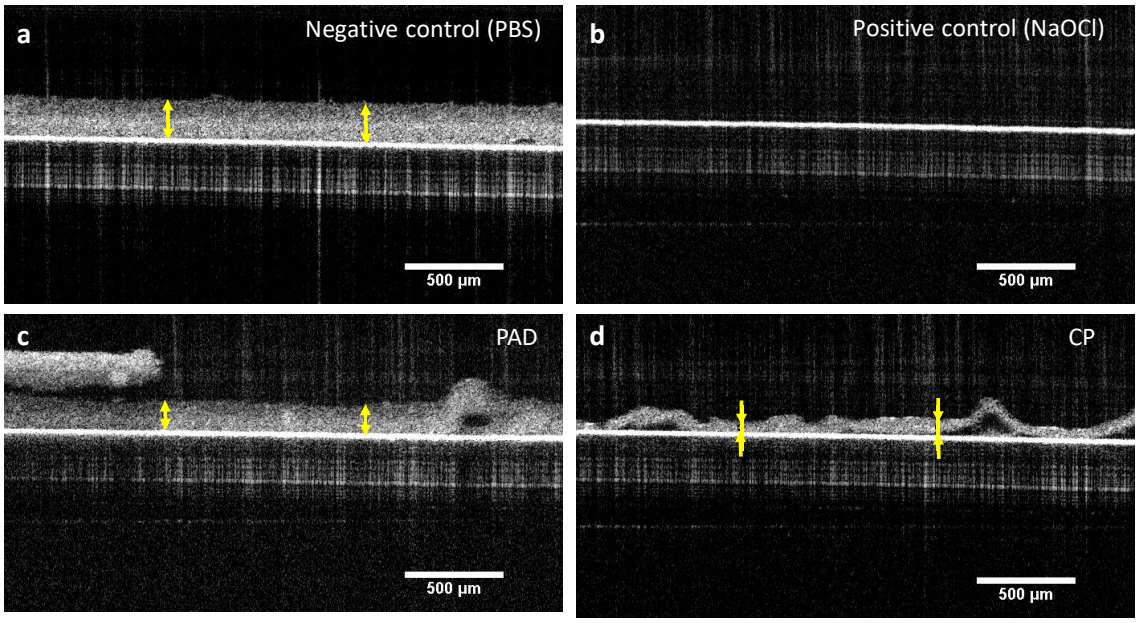

Figure 55: OCT images showing cross sections of biofilm samples after treatment, with yellow arrows indicating thickness measurements at 1000 µm intervals. a) Thick smooth biofilm after treatment with PBS, b) Lack of biofilm presence as seen in most air abrasion and NaOCl treated samples, c) Biofilm sample after PAD, showing some removal and dispersed biofilm structures on the left and d) Biofilm sample following cold plasma (CP) treatment showing a condensed biomass.

Thickness measurements carried out at the same five areas on each 5 biofilms for all the treatments resulted in similar trends as shown by the paper point sampling. Apart from the PAD, all the treatments led to a biofilm with significantly lower thickness ($p<0.001$). Treatment with air abrasion resulted in a lower biofilm thickness than the other treatments, significantly so for PBS and PAD ($p<0.001$) Figure 56a, b).

a

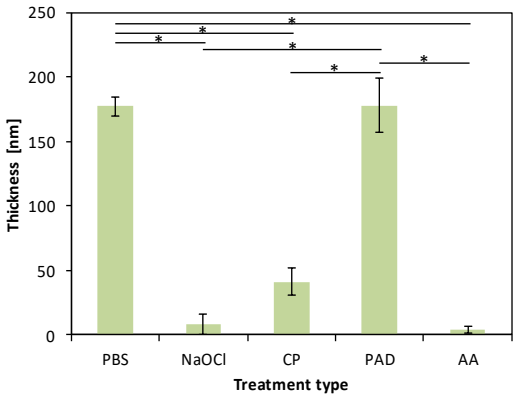

b

Treatment	Average Thickness [µm]	Stdev
PBS	177.09	15.68
NaOCl	8.08	18.07
CP	41.41	24.51
PAD	177.82	47.03
AA	4.00	5.66

Figure 56: OCT biofilm thickness measurements. a) Average thickness with the standard error of the mean, b) Average thickness with the standard deviation (*$p<0.001$).

Surprisingly, remnant structures were identified in one of the positive controls, as shown in Figure 57. Fluorescence analysis and CFU showed proportionally much lower/negligible signals for the positive control, suggesting that these remaining structures are most likely non-vital. The OCT images have the advantage of being label-free and allow for quick optical sectioning, providing a valuable technique to study biofilm growth and structure. However, as a detection method, it may be limited, as there is no indication of the vitality of the visible structures (Huang et al., 1991; Xi et al., 2006).

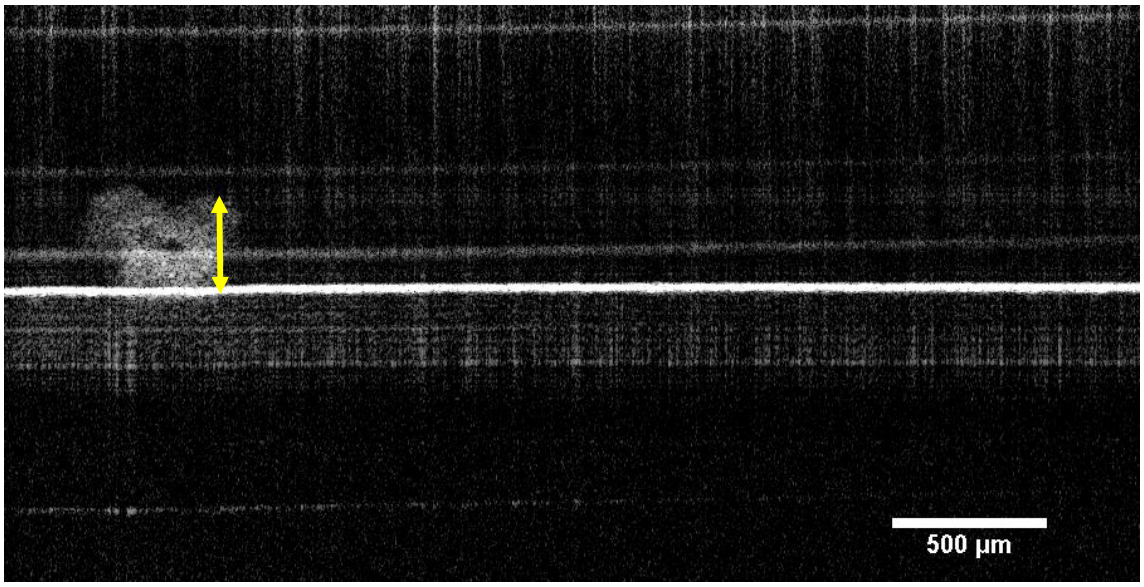

Figure 57: OCT image showing some residual biomass in one of the positive controls.

4.3 Conclusion

It is important to note that this study aimed to compare various detection methods in their efficiency to detect residual vital bacteria after disinfection procedures. Conclusions on which disinfection methods are superior in disinfection of implant-related infections must be taken with caution; incubation times and alterations to the incubation and treatment time as well as alterations in the precise application of each disinfection method would alter the outcome. Furthermore, disinfection is often carried out by combining multiple disinfection methods. As biofilm removal with air abrasion consistently resulted in lower detection throughout these studies, it can be suggested, that the element of physical removal is of great importance when attempting disinfection of biofilm-infected surfaces.

Comparison of fluorescence imaging and spectral analysis generally resulted in similar levels of detection (Figure 53). However, where the presence of an overlapping autofluorescent signal was present, the software analysis of the spectral data was able to unmix the signal using curve-fitting. The wide-field fluorescence microscopy, measuring all green fluorescence intensity within a bandwidth cannot distinguish when overlapping spectra are involved (Figure 53a). All the fluorescence methods were able to detect residual vital bacteria following the tested treatments, with a lack of signal for the positive control of NaOCl.

OCT analysis is a rapid label-free method, which provides information on biofilm thickness and structure, as shown in Figure 55 as the use of coverslips is not necessary. The optical sectioning possible with OCT provides an important tool to study biofilm growth and structures. Unfortunately, OCT does not give any information on the vitality of the biofilm structures present and has a more limited resolution compared to some microscopy techniques.

In contrast to current methods, which often rely on either culturing methods (Eick et al., 2013) or live/dead staining with fluorescence microscopy (Bürgers et al., 2012; Gosau et al., 2010; Rupf et al., 2011), the spectral detection of a calcein signal from residual bacteria can provide an immediate and user-friendly method for evaluation of antimicrobial agents.

Chapter 5 *Clinical Trial: Bacterial Detection in Root Canals*

5.1 Introduction

A ten-year study, retrospectively reviewing the outcomes of RCTs in the General Dental Services of the NHS, revealed that only 74% of RCTs pass through ten years without the need for secondary treatment or extraction (Lumley et al., 2008). The costs generated by this are substantial: in the UK alone, 1'001'675 RCTs at a cost of £50.5 million were placed in the General Dental Services. Similar costs are likely to be associated with the numerous RCTs undertaken in the private sector (Lumley et al., 2008). Similar failure rates of RCTs have also been shown in short-term prospective clinical trials, with the use of CBCT scans to assess the healing process of lesions following treatment (Patel et al., 2012).

Failure of endodontic treatment, even in cases where the treatment is of a high standard, are mostly due to the persistence of bacteria in the apical area of the root (Siqueira, 2001). As shown in a clinical study by Sjogren *et al.* as well as an animal study by Fabricious *et al.,* residual bacteria following treatment have a negative impact on the healing of teeth (Fabricius et al., 2006; Sjögren et al., 1991). Bacteria can survive in nutrient stressed and hostile conditions by adapting to life as highly resistant multispecies biofilms (Chávez de Paz, 2007). Factors including highly variable shapes and curvatures of the RC, the 'blind' nature of the treatment as well as the resistance of biofilms, lead to RCT's being a technically challenging procedure (Chávez de Paz, 2007; Peters, 2004).

Current means of detecting residual bacteria rely on subjective methods, such as the detection of clear irrigant solution, smell, a lack of dry paper points taken from the canals. Scientific or reproducible detection methods are largely limited to academic research, using methods such as CFU counting or PCR (Anderson et al., 2012; Sathorn et al., 2007; Kato, a Yoshida, et al., 2007). More recent approaches make use of autofluorescence or the detection of ATP activity. However, much like some academic research methods, these lack information on the vitality of residual bacteria or are too time-consuming to be seen as feasible for clinical use (Tan et al. 2015; Sato et al. 2012; Sainsbury et al. 2009c).

The *in-vitro* studies in Chapter 3 demonstrated the potential of both *in-* and *ex-situ* detection of vital bacteria, using CAM as a fluorescence dye to indicate bacterial vitality within a stressed endodontic biofilm. Software-supported spectral analysis provides a rapid, objective way to determine the presence of residual vital bacteria, the *ex-situ* method provided a solution

directly applicable to clinical research. Endodontic paper points, as used to dry the RC space before obturation (Pumarola-sufi et al., 1998), can be used to sample for remnant bacteria. They have the same taper as the rotary instruments used for the preparation of the RC space: combined with their absorbent nature, this makes them ideal for sampling and, by capitalising on otherwise discarded material, no additional time is spent.

To confirm the transition of the *in-vitro* studies into a clinical setting, a clinical trial (n = 53) was carried out, with samples taken at three time-points throughout treatment. Where patients gave additional consent, a cone-beam computer tomography (CBCT) scan was taken before treatment and after one year as a follow-up, in order to verify the relevance of the presence of detectable levels of residual bacteria at the end of the treatment.

5.2 Materials and methods

5.2.1 Sampling and analysis

Following ethical approval (REC ref: 05/Q0705/051), patients (n = 53) undergoing primary RCTs were selected and informed consent was obtained for the sampling of the RC space. The teeth included in the study had been referred to a specialist centre for the treatment of endodontic infection. They all responded negatively to vitality tests and presented pre-operative apical radiolucencies. The source population were adults aged 18-65, referred by their general dental practitioner into specialist endodontic clinics of Guy's Hospital, King's College London Dental Institute. Both single- and multi-rooted teeth were included in the study. Treatments on the 53 teeth (114 roots) were carried out by a total of 19 postgraduate endodontic students. In addition, informed consent was obtained for a follow up study using CBCT to assess the success of the treatment one-year post-treatment (REC ref: 08/H0804/79). As outlined in the patient information sheet (see appendix) the danger of harm occurring from the CBCT scan is very low as the radiation dose of a CBCT is equivalent to 3-4 days of background radiation.

Endodontic paper points were used to sample the RC space at three time-points during treatments: immediately after accessing the RC space, at the midpoint of the treatments (after shaping with shaping file S2, ProTaper universal, Dentsply, UK) and immediately pre-obturation. Therefore, where the treatment was carried out in multiple visits, the final sample was taken during the last visit. Pre-treatment, the mouth was disinfected using 0.2% chlorhexidine, followed by placement of a rubber dam, disinfected with 1% NaOCl to avoid contamination of the samples. Before sampling with the paper points the RC space was thoroughly rinsed out using a sterile saline solution, in order to remove any remnant irrigant solutions used during treatment (1% NaOCl and EDTA). Each canal was then sampled with 2 paper points; the first one to remove excess moisture and the second one with the sole purpose of sampling. The sampling protocol given to practitioners is described in the appendix.

Immediately after sampling, the paper points were stained in eppendorf tubes containing optimal concentrations of CAM (15 µl/ml) and incubated for 5 minutes at room temperature in a dark environment, before rinsing with sterile PBS. For every sampled tooth, stained sterile paper points were also tested as a quality control. Finally, the paper points were pressed between two sterile microscope slides (N/A131, Thickness 1-1.2 mm, Academy, UK),

removed and transferred into glass bottom well plates. Slides were checked and showed only minimal transfer of fluorescent material. 20 spectral readings were taken at 500 µm intervals, using a motorised x-y stage, starting from the tip of the paper point.

For the spectral analysis during the clinical trial, the proportion of the calcein signal, P_C (Equation 2), was used to quantify the bacterial activity (amount of vital cells) of the samples:

$$P_C[\%] = 100 \times \frac{\sum f_S}{\sum f_S + \sum f_B}$$

Equation 2

Where f_s is the fitting coefficient of the signal spectra and f_B is the fitting coefficient of the signal spectra. The proportional calcein signal (P_C) was made use of throughout the clinical trial and for simplicity, will be referred to as 'calcein signal'. The base spectra used for the spectral unmixing of these patient samples are shown in Figure 58. The use of spectral unmixing and base spectra is outlined in section 3.2.3. Multiple Background spectra (S_B) of paper point spectra were used here to get a more accurate fit, as the autofluorescence spectra of the paper point varied slightly.

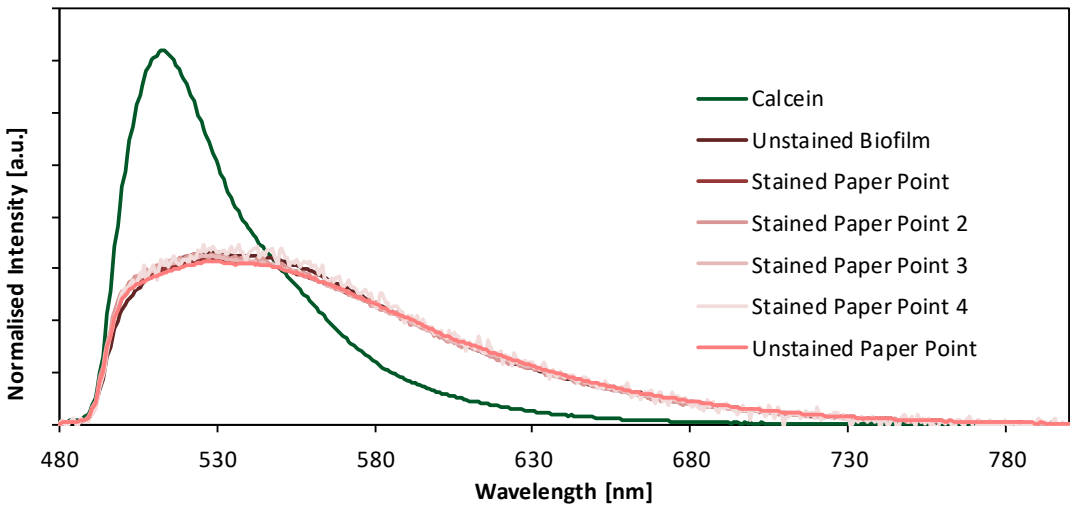

Figure 58: Normalised base spectra used for spectral un-mixing used for patient sample analysis, with signal spectra in green and background spectra in red

To establish a minimum detection threshold for vital biofilm detection, 200 spectra of 10 stained sterile endodontic paper points were recorded. The maximum calcein signal (P_C) was 2.18%. To avoid false positives, only readings recorded above twice this value (4.35%) were deemed as positive for bacterial detection (potential changes to the threshold will be discussed in 6.2).

The paper point patient samples were then transferred into eppendorf tubes containing 1 ml of PBS. Before plating on FAA plates, samples were vortexed with sterile glass beads (2 mm, Z273627, Sigma-Aldrich, United Kingdom) for 30 sec to ensure the bacteria detached from the paper points. CFU counts were then conducted on all the samples after 7 days and compared with the calcein signal.

Where statistical analysis was applied to compare experimental groups, the one-way ANOVA test with the Holm-Sidak method was performed.

5.2.2 Cytotoxic effect of CAM on CFU formation.

The number of patient samples, in which a CAM signal was detected, was compared to the number of patient samples which produced CFUs. As sampling the same RC with multiple paper points did not necessarily result in the same detection for each paper point, it was established that using the same paper point for imaging and culturing would provide a more reliable comparison. However, adverse effects of the CAM staining on CFU formation would skew this data. Three mature endodontic biofilms (as described in section 3.2.1.) were grown and nutritionally stressed for 7 days. Following this, half of the biofilm on each disc was removed using a sterile scalpel blade (Swann-Morton, Sheffield, UK) and dispersed into 1 mL of PBS, by vortexing. After serial dilution in PBS, aliquots (100 µl) were plated onto FAA plates and incubated anaerobically for 7 days, and the colonies were counted. The other half of the biofilms were incubated in 15 µg/ml CAM for 5 minutes before carrying out the same procedure of serial dilution and plating.

The effect of CAM on the vitality of bacteria in a mature endodontic biofilm is shown in Figure 59. To ensure reliable comparison discs containing the biofilms were separated into two halves rather than using separate biofilms. The results demonstrate no significant difference between the biofilms incubated in CAM for 5 minutes compared to the counterparts which were cultured directly. Nutritionally stressed anaerobically grown endodontic biofilms were used as

these conditions are common for endodontic biofilms, especially for the environment in the apical region or RCs (Chávez de Paz, 2007). The lack of significant toxic effects of CAM were confirmed on bacterial cells in mature nutritionally starved endodontic biofilms.

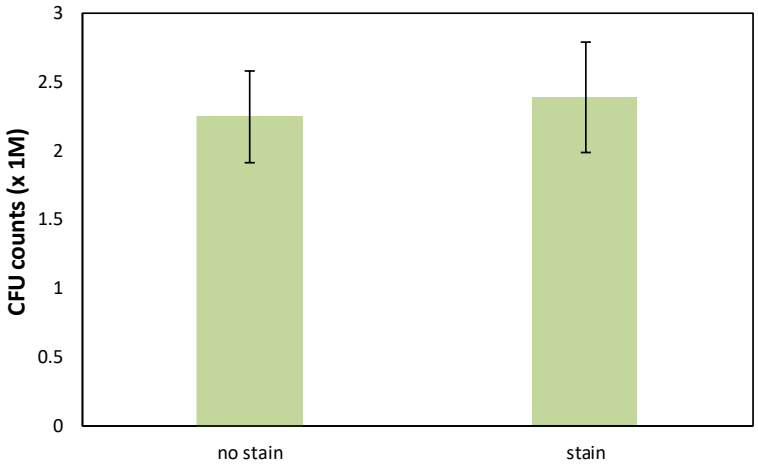

Figure 59: Comparison of E. faecalis CFUs before and after fluorescent staining, showing no significant difference. Error bars represent standard deviation.

5.2.3 Calcein AM stability and storage

The non-fluorescent CAM converts into fluorescent calcein by hydrolysis. The stock solutions are therefore recommended to be solubilised in anhydrous DMSO and stored in a frozen state. Working solutions are further diluted in PBS (established to be suitable for rapid biofilm staining at concentrations of 15 µg/ml). Once in a hydrous solution such as PBS, CAM gradually converts into calcein. For practical storage in a clinical setting, various storage methods were explored:

- Recommended storage of CAM in DMSO at -20 °C followed by dilution into working solutions in 15 µg/ml PBS directly before use.
- Storage of CAM in DMSO at 4 °C followed by dilution into working solutions in 15 µg/ml PBS directly before use.
- Storage of CAM in DMSO at room temperature followed by dilution into working solutions in 15 µg/ml PBS directly before use.
- Storage of working solution at -20 °C.
- Storage of working solution at 4 °C.
- Storage of working solution at room temperature.

All samples were stored in a dark environment and remained in an airtight container until used for imaging. 500 µl of each working solution was transferred into well-plates before imaging with blue LED excitation (M470L3 Blue, 470 nm, Thorlabs, UK) using a FITC filter cube with excitation filters of 467 - 498 nm and emission of 513 - 556 nm. Each solution was imaged after 1, 3, 14 and 30 days. Images were then analysed using ImageJ (Schneider et al., 2012), measuring the mean intensity values.

5.3 Results and Discussion

5.3.1 Detection in clinical samples

Sterile paper points identified a broad autofluorescence spectrum as shown in Figure 60a, which increased in intensity as the taper of the paper point increased (Figure 60b).

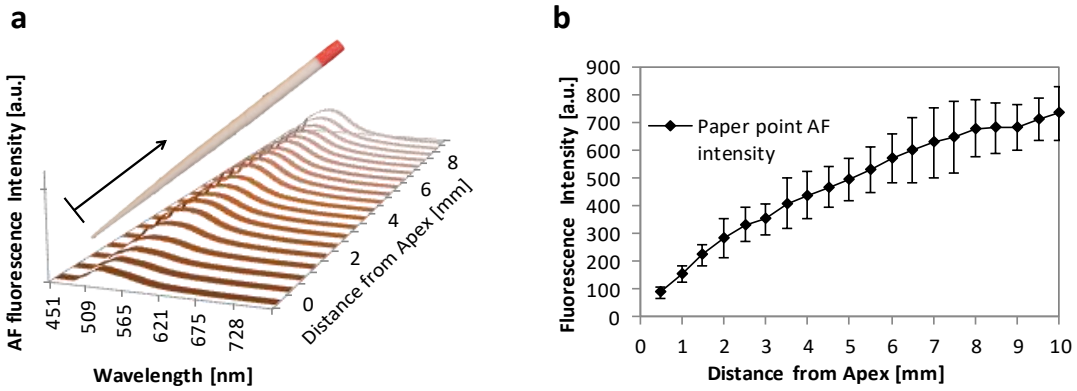

Figure 60: Characterisation of background autofluorescence: a) Example of raw paper point autofluorescence spectra. b) Increase of paper point autofluorescence intensity as the paper point taper increases.

Using endodontic paper points, samples were taken from 53 patients undertaking RCTs. The samples were tested for vital cells using the described methodology in this chapter. Detection of vital bacteria inside RCs during RCTs was carried out by sampling immediately after access (i), post shaping (ii) and pre-obturation (iii). Figure 61 shows an example of a stained sample from a clinical case with a very high calcein signal at the tip, which decreases along the paper point. The strong signal at the tip (top insert) can be attributed to a larger amount of bacteria, while further along the paper point shaft, the contribution of the background autofluorescence is dominant (bottom insert).

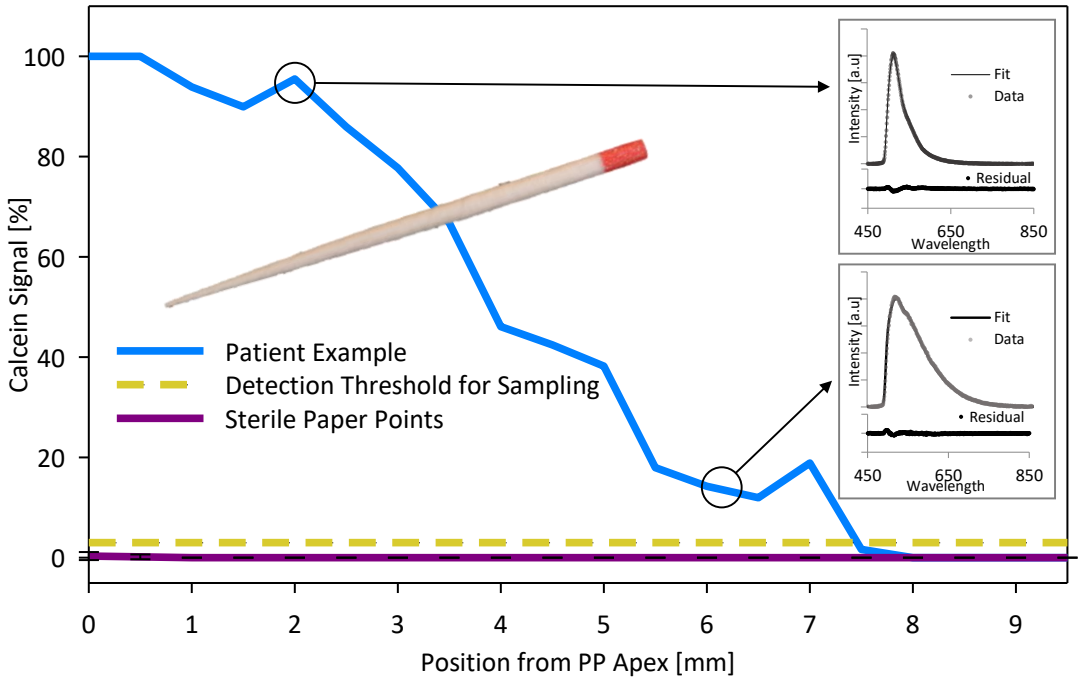

Figure 61: Signal detection from a patient sample. The spectral unmixing is shown at two different points on the patient sample. The low signal from the sterile stained paper points and the determined detection threshold for sampling are indicated.

Typically, a large amount of signal was detected in the primary sample (post access) with decreasing signal in the secondary sample (post shaping). The final sample (pre-obturation) typically produced a signal at the same level observed in the negative control. However, in some cases the calcein signal was greater than the 4.35% detection threshold, indicating the presence of remaining vital bacteria in the apex of the RC post-RCT.

Analysing the paper point samples from roots which were above the detection threshold, revealed a pattern: A high calcein signal was found at the tip of the sampled paper point. For the pre-obturation samples the tip corresponds to the apex of the root. This is in agreement with the literature, which suggests persistent infections to be located in the apical regions of the roots (Siqueira, 2001). Figure 62 shows the average calcein signal for all the pre-obturation paper points collected during this study, both for ones above and below the detection threshold.

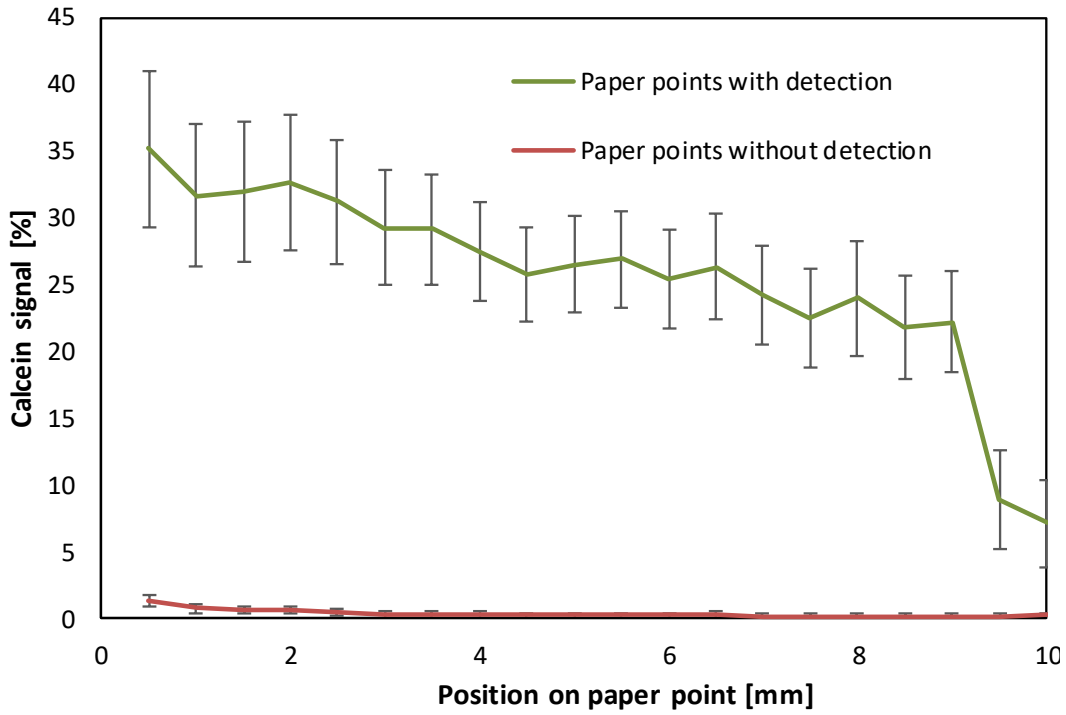

Figure 62: Average unmixed calcein signal shown for paper point patient samples with detection over and below the detection threshold, respectively. As this is the proportional value, it is, in effect, relative to the autofluorescence of the paper point. Error bars represent standard error of the mean.

As paper points positive for vital cells always maintained maximum signal towards the tip, the fitting results of the first three recorded locations along the paper point (starting at the tip) were averaged, in order to get one value per paper point to compare the different RCT stages. We predicted a large amount of detection for the initial sample (post-access), which would decrease throughout the treatment. The data collected, as expected, demonstrated a decrease in calcein signal throughout the endodontic treatment. When examining all of the sampled paper points (with and without signal detection), the results revealed in an overall decrease in calcein signal, with a significant decrease from the post-access sample to post-shaping ($p < 0.001$) and from post-access to pre-obturation ($p < 0.001$).

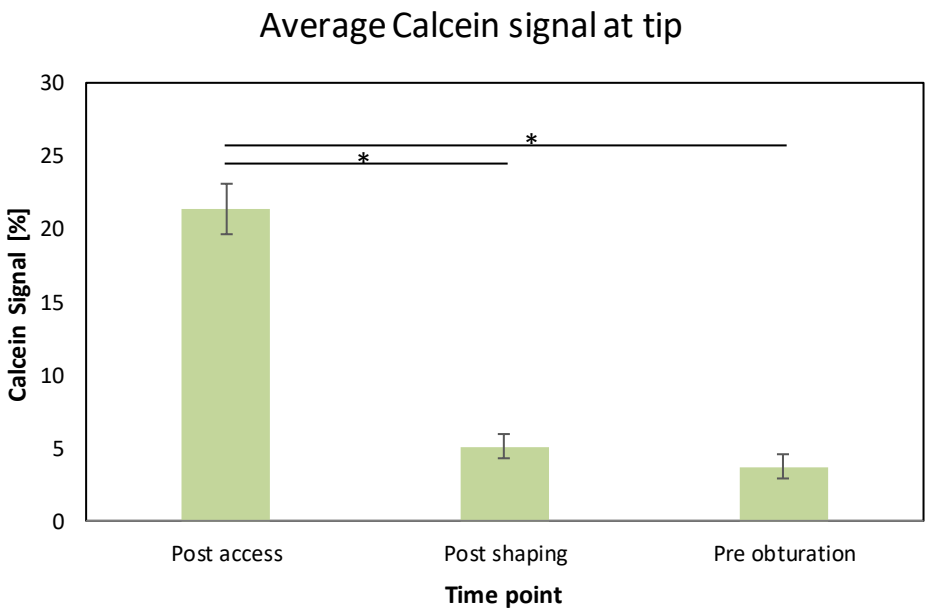

Figure 63: average calcein signal taken from the tip over the paper point at different time-points throughout 53 RCTs. Error bars represent standard error of the mean.

The data demonstrated that roots with detection over the threshold decreased in number with increasing treatment: from 74.6% post-access, to 29.8% after shaping and 18.4% pre-obturation (Figure 64). The decrease in a detectable vital signal shows that during the chemo-mechanical treatment, a majority of bacteria are removed. The calcein signal distribution of the pre-obturation samples is shown in Table 12, indicating the majority of roots being below detection limits. Table 12 also shows the number of roots which were positive for culture pre-obturation at the various corresponding calcein signals. The CFU/ml for these is also provided, however, due to the small sample size of roots from which bacteria were culturable, these numbers cannot be seen as representative. Despite the lower numbers of RCs with a detectable signal in the apex at the end of the treatment, clinically this results in 35.8% of teeth sampled showing a signal above the detection threshold. Furthermore, fluorescence detection proved to be more sensitive to vital bacteria than CFUs; A calcein signal was detected pre obturation in 18.4% of roots compared to 6.1% using culturing (Figure 64).

Table 12: Calcein signal distribution pre-obturation

Calcein Signal %	**Number of Roots**	Number of Roots positive for culture	Average CFU/ml (with standard deviation)
>4.35 (Clean)	93	1	10
4.4-21.7 %	14	3	31.7 (14.4)
21.7-65.2%	6	2	3302.5 (1762.5)
65.2-100 %	1	1	180

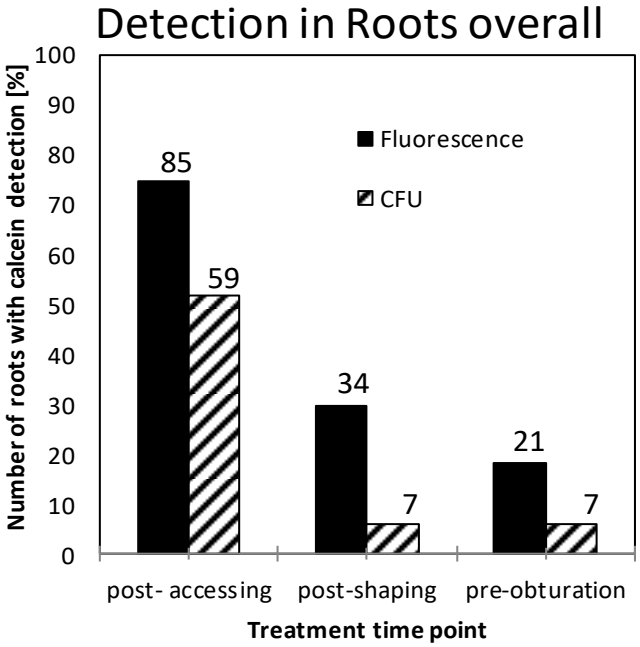

Figure 64: Clinical trial: Percentage of roots in which a signal was detected at different time-points throughout the treatment, as well as the comparison to CFU detection.

In order to optimise the sampling protocol, analysis from the first and second paper point from each root was compared. Detection increased for the second paper point at every sampling time point, as shown in Table 13.

Table 13: Percentage of roots with calcein signal detection, comparing first to second paper point

Time-point	Post accessing	Post-shaping	Pre-obturation
First paper point	56.1%	20.2%	10.5%
Second paper point	62.3%	22.8%	15.8%

Sampling with the second paper point was expected to provide higher detection numbers, as the first paper point would absorb and potentially be saturated by the excess liquid remaining in the RC space, following the rinsing with PBS (Figure 65). The paper points, as a sampling instrument have the benefit of having an absorbent nature, thus being likely to draw out fragments of bioburden and vital pulp cells from hard to reach areas.

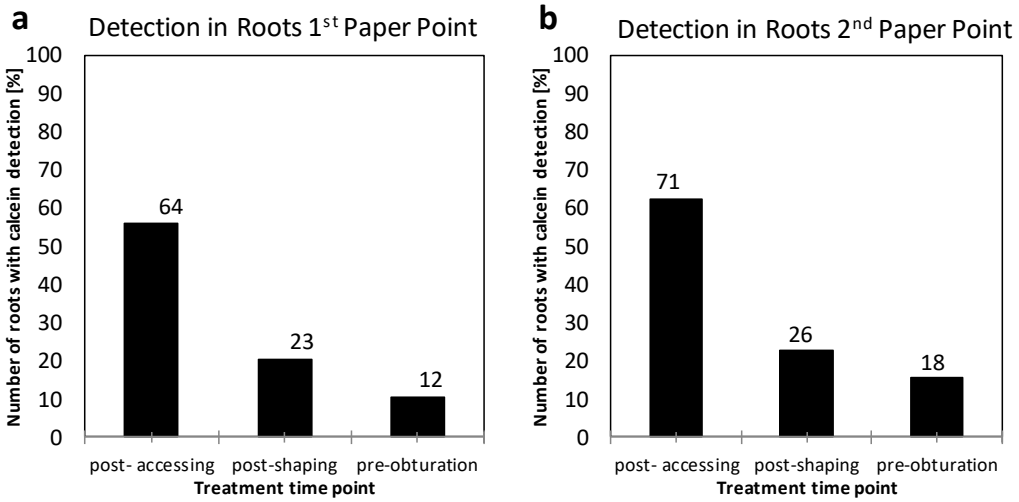

Figure 65: Comparison of calcein detection in all the roots from a) First and b) Second paper point taken from root canals during treatment.

Interestingly, however, in some cases detection was limited to the first of the two paper points collected – as shown by the increased number of roots when including both paper point samples. The detection increased at all time points when including both paper point samples, as shown in Table 14.

Table 14: Percentage of roots with calcein signal detection, comparing second to both paper points.

Time-point	Post accessing	Post-shaping	Pre-obturation
Second paper point	62.3%	22.8%	15.8%
Both paper points	74.6%	29.8%	18.4%

For the detection method, the interest lies in the numbers and percentages of roots in which bacteria have been detected. Clinically, the number of teeth with residual bacteria in the roots at time of obturation is also of importance: to lead to failure, multi-rooted teeth require only one root to cause a persisting infection. Detection including both sampled paper points at each time-point throughout treatment produced a similar trend when applying the data to detection in teeth, rather than roots. Teeth with any detection over the threshold decreased throughout the

treatment, from 81.1% immediately after access, to 52.3% after shaping and 35.8% pre obturation (Figure 66).

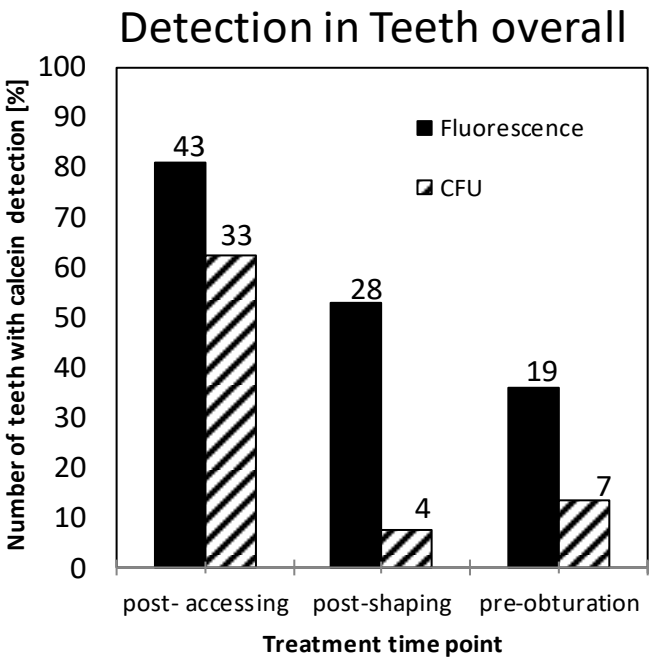

Figure 66: Clinical trial: Percentage of teeth in which a signal was detected at different time-points throughout the treatment, as well as the comparison to CFU detection.

The difference in detection for the two paper point samples also showed increased detection in the second paper point. Detection increased from 67.9%, 37.7% and 20.8% throughout the treatment for the first paper point to 73.6%, 43.4% and 30.2% for the second (Figure 67). However, as when analysing the roots individually, optimal detection was achieved when including both paper point samples, which when compared to the second paper point only increased from 73.6%, 43.4% and 30.2% to 81.1%, 53.8% and 35.8%, respectively. The results suggest that it may be beneficial to collect and analyse the initial paper point (primarily intended to absorb excess PBS), as well as the second one.

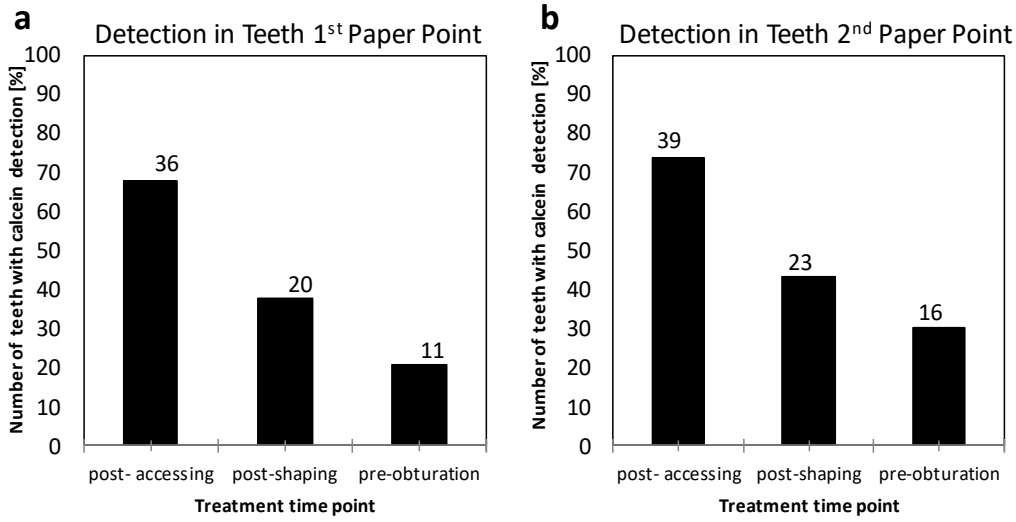

Figure 67: Comparison of calcein detection in all the teeth from a) First and b) Second paper point taken from root canals during treatment.

Interestingly, the detection of vital cells in 19 out of 53 of sampled teeth (35.8%) exceeds the percentage of RCT failures typically suggested by literature assessing RCT using periapical radiographs (24%) (Lumley et al., 2008; Ng et al., 2007). However, there is substantial agreement between the percentage of positively sampled teeth in the present study and the radiographic failure rate observed in CBCT studies in primary RCTs, where the percentage of teeth completely healed at the 1-year recall was a mere 62.5% in primary treatments (Patel et al., 2012) and 61% in re-treatments (Davies et al., 2015). Quantification of bacteria, especially in natural environments, is a contested issue, due to some bacteria being non-culturable or in non-culturable states (Li et al., 2014; Shen et al., 2010). Also, RC obturations have the potential of limiting the proliferation of the remaining bacteria. Reviewing patients included in the trial after 1 year aims to shed light on this issue and will allow to adjust detection threshold in respect to failures of the RCTs.

Overall, this clinical trial demonstrated the feasibility of this technique in a practical clinical setting. RCs were sampled and spectrally analysed immediately after accessing the RC space, after shaping and pre-obturation. Spectral analysis of control stained sterile paper points led to a threshold of 4.35%. A clear decrease in vital biofilm detection from the samples taken immediately after access compared to samples taken during and post-treatment was observed. While the majority of pre-obturation samples did not exceed the detection threshold, remaining vital bacteria were detected at the apex of the RC space in 18.4% of roots. Detection in the

apex is in accordance with current literature, explaining the RC apex to be the most challenging area for successful disinfection (Baugh and Wallace, 2005). Furthermore, similarly to the *in-vitro* detection of bacteria in a stressed state, the clinical trial showed that fluorescent analysis led to the detection of vital cells in more cases than CFU counting which only identified remnant bacteria in 7 teeth.

Detection by paper point sampling relies on the clinician correctly locating and accessing the RC, as the sampling is restricted to the general pre-created pathway of the endodontic instruments. However, endodontic paper points have the benefit of having identical tapers to the rotary instruments, being absorbent and flexible, as well as having constant and low autofluorescence, thus enhancing the detection of vital cells on the RC's apex and walls which remain untouched by mechanical instrumentation (Peters et al., 2003). Paper point sampling may not reach the apical portion during the initial post-access sample due to restrictions of the unshaped root as well as the taper of the paper point, however, for the pre-obturation sample this issue would not occur due to the identical tapers.

The teeth chosen for this study responded negatively to vitality tests and presented pre-operative apical radiolucencies. Therefore, the assumption can be made that no vital host cells would be present in the root canal space. As referred to previously, many fluorescent stains, including calcein AM do not differentiate between cells of bacterial or host origin. However, even when considering the RCT of roots with a vital pulp, the detection of vital cells in the root canal space, whether of bacterial or host cell nature, require removal as remnant pulp tissue can act as a source of nutrition for pathogenic bacteria (Haapasalo et al., 2003)

The recalls of patients, which are to be diagnosed with CBCT one year following the treatment, are currently in progress. To this date, 30 patients have had a check-up at this one-year time-point. Of these 30 patients, 9 showed a fluorescence detection above the preliminary set threshold. The recalled patients were all diagnosed by a senior consultant. Of the 9 patients in which a fluorescence signal above the threshold was detected, 5 were diagnosed as failures and 4 were seen to be healing. Of the 21 patients that produced a fluorescent signal below the threshold, 19 were diagnosed as healing and 2 as failing. Table 15 provides a summary of the recalled patients. A "True Positive" refers to a case where fluorescence detection led to a CBCT diagnosed failure and a "True Negative" to a case where a lack of fluorescence detection leads to a diagnosed healing. Overall, this results in an accuracy of 80%. Given that bacterial remnants do not lead to failure in all cases and other factors can lead to failure, these numbers

are promising for a tool to be used in clinical situations (Sjögren et al., 1997; Fabricius et al., 2006). Once a larger number of patients has been recalled, the threshold can potentially be adjusted to a more clinically relevant level. Only 2 of the recalled patients were positive for culturing pre-obturation, one of which lead to failure, the other healed. This demonstrates the difficulty of using culturing as a tool for detection especially when dealing with bacteria in hostile environments.

Table 15: Summary of recalled patients

True Positive	5
True Negative	19
False Positive	4
False Negative	2
Total Population	30
Accuracy	**80%**
Sensitivity **Specificity**	**71%** **83%**

5.3.2 Clinical application and commercialisation

The *in-vitro* studies as well as the clinical trial described here have been presented and communicated on various occasions. Communication of the described results, combined with the contacts and expertise made available by this CASE studentship, resulted in the generation of further interest by charities and research councils and allowed the securing of additional funding for further development. Funding received so far includes:

- KCL Commercialisation Institute £27,500
- EPSRC Impact Accelerator Award 48,040
- Design Council Spark £15,000

The next steps and potential partnerships to transfer the patent protected methodology into clinical use are currently in discussion. Efforts are currently focusing on development and use of prototypes for further trials and commercialisation. There are also ongoing negotiations with commercial partners to increase the volume and speed of these next steps.

The EPSRC Impact Accelerator Award has led to the construction of two early prototypes, miniaturised for bench side use. The principle of both prototypes is as described is this thesis, one differing in the fact that a fluorescence image will be recorded rather than a spectrum. Both prototypes will make an initial baseline measurement, as soon as the sample has been introduced into the fluorescent stain, followed by a second measurement to monitor any change in the fluorescence. Recording of a baseline measurement is especially important where an image is taken instead of a spectrum – autofluorescence must be taken into consideration and only in the presence of vital cells would there be a significant change in the fluorescence intensity over a short period of time. Figure 68 shows a depiction of the micro-spectrometer setup being used throughout this study, as well as an early miniaturised prototype which could feasibly be used bench-side in clinics.

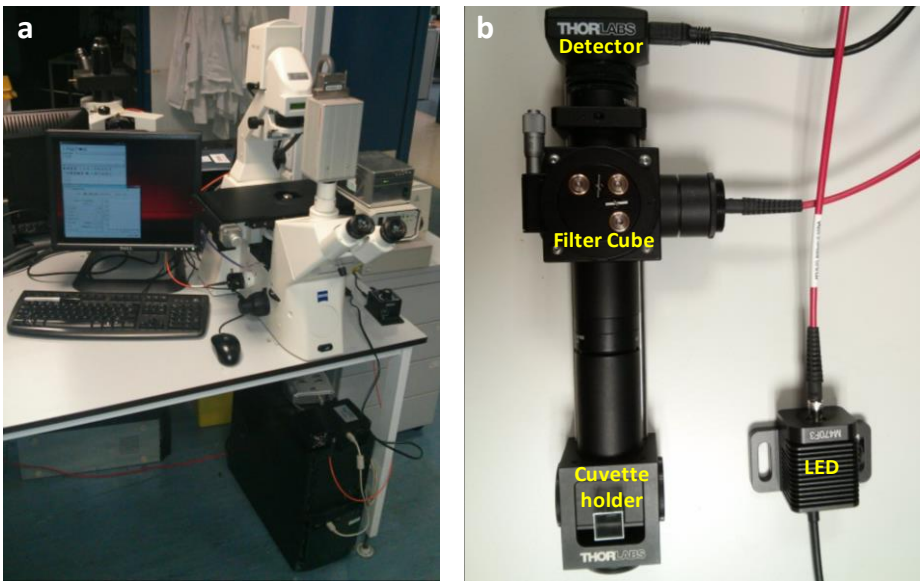

Figure 68: Detection of clinical samples a) Initial setup with spectrometer coupled to a wide-field fluorescence microscope. b) Miniaturised prototype with the essential components: Blue LED light source, filter cube with dichroic mirror and Ex/Em filters for green emission, a cuvette holder for the sample and a CCD detector.

An important aspect for the future prototype design is the development of a 'cassette' in which the sampled paper points can be placed and exposed to the CAM in a secure user-friendly manner. For this purpose, we worked together with the design and development company Kinnier Dufort. The final concept is outlined in Figure 69. The cassette provides four slots, into which the paper points used for sampling can easily be inserted into. The tips of the paper points are then guided to an optical window to be analysed by either a CCD camera or a spectrometer. Where using the fluorescence imaging technique all four paper points can be analysed at the same time, by defining regions of interest and measuring the fluorescence intensity increase for each paper point tip. Development of the cassette as an early step will allow to compare the prototype setups in upcoming clinical trials, both to each other as well as to the current lab setup. Furthermore, feedback on the usability in clinical settings will be collected from nurses as well as dentists.

Calcein AM stability and storage

For storage in clinical settings, various storage options of both stock solutions in DMSO and working solutions in PBS were examined. Where necessary, the stock solutions were made up into working solutions before fluorescence imaging and measuring of the mean fluorescence. As shown in Figure 70, CAM storage in DMSO does not result in a fluorescence increase

independent of the storage conditions, hence for the cassette design the blister packs were chosen, to separate the CAM in DMSO from the PBS. When stored at -20º, the CAM working solution in PBS also doesn't show an increase in fluorescence. However, after 5 days of storage at 4º, the fluorescence intensity of the working solution begins to increase. Stored at room temperature (RT), there is an immediate increase from day one. Provided it is stored in an airtight container, storage of CAM in DMSO remains stable, due to the anhydrous nature of DMSO. Once it is further diluted in PBS, is begins to gradually hydrolyse. For short-term storage, the working solution can be refrigerated at 4º or frozen at -20º.

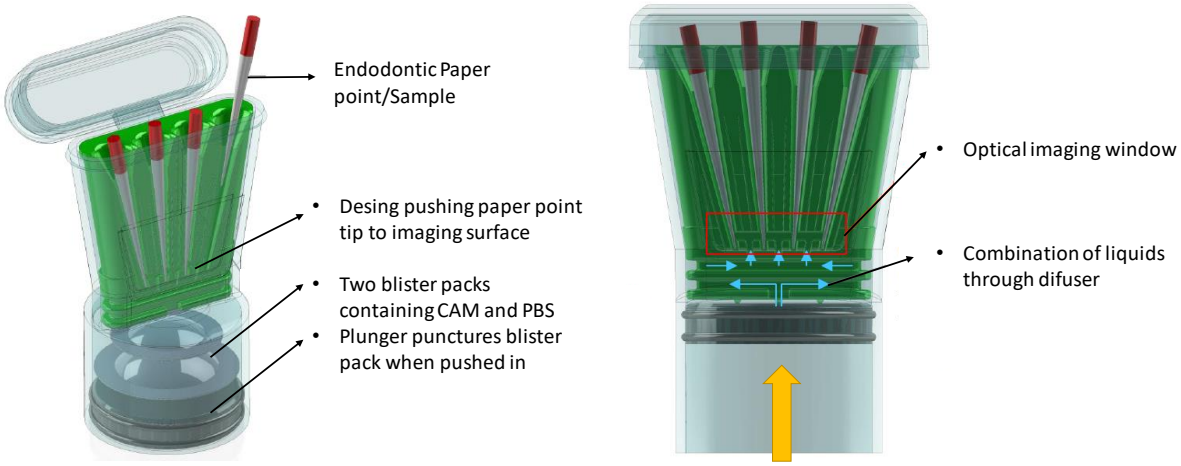

Figure 69: Concept design of cassette to be used in future prototypes. After sampling, paper points are inserted from the top. Pushing the plunger from below punctures blister packs containing CAM and PBS which then get combined through a diffuser before reaching the paper point tips.

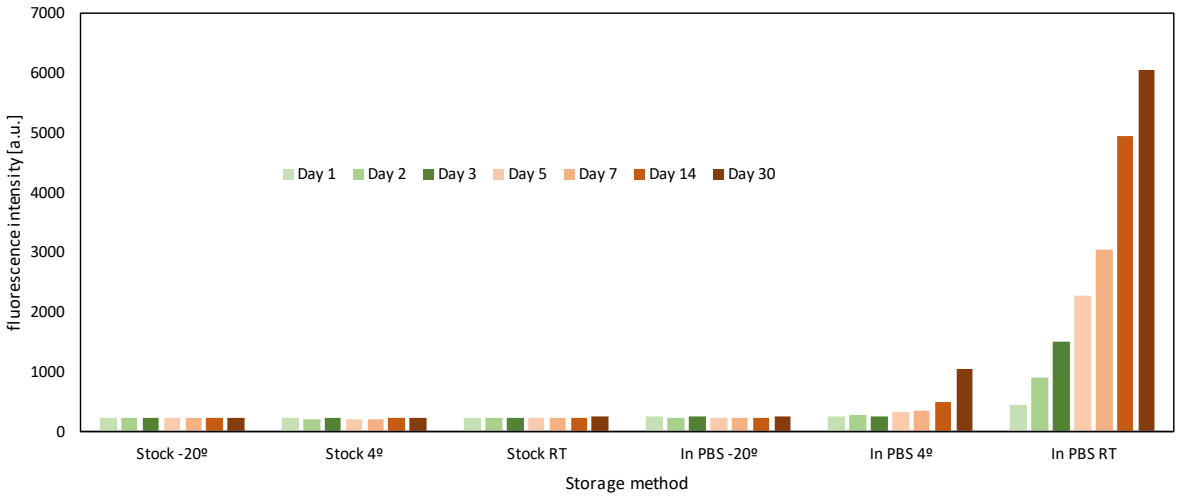

Figure 70: Fluorescence intensity of CAM stored either in stock (DMSO) or working solutions (in PBS) for 1 – 30 days. Storage conditions were room temperature (RT), 4º or frozen at -20º.

5.4 Conclusion

The aim of this clinical trial was to validate the translation of the results gained for the *ex-situ* approach into a clinical setting, with the ultimate goal of paving the way for a rapid, user-friendly bench-side device.

As with the *in-vitro* study, characterising base spectra for the spectral analysis was carried out by recording the paper point autofluorescence spectrum as well as that of hydrolysed CAM. Recruitment was carried out for patients undergoing primary RCT's, as this would be the main application for this methodology and would ensure more control over the consistent quality of the treatment.

The patient samples were taken at three time-points throughout the treatment. Detection was possible at all time-points, indicating that residual bacteria could not only be detected early on in the treatment but also following the chemo-mechanical treatment, just before obturation. The study showed a decrease in the percentage of roots and teeth with detection as the treatment progressed, demonstrating the effect of the treatment. Finally, the paper point samples were also used for bacterial culturing, suggesting, as seen in the *in-vitro* studies, fluorescence detection of vital cells was possible where no CFU grew.

From a clinical perspective, the final sample was the one of most importance, as residual bacteria in the RC pre-obturation could lead to failure of the treatment. Currently, the patient trial is being continued, restricted to the pre-obturation sample. In order to gain information on the relevance of detecting residual vital cells, CBCT scans treated teeth are being carried out before, and one-year post treatment.

This chapter has demonstrated the feasibility of and potential advantages and clinical relevance of fluorescent staining in combination with spectral analysis. The *ex-situ* approach provides a viable technique for introduction into the current workflow, capitalising on otherwise discarded biological material. As opposed to the recently published technique using an ATP assay, which also offers a rapid and sensitive detection method [12], we demonstrated the detection of the remnant bacteria directly on the paper point. By avoiding additional preparation, sampling and vortexing, valuable time is saved as the paper point measurements can be fully automated. It has the potential to minimise persistent infections, reduce treatment cost and avoid unnecessary secondary visits when no residual bacteria are detected.

Finally, this method offers the flexibility to be applied to other substrates and systems, potentially increasing the range of its clinical functions such as bacterial detection during wound infection and peri-implantitis treatment. Additionally, for research on disinfection techniques, it could provide a more rapid and user-friendly alternative to fluorescence microscopy.

Chapter 6 *Conclusions and Future Work*

6.1 Conclusions

The focus of this thesis was to utilise fluorescent staining and micro-spectroscopy to develop a rapid user-friendly method to detect vital cells in mature bacterial biofilms following RCTs, as well as to show additional applications of this technology.

Proof of concept studies using fluorescent beads as a simulation of fluorescently stained bacteria demonstrated, that under ideal conditions, small fluorescent particles could be detected in endodontic settings: both for an *in-situ* endoscopic approach of contaminated RC spaces as well as an *ex-situ* approach, which involves sampling of the RC space with endodontic paper points. In addition, it was shown that with similar equipment no discernible autofluorescence was detected during RCT, highlighting the need for induced fluorescence.

In-vitro studies evaluated a number of fluorescent dyes, characterising them for the suitability of rapid staining of vital cells in mature endodontic biofilms. To comply with a clinical workflow, incubation in the fluorescent dyes was limited to 5 minutes. Calcein AM, a fluorescent stain which is intrinsically non-fluorescent until cleaved by endogenous enzymes into the fluorescent calcein, was shown to be a suitable live stain. The green fluorescent signal only occurred in the presence of vital cells and produced very little to no background staining (both in the presence of non-vital cells and the HA and paper point substrates). *In-vitro* studies on the *in-situ* approach demonstrated the possibility of remote detection (using an optical glass fibre cable) by spectral analysis after 5 minutes of live/dead staining. The spectral analysis could generally be seen as a simple alternative to the more laborious analysis of conventional live/dead microscopy. Fluorescence detection was further shown to be more sensitive than the gold standard of CFU counting in detecting residual vital cells in a stressed endodontic biofilm. In order to simulate conditions during a RCT, nutritionally starved endodontic biofilms were treated with 1% NaOCl for various time periods. Spectral analysis of the samples showed a live signal coming from residual cells after they had lost the ability to be cultured. The *ex-situ* approach, involving paper point sampling of the RC space, proved to be a feasible method for detection of vital bacteria, whilst avoiding potential biocompatibility issues of introducing fluorescent stains into the RC space directly. Applying spectral un-mixing software enabled unbiased quantification of both the stained biofilm fluorescence and the presence of substrate autofluorescence.

After successfully determining Calcein AM to be a suitable fluorescent stain for endodontic biofilms and establishing an accurate, rapid way of analysing recorded spectra using software for spectral unmixing, the methodology was tested on disinfection techniques used in peri-implantitis. The same 5-minute time restriction was applied and various fluorescence based imaging techniques were used. The fluorescence based techniques were compared to each other, as well as to cell culturing and OCT imaging. Fluorescence imaging, using FITC filter cubes to measure green fluorescence intensity, and spectral analysis resulted in similar detection levels. However, it was demonstrated that, in the presence of any significant autofluorescence overlapping the calcein spectrum, the fluorescence intensity can be skewed. Using spectral unmixing to analyse a recorded spectrum, overlapping spectra can be distinguished from each other, giving a more reliable result. OCT, a label-free method using far-red light for deep sectioning was shown to be an excellent method for studying biofilm structure and thickness. Despite being a label-free non-invasive technique which rapidly records 3D images it has limited suitability for assessing successful disinfection, as it gives no indication on the vitality of the cells in residual structures.

These lab-based experiments laid out the ground work and established and refined the methodology, thus enabling a clinical trial to be carried out. The clinical trial was based on the *ex-situ* approach, taking samples from the RC space followed by *ex-situ* staining and analysis. The aim of this was to validate the translation of the discussed results into clinical situations. Recruitment of patients undergoing primary RCT was carried out. During the treatment, samples were taken at three time-points: Directly after accessing the RC space, following shaping of the canals and lastly, immediately before obturation. Samples were fluorescently stained, analysed and also cultured for CFU counting. As expected, the number of teeth with vital detection decreased throughout the treatment, showing the chemo-mechanical treatment removing vital biofilms. Clinically, the pre obturation sample was of most importance as bacteria remaining in the RC at this point could lead the failure of the treatment. Detection of a vital signal pre obturation was shown in 18.4% of roots sampled (35.8% of teeth) and resulted in detection in more teeth then CFU counting at all time-points. The clinical trial demonstrated the feasibility of fluorescent staining in combination with spectral analysis for clinical use, as well as highlighting advantages compared to bacterial culturing. By sampling the RC space with endodontic paper points followed by *ex-situ* fluorescent staining and analysis, this provides a patient-friendly, simple-to-use and rapid method with the potential to be used as a bench-side tool.

6.2 Future work

Ongoing clinical trials are being carried out to establish a suitable detection threshold to predict the likelihood of treatment failure. Establishment of treatment failure involves CBCT scans to be taken before and 1-year post treatment of patients undergoing RCTs. Detection levels pre obturation can then be compared to the treatment outcome. Very small amounts of remnant vital bacteria may not be sufficient to result in treatment failure, low levels of detection may not justify further treatment and weakening of the root. By comparing levels of detection on patients which have failing treatments, an appropriate threshold can be established.

To simplify ongoing and future clinical trials as well as moving towards commercialisation, bench side prototypes must be established: Either to be a miniaturised version of the current micro-spectrometer setup, or even a device which simply measures the fluorescence intensity. For the latter, an initial baseline reading would be of necessity to distinguish CAM induced fluorescence from autofluorescence. By having a baseline fluorescence measurement, the change in fluorescence intensity can be measured with great accuracy, which would only occur through the conversion of CAM to the fluorescent calcein by vital cells.

Within the scope of this project, CAM was characterised on a mixed species endodontic biofilm, applied to planktonic *E. faecalis* as well as a *P. gingivalis* biofilm and biofilms sampled from patients RC spaces. However, to further establish the suitability and explore limitations of the use of this fluorescent stain, it may be of use to characterise it on a large number of individual bacterial strains involved with endodontic or implant-related diseases. With regards to future applications outside of *in-vitro* studies and the detection in controlled areas such as RCs, the exploration and development of stains that specifically stain for vital bacteria (potentially specific species) could open up many further applications for this type of detection, especially for an *in-situ* approach.

More immediate applications could lead to the development of prototypes similar to the bench side device for use in dental clinics, but aimed at *in-vitro* disinfection studies. A method for quick evaluation of disinfection techniques without the need for a trained microscopist could have a range of applications in bacteriology and pre-clinical trials.

Appendix

Appendix Table 1: Detailed information of the BLAST results.

Query sequence	Query length [nt]	Hit HOT	Hit HOMD files	HOMD clone name	Identities (%)	Mismatch	Identities (no gaps & non-AGCTU)(%)	Mismatch (no gaps & non-AGCTU)	Score (bits)	Query Start	Subject Start
AR_RT2_1C10_O2_ii	577	746	746_1986	Actinomyces radicidentis Oral Taxon 746 {AJ251986} [1]	99.8	1/576	99.8	1/576	896	1	371
SE_6FA_14	583	601	601_3363	Staphylococcus epidermidis Oral Taxon 601 {D83363} [64]	99.8	1/584	100	0/583	907	1	38
EF_O2	618	604	604_8293	Enterococcus faecalis Oral Taxon 604 {Y18293} [34]	99.5	3/618	100	0/615	951	1	37
Smo_2B_23F	488	677	677_3929	Streptococcus mitis Oral Taxon 677 {AF003929} [999+]	98.8	6/486	99	5/485	736	2	33
PA_3BF_21	604	530	530_5256	Propionibacterium acnes Oral Taxon 530 {AF145256} [1]	99.8	1/604	100	0/603	938	1	36

Patient information sheet and Consent form for CBCT scans

REC Study Number: 08/H0804/79
Patient Identification Number for this trial:

PATIENT INFORMATION (version 5 14.10.15)

Title of investigation: Cone beam computed tomography study 2

Name of Researcher: Mr. Shanon Patel

You are being invited to take part in a research study. Before you decide to take part it is important for you to understand why the research is being done and what it will involve. Please take time to read the following information carefully. Ask us if there is anything that is not clear or if you would like more information. Take time to decide whether or not you wish to take part.

What is the purpose of this study?

Dental radiographs (X rays) are usually taken immediately after completion of treatment and on a periodic basis (review appointments), usually after 1 and 2 years after treatment has been completed to assess how successful treatment has been. The amount of information gained from conventional dental radiographs is limited as the images produced are only 2 dimensional (like a photograph).

Immediately before root canal treatment is commenced and at your review appointments in addition to the conventional radiograph we would also like to take an additional specialised 3-dimensional scan of the tooth. This 3-dimensional scan is called a 'Cone Beam Computed Tomography scan' and is the latest technology for imaging teeth. It allows us to assess your tooth in *3-dimensions* and therefore generates potentially more useful information about your tooth including the degree of healing. This specialised Cone Beam CT scan may give us a better understanding of the anatomy of your tooth Review appointments will also be arranged 1 and 2 years after the completion of your root canal treatment. If we are uncertain as to the degree of healing at this time, an additional review and scan may be required 4 years after completion of your treatment. However, this is not common. The additional radiation dose to the patient is in the same order of magnitude as a conventional dental X ray. The additional 3D scan would take 5-10 minutes to be carried out.

By taking 2 different types of images of your tooth (the conventional 2-dimensional radiograph and a
3-dimensional limited Cone Beam Computed Tomography scan) and comparing them we are aiming to scientifically confirm that this new 3-dimensional scanning technique is more accurate and helpful in assessing healing of root canal treatment.
The additional scan will taken straight after the conventional radiograph, and therefore will only add another 5-10 minutes to your appointment. The additional radiation dose from this second scan is minimal and is very similar to the conventional radiograph.

Ask us if there is anything that is not clear or if you would like more information. Take time to decide whether or not you wish to take part.

Do I have to take part?

It is up to you to decide. We will describe the study and go through this information sheet, which we will then give to you. If you agree to take part in the study we will then ask you to sign a consent form to show you have agreed to take part. You are free to withdraw at any time, without giving a reason. This would not affect the standard of treatment you receive.

What are the other possible disadvantages and risks of taking part?

The chance of any harm occurring to the patient as a result of exposure to dental X ray radiation is very small. The effective dose of each of these cone beam computed scans is equivalent 3-4 days of annual background radiation, so for the whole study the extra scans are equivalent to less than 10 days of background radiation. To put this in perspective, the effective dose from cosmic radiation on board an aircraft flying a round trip from Paris to Tokyo is equivalent to 15 days of annual background radiation.

What are the possible benefits of taking part?

The specialised 'Cone Beam Computed Tomography scan' could allow us to accurately and objectively assess how successful your treatment has been.

What will happen to the results?

The results of this study will be presented at national and international scientific meetings, and also published in dental journals.

Who is funding this study?

This study is being funded by the Department of Restorative Dentistry.

Will my taking part in this study be kept confidential?

Each patient will be given a unique identification number which will be used throughout the study. Only authorised people will have access to your records, they will have a duty of confidentiality to you as a research participant and we will do our best to meet this duty.
The information we collect will be kept securely for seven years, after which it will be disposed of securely.

What if there is a problem?

If you have a concern or any questions about any aspect of this study, you should ask to Mr Shanon Patel who will do his best to answer your questions. If you remain unhappy and wish to complain formally, you can do this through the NHS Complaints Procedure.

Contact details:

Mr Shanon Patel Endodontic Consultant/Honorary Senior Lecturer Unit, Floor 25 Guy's Tower, Guy's Hospital, London, SE1 9RT tel 020 7188 1605)

KING'S College LONDON
University of London

Guy's and St Thomas' NHS
NHS Foundation Trust

Guy's Hospital Great Maze Pond

London SE1 9RT

Main switchboard: 020 7188 7188

REC Study Number: 08/H0804/79

Patient Identification Number for this trial:

CONSENT FORM

(version 5 08/07/2015)

Title of Project: Cone beam computed tomography study 2

Name of Principle investigator: Mr. Patel

Please initial box

1. I confirm that I have read and understand the information sheet (Version 5dated 08/07/2015) for the above study and have had the opportunity to ask questions.

2. I understand that my participation is voluntary and that I am free to withdraw at any time, without giving any reason, without my medical care or legal rights being affected.

3. I understand that sections of any of my medical notes may be looked at by responsible individuals from [company name] or from regulatory authorities where it is relevant to my taking part in research. I give permission for these individuals to have access to my records.

4. I agree to take part in the above study.

_____ _____ _____

Name of Patient Date Signature

	Date	Signature
Name of Person taking consent (if different from researcher)		
	Date	Signature
Researcher		

1 for patient; 1 for researcher; 1 to be kept with hospital notes

Protocol for paper point sampling for fluorescence staining

In order to standardise the sampling procedure, the following protocol was established and distributed to all the clinicians participating in the study.

Initial Sample (Baseline):

Immediately after creating access cavity

- Disinfection/rinse mouth with chlorhexidine 0.2%
- Placement of rubber dam
- Disinfection of rubber dam with NaOCl
- Creation of access cavity
- Rinse with sterile saline (1 ml in sterile monoject syringe), leaving a drop inside the canal space
- Insertion of the paper point (F2) in the canal of choice, insert to achievable length
- Following removal of first paper point, insert second paper point and rub against the root canal walls

Paper Points per canal: 2Second Sample (Intermediate):

Post shaping with S2

- Rinse with sterile saline (1 ml in sterile monoject syringe), leaving a drop inside the canal space
- Insertion of the paper point (F2) into each canal, insert as close to the working length as possible
- Following removal of first paper point, insert second paper point and rub against the root canal walls

Paper Points per canal: 2

Final Sample (prior to obturation):

Pre-filling of the root canal space, after finishing files and passive ultrasonic irrigation

- Irrigants used by this point: 2% sodium hypochlorite with 17% EDTA
- Rinse with sterile saline (1 ml in sterile monoject syringe), leaving a drop inside the canal space
- Insertion of the paper point (F2) into each canal (where canals meet insert into the canal that will be filled to the working length), insert to the working length, rub against the root canal walls

Paper Points per canal: 2

Control Sample

- One sterile paper point to be incubated directly in staining solution without root canal contact as negative control

Paper points: 1

Total Paper Points to image: 7 (per canal) in multi-rooted teeth could have up to 28 if 4 separate canals) and 1 negative control

After removal from root canal, paper points are immediately incubated in an Eppendorf tube containing 0.5 ml of staining solution for 5 minutes in a dark environment. Following incubation, paper points are rinsed in PBS and stored in sterile eppendorf tube in a dark environment.

In the case of multiple appointments, the final sample is to be taken on the last appointment, pre obturation.

References

Alavi, M. R., Stojadinovic, A., Izadjoo, M. J., Chief, D., Jackson, H. M., Program, I., Medical, D., Operational, B., Award, S., Initiative, C. W. & Foundation, M. J. (2012) An overview of biofilm and its detection in clinical samples. *Journal of Wound Care*. 21 (8), 376–383.

Albrektsson, T., Zarb, G., Worthington, P. & Eriksson, A. R. (1986) The long-term efficacy of currently used dental implants: a review and proposed criteria of success. *The International journal of oral & maxillofacial implants*. 1 (1), 11–25.

Alla, R. K., Ginjupalli, K., Upadhya, N., Shammas, M., Ravi, R. K. & Ravichandra Sekhar (2011) Surface Roughness of Implants: A Review. *Trends Biomater. Artif. Organs*. 25 (3), 112–118.

Almatroudi, A., Gosbell, I. B., Hu, H., Jensen, S. O., Espedido, B. A., Tahir, S., Glasbey, T. O., Legge, P., Whiteley, G., Deva, A. & Vickery, K. (2016) Staphylococcus aureus dry-surface biofilms are not killed by sodium hypochlorite: Implications for infection control. *Journal of Hospital Infection*. [Online] 93 (3), 263–270.

Amoroso, P. F., Pier-Francesco, A., Adams, R. J., Waters, M. G. J. & Williams, D. W. (2006) Titanium surface modification and its effect on the adherence of Porphyromonas gingivalis: an in vitro study. *Clinical oral implants research*. [Online] 17 (6), 633–637.

Amos, W. B. & White, J. G. (2003) How the Confocal Laser Scanning Microscope entered Biological Research. *Biology of the Cell*. [Online] 95 (6), 335–342.

Anderson, A. C., Hellwig, E., Vespermann, R., Wittmer, A., Schmid, M., Karygianni, L. & Al-Ahmad, A. (2012) Comprehensive analysis of secondary dental root canal infections: a combination of culture and culture-independent approaches reveals new insights. *PloS one*. [Online] 7 (11), e49576.

Ando, T., Kobayashi, E., Liao, H., Maruyama, T., Muragaki, Y., Iseki, H., Kubo, O. & Sakuma, I.

(2011) Precise comparison of protoporphyrin IX fluorescence spectra with pathological results for brain tumor tissue identification. *Brain Tumor Pathology*. [Online] 28 (1), 43–51.

Anusavice, K. J., Chiayi, S. & Rawls, H. R. (2013) *Philips' science of dental materials*. Twelfth ed. St. Louis. Mo. : Elsevier/Saunders.

Anwar, H., Strap, J. L., Chen, K. & Costerton, J. W. (1992) Dynamic interactions of biofilms of mucoid *Pseudomonas aeruginosa* with tobramycin and piperacillin. *Antimicrob Agents Chemother*. [Online] 36 (6), 1208–1214.

Ata-Ali, J., Candel-Marti, M. E., Flichy-Fernández, A. J., Peñarrocha-Oltra, D., Balaguer-Martinez, J. F. & Diago, M. P. (2011) Peri-implantitis: Associated microbiota and treatment. *Medicina Oral, Patologia Oral y Cirugia Bucal*. [Online] 16 (7), e937-43.

Bachmann, L. (2006) Fluorescence Spectroscopy of Biological Tissues. *Applied Spectroscopy Reviews*. [Online] 41 (6), 575–590.

Bago, I., Plečko, V., Gabrić Pandurić, D., Schauperl, Z., Baraba, A. & Anić, I. (2013) Antimicrobial efficacy of a high-power diode laser, photo-activated disinfection, conventional and sonic activated irrigation during root canal treatment. *International Endodontic Journal*. [Online] 46 (4), 339–347.

Ball, D. W. (2006) *Field Guide to Spectroscopy*. [Online]. SPIE.

Banerjee, A. & Watson, F. T. (2015) *Minimally Invasive Operative Dentistry*. tenth. Oxford: Oxford University Press.

Banerjee, A. & Watson, T. F. (2002) Air abrasion: its uses and abuses. *Dent Update*. 29 (7), 340–346.

Baugh, D. & Wallace, J. (2005) The role of apical instrumentation in root canal treatment: a review of the literature. *Journal of endodontia*. [Online] 31 (5), 333–340.

Bazrafshan, N. & Darby, I. (2014) Retrospective success and survival rates of dental implants placed with simultaneous bone augmentation in partially edentulous patients. *Clinical oral implants research*. [Online] 25 (7), 768–773.

de Beer, D. (1997) Measurement of local diffusion coefficients in biofilms by micro-injection and confocal microscopy. *Biotechnology and Bioengineering*. 53151–158.

Berg, I. C. H., Rutland, M. W. & Arnebrant, T. (2003) Lubricating properties of the initial salivary pellicle--an AFM study. *Biofouling*. [Online] 19 (6), 365–369.

Black, R. B. (1945) Technic for Nonmechanical Preparation of Cavities and Prophylaxis. *The Journal of the American Dental Association*. [Online] 32 (15), 955–965.

Bleich, R., Watrous, J. D., Dorrestein, P. C., Bowers, A. A. & Shank, E. A. (2015) Thiopeptide antibiotics stimulate biofilm formation in Bacillus subtilis. *Proceedings of the National Academy of Sciences of the United States of America*. [Online] 112 (10), 3086–3091.

Blome, B., Braun, A., Sobarzo, V. & Jepsen, S. (2008) Molecular identification and quantification of bacteria from endodontic infections using real-time polymerase chain reaction. *Oral Microbiology and Immunology*. [Online] 23 (5), 384–390.

Bollen, C. M. L., Papaioanno, W., Van Eldere, J., Schepers, E., Quirynen, M. & van Steenberghe, D. (1996) The influence of abutment surface roughness on plaque accumulation and peri-implant mucositis. *Clinical Oral Implants Research*. [Online] 7 (3), 201–211.

Borriello, G., Werner, E., Roe, F., Kim, A. M., Ehrlich, G. D. & Stewart, P. S. (2004) *Oxygen Limitation Contributes to Antibiotic Tolerance of Pseudomonas aeruginosa in Biofilms*. [Online] 48 (7), 2659–2664.

Brånemark, P. I., Hansson, B. O. A., Breine, R., Lindström, U., J. Hallén, O. & Ohman, A. (1977) Osseointegrated implants in the treatment of the edentulous jaw. Experience from a 10-year period. *scand. J. Plast. Reconstr. Surg.* 161–132.

British Dental Health Foundation (n.d.) *Cosmetic Dentistry: Implants* [online]. Available from: https://www.dentalhealth.org/tell-me-about/topic/cosmetic-dentistry/implants.

Bürgers, R., Gerlach, T., Hahnel, S., Schwarz, F., Handel, G. & Gosau, M. (2010) In vivo and in vitro biofilm formation on two different titanium implant surfaces. *Clinical oral implants research*. [Online] 21 (2), 156–164.

Bürgers, R., Witecy, C., Hahnel, S. & Gosau, M. (2012) The effect of various topical peri-implantitis antiseptics on Staphylococcus epidermidis, Candida albicans, and Streptococcus sanguinis. *Archives of oral biology*. [Online] 57 (7), 940–947.

Busscher, H. J., Rinastiti, M., Siswomihardjo, W. & van der Mei, H. C. (2010) Biofilm formation on dental restorative and implant materials. *Journal of dental research*. [Online] 89 (7), 657–665.

Byrne, G. (2014) *Fundamentals of Implant Dentistry*. first. Wiley.

Byström, A. & Sundqvist, G. (1981) Bacteriologic evaluation of the efficacy of mechanical root canal instrumentation in endodontic therapy. *Scandinavian journal of dental research*. 89 (4), 321–328.

Carrotte, P. (2004) Endodontics: Part 9. Calcium hydroxide, root resorption, endo-perio lesions. *British dental journal*. [Online] 197 (12), 735–743.

Castonguay, M. H., van der Schaaf, S., Koester, W., Krooneman, J., van der Meer, W., Harmsen, H. & Landini, P. (2006) Biofilm formation by Escherichia coli is stimulated by synergistic interactions and co-adhesion mechanisms with adherence-proficient bacteria. *Research in Microbiology*. [Online] 157 (5), 471–478.

Chao, Y. & Zhang, T. (2011) Optimization of fixation methods for observation of bacterial cell morphology and surface ultrastructures by atomic force microscopy. *Applied microbiology and biotechnology*. [Online] 92 (2), 381–392.

Chatterji, D. & Kumar Ojha, A. (2001) Revisiting the stringent response, ppGpp and starvation signaling. *Current Opinion in Microbiology*. [Online] 4 (2), 160–165.

Chávez de Paz, L. (2007) Redefining the persistent infection in root canals: possible role of biofilm communities. *Journal of endodontics*. [Online] 33 (6), 652–662.

Chávez de Paz, L. E. (2012) Development of a multispecies biofilm community by four root canal bacteria. *Journal of endodontics*. [Online] 38 (3), 318–323.

Colvin, K. M., Gordon, V. D., Murakami, K., Borlee, B. R., Wozniak, D. J., Wong, G. C. L. &

Parsek, M. R. (2011) The pel polysaccharide can serve a structural and protective role in the biofilm matrix of Pseudomonas aeruginosa. *PLoS Pathogens*. [Online] 7 (1), e1001264.

Croneya, J. C., Jamesona, D. M. & Learmonthb, R. P. (2001) Fluorescence spectroscopy in biochemistry: teaching basic principles with visual demonstrations. *Biochemistry and Molecular Biology Education*. 2960–65.

Dahlen, G., Samuelsson, W., Molander, A. & Reit, C. (2000) Identification and antimicrobial susceptibility of enterococci isolated from the root canal. *Oral Microbiology and Immunology*. [Online] 15 (5), 309–312.

Davey, M. E., George, A. O. & Toole, G. A. O. (2000) Biofilms : from Ecology to Molecular Genetics. *Microbial and Molecular Biology Reviews*. [Online] 64 (4), 847–867.

Davies, A., Mannocci, F., Mitchell, P., Andiappan, M. & Patel, S. (2015) The detection of periapical pathoses in root filled teeth using single and parallax periapical radiographs versus cone beam computed tomography - a clinical study. *International Endodontic Journal*. [Online] 48 (6), 582–592.

Davies, D. (2003) Understanding biofilm resistance to antibacterial agents. *Nature reviews. Drug discovery*. [Online] 2 (2), 114–122.

Dentistry, A. A. of I. (n.d.) *Dental Implants Facts and Figures* [online]. Available from: http://www.aaid.com/about/press_room/dental_implants_faq.html (Accessed 12 February 2016).

Dickinson, M. E. & Davidson, M. W. (2017) *Introduction to Spectral Imaging and Linear Unmixing* [online]. Available from: http://zeiss-campus.magnet.fsu.edu/articles/spectralimaging/introduction.html (Accessed 1 August 2016).

Diéguez, L., Darwish, N., Mir, M., Martínez, E., Moreno, M. & Samitier, J. (2009) Effect of the Refractive Index of Buffer Solutions in Evanescent Optical Biosensors. *Sensor Letters*. [Online] 7 (5), 851–855.

Dietel, W., Pottier, R., Pfister, W., Schleier, P. & Zinner, K. (2007) 5-Aminolaevulinic acid (ALA) induced formation of different fluorescent porphyrins: A study of the biosynthesis of porphyrins by bacteria of the human digestive tract. *Journal of Photochemistry and Photobiology B: Biology*. [Online] 86 (1), 77–86.

Distel, J. W., Hatton, J. F. & Gillespie, M. J. (2002) Biofilm formation in medicated root canals. *Journal of endodontics*. [Online] 28 (10), 689–693.

Donlan, R. M. & Costerton, J. W. (2002) *Biofilms : Survival Mechanisms of Clinically Relevant Microorganisms*. [Online] 15 (2), 167–193.

Donnell, G. M. C. (1999) *Antiseptics and Disinfectants : Activity , Action , and Resistance*. 12 (1), 147–179.

Drago, L., De Vecchi, E., Torretta, S., Mattina, R., Marchisio, P. & Pignataro, L. (2012) Biofilm formation by bacteria isolated from upper respiratory tract before and after adenotonsillectomy. *Apmis*. [Online] 120 (5), 410–416.

Dreszer, C., Wexler, A. D., Drusova, S., Overdijk, T., Zwijnenburg, A., Flemming, H. C., Kruithof, J. C. & Vrouwenvelder, J. S. (2014) In-situ biofilm characterization in membrane systems using Optical Coherence Tomography: Formation, structure, detachment and impact of flux change. *Water Research*. [Online] 67 (0), 243–254.

Duan, Y., Huang, C. & Yu, Q. S. (2007) Cold plasma brush generated at atmospheric pressure. *Review of Scientific Instruments*. [Online] 78 (1), .

Ebenezar, J., Aruna, P. R. & Ganesan, S. (2015) Native fluorescence spectroscopic characterization of DMBA induced carcinogenesis in mice skin for the early detection of tissue transformation. *The Analyst*. [Online] 140 (12), 4170–4181.

Ehrhardt, A., Leonhard, M., Reulen, H. J., Stummer, W., Stepp, H. & Mo, G. (1998) Technical Principles for Protoporphyrin-IX-Fluorescence Guided Microsurgical Resection of Malignant Glioma Tissue. *Acta Neurochirurgica*. 140995–1000.

Eick, S., Markauskaite, G., Nietzsche, S., Laugisch, O., Salvi, G. E. & Sculean, A. (2013) Effect of photoactivated disinfection with a light-emitting diode on bacterial species and biofilms

associated with periodontitis and peri-implantitis. *Photodiagnosis and photodynamic therapy*. [Online] 10 (2), 156–167.

Ercan, E., Ozekinci, T., Atakul, F. & Gül, K. (2004) Antibacterial activity of 2% chlorhexidine gluconate and 5.25% sodium hypochlorite in infected root canal: in vivo study. *Journal of endodontics*. [Online] 30 (2), 84–87.

Evans, R. C. & Holmes, C. J. (1987) Effect of vancomycin hydrochloride on Staphylococcus epidermidis biofilm associated with silicone elastomer. *Antimicrobial Agents and Chemotherapy*. [Online] 31 (6), 889–894.

Fabricius, L., Dahlén, G., Sundqvist, G., Happonen, R.-P. & Möller, A. J. R. (2006) Influence of residual bacteria on periapical tissue healing after chemomechanical treatment and root filling of experimentally infected monkey teeth. *European journal of oral sciences*. [Online] 114 (4), 278–285.

Flemming, H.-C. & Wingender, J. (2010) The biofilm matrix. *Nature reviews. Microbiology*. [Online] 8 (9), 623–633.

Frank, K. L. & Patel, R. (2007) Poly-N-acetylglucosamine is not a major component of the extracellular matrix in biofilms formed by icaADBC-positive Staphylococcus lugdunensis isolates. *Infection and immunity*. [Online] 75 (10), 4728–4742.

Froum, S. J., Dagba, A. S., Shi, Y., Perez-Asenjo, A., Rosen, P. S. & Wang, W. C. W. (2016) Successful Surgical Protocols in the Treatment of Peri-Implantitis. *Implant Dentistry*. [Online] 25 (3), 416–426.

Fux, C. A., Costerton, J. W., Stewart, P. S. & Stoodley, P. (2005) Survival strategies of infectious biofilms. *Trends in Microbiology*. [Online] 13 (1), 34–40.

Garini, Y., Young, I. T. & McNamara, G. (2006) Spectral Imaging: Principles and Applications. *Cytometry. Part A : the journal of the International Society for Analytical Cytology*. [Online] 69 (8), 735–747.

Gernhardt, C. R., Eppendorf, K., Kozlowski, A. & Brandt, M. (2004) Toxicity of concentrated sodium hypochlorite used as an endodontic irrigant. *International Endodontic Journal*.

[Online] 37 (4), 272–280.

Giana, E., Jr, L. S., Zangaro, R. A. & Pacheco, M. T. T. (2003) Rapid Identification of Bacterial Species by Fluorescence Spectroscopy and Classification Through Principal Components Analysis. *Journal of Fluorescence*. 13 (6), 489–493.

Giardino, L., Ambu, E., Savoldi, E., Rimondini, R., Cassanelli, C. & Debbia, E. A. (2007) Comparative Evaluation of Antimicrobial Efficacy of Sodium Hypochlorite, MTAD, and Tetraclean Against Enterococcus faecalis Biofilm. *Journal of Endodontics*. [Online] 33 (7), 852–855.

Di Giulio, M., Traini, T., Sinjari, B., Nostro, A., Caputi, S. & Cellini, L. (2015) Porphyromonas gingivalis biofilm formation in different titanium surfaces, an in vitro study. *Clinical oral implants research*. [Online] 27 (7), 918–925.

GmbH, R. P. (2017) *Piezobrush PZ2* [online]. Available from: http://www.piezobrush.com/wp-content/uploads/2015/10/piezobrush-zubehoer-nearfield-duese-anwendung.jpg (Accessed 17 January 2017).

Gomes-Filho, J. E., Aurélio, K. G., Costa, M. M. T. D. M. & Bernabé, P. F. E. (2008) Comparison of the biocompatibility of different root canal irrigants. *Journal of applied oral science : revista FOB*. [Online] 16 (2), 137–144.

Gomes, B. P. F. a, Pinheiro, E. T., Gadê-Neto, C. R., Sousa, E. L. R., Ferraz, C. C. R., Zaia, a a, Teixeira, F. B. & Souza-Filho, F. J. (2004) Microbiological examination of infected dental root canals. *Oral microbiology and immunology*. 19 (2), 71–76.

Gonçalves, L. S., Rodrigues, R. C. V., Andrade Junior, C. V., Soares, R. G. & Vettore, M. V. (2016) The effect of sodium hypochlorite and chlorhexidine as irrigant solutions for root canal disinfection: A systematic review of clinical trials. *Journal of Endodontics*. [Online] 42 (4), 527–532.

Gosau, M., Hahnel, S., Schwarz, F., Gerlach, T., Reichert, T. E. & Bürgers, R. (2010) Effect of six different peri-implantitis disinfection methods on in vivo human oral biofilm. *Clinical oral implants research*. [Online] 21 (8), 866–872.

Gristina, A. G., Hobgood, C. D., Webb, L. X. & Myrvik, Q. N. (1987) Adhesive colonization of biomaterials and antibiotic resistance. *Biomaterials*. [Online] 8 (6), 423–426.

Guggenheim, B., Giertsen, E., Schupbach, P. & Shapiro, S. (2001) Validation of an in vitro Biofilm Model of Supragingival Plaque. *Journal of Dental Research*. [Online] 80 (1), 363–370.

Gulabivala, K. & Ng, Y.-L. (2014) 'Aetiopathogenesis of periapical disease', in *Endodontics*. 4th edition Elsevier Health Sciences UK. p. 399.

Haapasalo, M., Udnæs, T. & Endal, U. (2003) Persistent , recurrent , and acquired infection of the root canal system post-treatment. *Endodontic Topics*. [Online] 629–56.

Haisch, C. & Niessner, R. (2007) Visualisation of transient processes in biofilms by optical coherence tomography. *Water Research*. [Online] 41 (11), 2467–2472.

Hall-Stoodley, L., Costerton, J. W. & Stoodley, P. (2004) Bacterial biofilms: from the natural environment to infectious diseases. *Nature reviews. Microbiology*. [Online] 2 (2), 95–108.

Hannig, M. & Balz, M. (2001) Protective Properties of Salivary Pellicles from Two Different Intraoral Sites on Enamel Erosion. *Caries Research*. [Online] 35 (2), 142–148.

Hargreaves, K. M. & Berman, L. H. (2015) *Cohen's Pathways of the Pulp Expert Consulte*.

Harmsen, M., Lappann, M., Knøchel, S. & Molin, S. (2010) Role of extracellular DNA during biofilm formation by listeria monocytogenes. *Applied and Environmental Microbiology*. [Online] 76 (7), 2271–2279.

Hassan, A., Usman, J., Kaleem, F., Omair, M., Khalid, A. & Iqbal, M. (2011) Evaluation of different detection methods of biofilm formation in the clinical isolates. *The Brazilian Journal of Infectious Diseases*. [Online] 15 (4), 305–311.

Ho, Q. V, George, R., Sainsbury, A. L., Kahler, W. a & Walsh, L. J. (2010) Laser fluorescence assessment of the root canal using plain and conical optical fibers. *Journal of endodontics*. [Online] 36 (1), 119–122.

Hoiby, N., Bjarnsholt, T., Givskov, M., Molin, S. & Ciofu, O. (2010) Antibiotic resistance of

bacterial biofilms. *International Journal of Antimicrobial Agents*. [Online] 35 (4), 322–332.

Hong, S. H., Hegde, M., Kim, J., Wang, X., Jayaraman, A. & Wood, T. K. (2012) Synthetic quorum-sensing circuit to control consortial biofilm formation and dispersal in a microfluidic device. *Nature communications*. [Online] 3 (3), 613.

Huang, D., Swanson, E. a, Lin, C. P., Schuman, J. S., Stinson, W. G., Chang, W., Hee, M. R., Flotire, T., Gregory, K., Puliafito, C. a & Fujimoto, J. G. (1991) Optical Coherence Tomography. *Science*. [Online] 254 (5035), 1178–1181.

Huffaker, S. K., Safavi, K., Spangberg, L. S. W. & Kaufman, B. (2010) Influence of a passive sonic irrigation system on the elimination of bacteria from root canal systems: A clinical study. *Journal of Endodontics*. [Online] 36 (8), 1315–1318.

Ito, Y., Sato, T., Yamaki, K., Mayanagi, G., Hashimoto, K., Shimauchi, H. & Takahashi, N. (2012) Microflora profiling of infected root canal before and after treatment using culture-independent methods. *Journal of Microbiology*. [Online] 50 (1), 58–62.

Jacobs, N. J., Jacobs, J. M. & Brent, P. (1970) Formation of protoporphyrin from coproporphyrinogen in extracts of various bacteria. *Journal of Bacteriology*. 102 (2), 398–403.

Joaquin, J. C., Kwan, C., Abramzon, N., Vandervoort, K. & Brelles-Mariño, G. (2009) Is gas-discharge plasma a new solution to the old problem of biofilm inactivation? *Microbiology*. [Online] 155 (3), 724–732.

Kanagasingam, S., Lim, C. X., Yong, C. P., Mannocci, F. & Patel, S. (2016) Diagnostic accuracy of periapical radiography and cone beam computed tomography in detecting rapical periodontitis using histopathological findings as a reference standard. *International endodontic journal*. [Online] 1–10.

Kato, H., Yoshida, A., Ansai, T., Watari, H., Notomi, T. & Takehara, T. (2007) Loop-mediated isothermal amplification method for the rapid detection of Enterococcus faecalis in infected root canals. *Oral microbiology and immunology*. [Online] 22 (2), 131–135.

Kato, H., Yoshida, a, Ansai, T., Watari, H., Notomi, T. & Takehara, T. (2007) Loop-mediated

isothermal amplification method for the rapid detection of Enterococcus faecalis in infected root canals. *Oral microbiology and immunology*. [Online] 22 (2), 131–135.

Keren, I., Kaldalu, N., Spoering, A., Wang, Y. & Lewis, K. (2004) Persister cells and tolerance to antimicrobials. *FEMS Microbiology Letters*. [Online] 230 (1), 13–18.

Kim, J., Hahn, J., Franklin, M. J., Stewart, P. S. & Yoon, J. (2009) Tolerance of dormant and active cells in Pseudomonas aeruginosa PA01 biofilm to antimicrobial agents. *Journal of Antimicrobial Chemotherapy*. [Online] 63129–135.

Köhler, T., Epp, S. F., Curty, L. K. & Pechère, J. (1999) Characterization of MexT , the Regulator of the MexE-MexF-OprN Multidrug Efflux System of Pseudomonas aeruginosa Characterization of MexT , the Regulator of the MexE-MexF-OprN Multidrug Efflux System of Pseudomonas aeruginosa. *Journal of Bacteriology*. 181 (20), 6300–6305.

Kolenbrander, P. E., Jr, R. J. P., Rickard, A. H., Jakubovics, N. S., Chalmers, N. I. & Diaz, P. I. (2006) Bacterial interactions and successions during plaque development. *Periodontology 2000*. 42 (5), 47–79.

Kostakioti, M., Hadjifrangiskou, M. & Hultgren, S. J. (2013) Bacterial biofilms: development, dispersal, and therapeutic strategies in the dawn of the postantibiotic era. *Cold Spring Harbor perspectives in medicine*. [Online] 3 (4), 1–23.

Kraus, B., Ziegler, M. & Wolff, H. (2007) Linear fluorescence unmixing in cell biological research. *Modern Research and Educational Topics in Microscopy*. 863–872.

Kuboniwa, M. & Lamont, R. J. (2013) Subgingival biofilm formation. *NIH Public Access*. [Online] 52 (1), 38–52.

Lakowicz, J. R. (2006) *Principles of Fluorescence Spectroscpy*. Third Edit. Baltimore: Springer.

Lane, D. J. (1991) '16S/23S rRNA sequencing', in *in Nucleic Acid Techniques in Bacterial Systematics (Stackebrandt, E. and Goodfellow, M., eds).* Chichester, United Kingdom: John Wiley & Sons, Inc. pp. 115–175.

Lang, N. P. & Lindhe, J. (2015) 'Clinical Periodontology and Implant Dentistry', in *Clinical*

Periodontology and Implant Dentistry. Wiley. pp. 505–508.

Lang, N. P., Lindhe, J. & Lang, N. P. (2015) 'Clinical Periodontology and Implant Dentistry', in *Clinical Periodontology and Implant Dentistry*. Wiley. pp. 861–864.

Lansford, R., Bearman, G. & Fraser, S. E. (2001) Resolution of multiple green fluorescent protein color variants and dyes using two-photon microscopy and imaging spectroscopy. *J Biomed Opt*. [Online] 6 (3), 311–318.

Lee, J.-K., Ha, B.-H., Choi, J.-H., Heo, S.-M. & Perinpanayagam, H. (2006) Quantitative three-dimensional analysis of root canal curvature in maxillary first molars using micro-computed tomography. *Journal of endodontics*. [Online] 32 (10), 941–945.

Leid, J. G., Willson, C. J., Shirtliff, M. E., Hassett, D. J., Parsek, M. R. & Jeffers, A. K. (2005) The exopolysaccharide alginate protects Pseudomonas aeruginosa biofilm bacteria from IFN-gamma-mediated macrophage killing. *Journal of immunology*. [Online] 175 (11), 7512–7518.

Li, L., Mendis, N., Trigui, H., Oliver, J. D. & Faucher, S. P. (2014) The importance of the viable but non-culturable state in human bacterial pathogens. *Frontiers in Microbiology*. [Online] 5 (258), 1–20.

Lifesciences (2013) *Calcein AM Spectrum* [online]. Available from: http://www.invitrogen.com/site/us/en/home/support/Product-Technical-Resources/Product-Spectra.481ph9.htmlNo Title.

Lüdecke, C., Jandt, K. D., Siegismund, D., Kujau, M. J., Zang, E., Rettenmayr, M., Bossert, J. & Roth, M. (2014) Reproducible biofilm cultivation of chemostat-grown escherichia coli and investigation of bacterial adhesion on biomaterials using a non-constant-depth film fermenter. *PLoS ONE*. [Online] 9 (1), e84837.

Lumley, P. J., Lucarotti, P. S. K. & Burke, F. J. T. (2008) Ten-year outcome of root fillings in the General Dental Services in England and Wales. *International endodontic journal*. [Online] 41 (7), 577–585.

Mah, T. F. & O'Toole, G. a (2001) Mechanisms of biofilm resistance to antimicrobial agents.

Trends in microbiology. 9 (1), 34–39.

Mahato, N., Wu, X. & Wang, L. (2016) Management of peri-implantitis : a systematic review , 2010 – 2015. *SpringerPlus*. [Online] 5 (105), 1–9.

Malet, J., Mora, F. & Bouchard, P. (2011) 'Implant Dentistry at a Glance', in *Implant Dentistry at a Glance*. Hoboken: John Wiley & Sons, Inc. pp. 22–23.

Malet, J., Mora, F. & Bourard, P. (2011) 'Implant Dentistry at a Glance', in *Implant Dentistry at a Glance*. Hoboken: John Wiley & Sons, Inc. pp. 20–21.

Mang, T. S. (2004) Lasers and light sources for PDT: Past, present and future. *Photodiagnosis and Photodynamic Therapy*. [Online] 1 (1), 43–48.

Marsh, R. L., Thornton, R. B., Smith-Vaughan, H. C., Richmond, P., Pizzutto, S. J. & Chang, A. B. (2014) Detection of biofilm in bronchoalveolar lavage from children with non-cystic fibrosis bronchiectasis. *Pediatric pulmonology*. [Online] 292 (March 2014), 284–292.

Mart, S. V, Zhurina, M. V, Registan, G. I. El & Plakunov, V. K. (2014) Activation of Formation of Bacterial Biofilms by Azithromycin and Prevention of This Effect. *Microbiology*. [Online] 83 (6), 723–731.

Martinho, F. C., Gomes, A. P. M., Fernandes, A. M. M., Ferreira, N. S., Endo, M. S., Freitas, L. F. & Camões, I. C. G. (2014) Clinical comparison of the effectiveness of single-file reciprocating systems and rotary systems for removal of endotoxins and cultivable bacteria from primarily infected root canals. *Journal of Endodontics*. [Online] 40 (5), 625–629.

Masataka, M. & Seiyo, S. (1971) Studies on the Formation of Protoporphyrin IX by Anaerobic Bacteria. *BIOCHIMICA ET BIOPHYSICA ACTA*. 264 (1972), 252–262.

McDowell, A., Valanne, S., Ramage, G., Tunney, M. M., Glenn, J. V, McLorinan, G. C., Bhatia, A., Maisonneuve, J.-F., Lodes, M., Persing, D. H. & Patrick, S. (2005) Propionibacterium acnes types I and II represent phylogenetically distinct groups. *Journal of clinical microbiology*. [Online] 43 (1), 326–334.

Metzger, Z., Solomonov, M. & Kfir, A. (2013) The role of mechanical instrumentation in the cleaning of root canals. *Endodontic Topics*. [Online] 29 (1), 87–109.

Miller, M. B. & Bassler, B. L. (2001) Quorum Sensing in Bacteria. *Annual Review of Microbiology*. 55165–199.

Mohammadi, Z., Jafarzadeh, H. & Shalavi, S. (2014) Antimicrobial efficacy of chlorhexidine as a root canal irrigant: a literature review. *Journal of Oral Science*. [Online] 56 (2), 99–103.

Moisan, M., Barbeau, J., Moreau, S., Pelletier, J., Tabrizian, M. & Yahia, L. (2001) Low-temperature sterilization using gas plasmas: A review of the experiments and an analysis of the inactivation mechanisms. *International Journal of Pharmaceutics*. [Online] 226 (1–2), 1–21.

Moter, A. & Göbel, U. B. (2000) Fluorescence in situ hybridization (FISH) for direct visualization of microorganisms. *Journal of microbiological methods*. 41 (2), 85–112.

Murad, C. F., Sassone, L. M., Faveri, M., Hirata, R., Figueiredo, L. & Feres, M. (2014) Microbial diversity in persistent root canal infections investigated by checkerboard DNA-DNA hybridization. *Journal of Endodontics*. [Online] 40 (7), 899–906.

Ng, Y.-L., Mann, V., Rahbaran, S., Lewsey, J. & Gulabivala, K. (2007) Outcome of primary root canal treatment: systematic review of the literature - part 1. Effects of study characteristics on probability of success. *International endodontic journal*. [Online] 40 (12), 921–939.

Nguyen, C. T., Robinson, S. R., Jung, W., Novak, M. A., Boppart, S. A. & Allen, J. B. (2013) Investigation of bacterial biofilm in the human middle ear using optical coherence tomography and acoustic measurements. *Hearing Research*. [Online] 301193–200.

Nguyen, D., Joshi-datar, A., Lepine, F., Bauerle, E., Olakanmi, O., Britigan, B. E. & Singh, P. K. (2011) Active Starvation Responses Mediate Antibiotic Tolerance in Biofilms and Nutrient-Limited Bacteria. *SCIENCE*. 334982–986.

Niazi, S. A., Al-Ali, W. M., Patel, S., Foschi, F. & Mannocci, F. (2015) Synergistic effect of 2% chlorhexidine combined with proteolytic enzymes on biofilm disruption and killing. *International Endodontic Journal*. [Online] 48 (12), 1157–1167.

Niazi, S. A., Clark, D., Do, T., Gilbert, S. C., Foschi, F., Mannocci, F. & Beighton, D. (2014) The effectiveness of enzymic irrigation in removing a nutrient-stressed endodontic multispecies biofilm. *International Endodontic Journal*. [Online] 47 (8), 756–768.

Niazi, S. A., Clarke, D., Do, T., Gilbert, S. C., Mannocci, F. & Beighton, D. (2010) Propionibacterium acnes and Staphylococcus epidermidis isolated from refractory endodontic lesions are opportunistic pathogens. *Journal of Clinical Microbiology*. [Online] 48 (11), 3859–3869.

Norowski, P. A. & Bumgardner, J. D. (2009) Biomaterial and antibiotic strategies for peri-implantitis: a review. *Journal of biomedical materials research. Part B, Applied biomaterials*. [Online] 88 (2), 530–543.

Norwood, D. E. & Gilmour, A. (2000) The growth and resistance to sodium hypochlorite of Listeria monocytogenes in a steady-state multispecies biofilm. *Journal of Applied Microbiology*. [Online] 88 (3), 512–520.

O'Toole, G. A. & Kolter, R. (1998) Initation of biofilm formation in Pseudomans fluorescens WC365 proceeds via multiple, convergent signalling pathways: a genetic analysis. *Molecular Microbiology*. 28449–461.

Ocean Optics (2016) *QE65000 Spectrometer* [online]. Available from: http://oceanoptics.com/wp-content/uploads/OceanOptics_Spectrometers.pdf.

Önçağ, Ö., Hoşgör, M., Hilmioğlu, S., Zekioğlu, O., Eronat, C. & Burhanoğlu, D. (2003) Comparison of antibacterial and toxic effects of various root canal irrigants. *International Endodontic Journal*. [Online] 36 (6), 423–432.

Orstavik, D. & Thomas, P. F. (2007) *Essential Endodontology: Prevention and Treatment of Apical Periodontitis, 2nd Edition*. Second. [Online]. Blackwell Munksgaar Ltd.

Osman, R. & Swain, M. (2015) A Critical Review of Dental Implant Materials with an Emphasis on Titanium versus Zirconia. *Materials*. [Online] 8 (3), 932–958.

Papaioannou, W., Panagopoulos, a, Koletsi-Kounari, H., Kontou, E. & Makou, M. (2012) Adhesion of porphyromonas gingivalis and biofilm formation on different types of

orthodontic brackets. *International Journal of Dentistry*. [Online] 2012471380.

Papaspyridakos, P., Chen, C.-J., Singh, M., Weber, H.-P. & Gallucci, G. O. (2012) Success criteria in implant dentistry: a systematic review. *Journal of dental research*. [Online] 91 (3), 242–248.

Park, J.-B., Koh, M., Jang, Y.-J., Choi, B.-K., Kim, K.-K. & Ko, Y. (2014) Removing bacteria from rough surface titanium discs with chlorhexidine and additional brushing with dentifrice. *Gerodontology*. [Online] 33 (1), 28–35.

Parsek, M. R. & Singh, P. K. (2003) Bacterial biofilms: an emerging link to disease pathogenesis. *Annual review of microbiology*. [Online] 57677–701.

Patel, S., Durack, C., Abella, F., Roig, M., Shemesh, H., Lambrechts, P. & Lemberg, K. (2014) European Society of Endodontology position statement: The use of CBCT in Endodontics. *International Endodontic Journal*. [Online] 47 (6), 502–504.

Patel, S., Wilson, R., Dawood, A., Foschi, F. & Mannocci, F. (2012) The detection of periapical pathosis using digital periapical radiography and cone beam computed tomography – Part 2 : a 1-year post-treatment. *International endodontic journal*. [Online] 45 (8), 711–723.

Paul, D., Kim, Y. S., Ponnusamy, K. & Kweon, J. H. (2009) Application of Quorum Quenching to Inhibit Biofilm Formation. *Environmental Engineering Science*. [Online] 26 (8), 1319–1324.

Persson, G. R. & Renvert, S. (2014) Cluster of bacteria associated with peri-implantitis. *Clinical implant dentistry and related research*. [Online] 16 (6), 783–793.

Peters, O. a (2004) Current challenges and concepts in the preparation of root canal systems: a review. *Journal of endodontics*. 30 (8), 559–567.

Peters, O. a, Peters, C. I., Schönenberger, K. & Barbakow, F. (2003) ProTaper rotary root canal preparation: effects of canal anatomy on final shape analysed by micro CT. *International endodontic journal*. 36 (2), 86–92.

Petersilka, G. J. (2011) Subgingival air-polishing in the treatment of periodontal biofilm infections. *Periodontology 2000*. [Online] 55 (1), 124–142.

Poole, K. (2012) Bacterial stress responses as determinants of antimicrobial resistance. *Journal of Antimicrobial Chemotherapy*. [Online] 672069–2089.

Portillo, M. E., Corvec, S., Borens, O. & Trampuz, A. (2013) Propionibacterium acnes: an underestimated pathogen in implant-associated infections. *BioMed research international*. [Online] 2013804391.

Prichard, J. (2012) Rotation or reciprocation: a contemporary look at NiTi instruments? *British dental journal*. [Online] 212 (7), 345–346.

Pumarola-sufi, J., Sold-vicens, L., Sentis-vilalta, J., Canalda-sahli, C. & Brau-aguadd, E. (1998) Absorbency Properties of Different Brands of Standardized Endodontic Paper Points. *Journal of endodontics*. 24 (12), 796–798.

Reylon Plasma GmbH (n.d.) *Atmospheric plasma sterilization (PB3 / PZ2)* [online]. Available from: https://www.relyon-plasma.com/applications/sterilization/?lang=en.

Rosan, B. & Lamont, R. J. (2000) Dental plaque formation. *Microbes and infection / Institut Pasteur*. [Online] 2 (13), 1599–1607.

Roy, S., Elgharably, H., Sinha, M., Ganesh, K., Chaney, S., Mann, E., Miller, C., Khanna, S., Bergdall, V. K., Powell, H. M., Cook, C. H., Gordillo, G. M., et al. (2014) Mixed-species biofilm compromises wound healing by disrupting epidermal barrier function. *Journal of Pathology*. [Online] 233 (4), 331–343.

Ruddle, C. J. (2005) The ProTaper technique. *Endodontic Topics*. [Online] 10 (1), 187–190.

Rupf, S., Idlibi, A. N., Marrawi, F. Al, Hannig, M., Schubert, A., von Mueller, L., Spitzer, W., Holtmann, H., Lehmann, A., Rueppell, A. & Schindler, A. (2011) Removing biofilms from microstructured titanium Ex Vivo: A novel approach using atmospheric plasma technology. *PLoS ONE*. [Online] 6 (10), e25893.

Sainsbury, A. L., Bird, P. S. & Walsh, L. J. (2009a) DIAGNOdent laser fluorescence assessment of endodontic infection. *Journal of endodontics*. [Online] 35 (10), 1404–1407.

Sainsbury, A. L., Bird, P. S. & Walsh, L. J. (2009b) DIAGNOdent laser fluorescence assessment

of endodontic infection. *Journal of endodontics*. [Online] 35 (10), 1404–1407.

Sainsbury, A. L., Bird, P. S. & Walsh, L. J. (2009c) DIAGNOdent laser fluorescence assessment of endodontic infection. *Journal of endodontics*. [Online] 35 (10), 1404–1407.

Sakka, S., Baroudi, K. & Nassani, M. Z. (2012) Factors associated with early and late failure of dental implants. *Journal of investigative and clinical dentistry*. [Online] 3 (4), 258–261.

Sánchez, M. C., Llama-Palacios, A., Fernández, E., Figuero, E., Marín, M. J., León, R., Blanc, V., Herrera, D. & Sanz, M. (2014) An in vitro biofilm model associated to dental implants: structural and quantitative analysis of in vitro biofilm formation on different dental implant surfaces. *Dental materials : official publication of the Academy of Dental Materials*. [Online] 30 (10), 1161–1171.

Sathorn, C., Parashos, P. & Messer, H. H. (2007) How useful is root canal culturing in predicting treatment outcome? *Journal of endodontics*. [Online] 33 (3), 220–225.

Sato, T., Yamaki, K., Ishida, N., Shoji, M., Sato, E., Abiko, Y., Hashimoto, K., Takeuchi, Y., Matsuyama, J., Shimauchi, H. & Takahashi, N. (2012) Rapid quantification of bacteria in infected root canals using fluorescence reagents and a membrane filter: a pilot study on its clinical application to the evaluation of the outcomes of endodontic treatment. *International journal of dentistry*. [Online] 2012 (172935), 1–4.

Schneider, C. a, Rasband, W. S. & Eliceiri, K. W. (2012) NIH Image to ImageJ: 25 years of image analysis. *Nature Methods*. [Online] 9 (7), 671–675.

Schwarz, F., Ferrari, D., Popovski, K., Hartig, B. & Becker, J. (2009) Influence of different air-abrasive powders on cell viability at biologically contaminated titanium dental implants surfaces. *Journal of Biomedical Materials Research - Part B Applied Biomaterials*. [Online] 88 (1), 83–91.

Schwarz, F., Sahm, N. & Becker, J. (2014) Combined surgical therapy of advanced peri-implantitis lesions with concomitant soft tissue volume augmentation. A case series. *Clinical Oral Implants Research*. [Online] 25 (1), 132–136.

Sedlacek, M. & Walker, C. (2007) Antibiotic resistance in an in vitro subgingival biofilm model.

Oral microbiology and immunology. 22333–339.

Shah, J., Mark, O., Weltman, H., Barcelo, N., Lo, W., Wronska, D., Kakkilaya, S., Rao, A., Bhat, S. T., Sinha, R., Omar, S., O'bare, P., et al. (2015) Fluorescence In Situ hybridization (FISH) assays for diagnosing malaria in endemic areas. *PLoS ONE*. [Online] 10 (9), 1–15.

Shen, Y., Stojicic, S. & Haapasalo, M. (2011) Antimicrobial efficacy of chlorhexidine against bacteria in biofilms at different stages of development. *Journal of endodontics*. [Online] 37 (5), 657–661.

Shen, Y., Stojicic, S. & Haapasalo, M. (2010) Bacterial viability in starved and revitalized biofilms: comparison of viability staining and direct culture. *Journal of endodontics*. [Online] 36 (11), 1820–1823.

Shuping, G. B., Orstavik, D., Sigurdsson, a & Trope, M. (2000) Reduction of intracanal bacteria using nickel-titanium rotary instrumentation and various medications. *Journal of endodontia*. [Online] 26 (12), 751–755.

Signoretto, C., Lleò, M. M., Tafi, M. C. & Canepari, P. (2000) Cell wall chemical composition of Enterococcus faecalis in the viable but nonculturable state. *Applied and environmental microbiology*. 66 (5), 1953–1959.

Simonis, P., Dufour, T. & Tenenbaum, H. (2010) Long-term implant survival and success: a 10-16-year follow-up of non-submerged dental implants. *Clinical oral implants research*. [Online] 21 (7), 772–777.

Siqueira, J. F. (2001) Aetiology of root canal treatment failure: why well-treated teeth can fail. *International endodontic journal*. 34 (1), 1–10.

Siqueira, J. F., Antunes, H. S., R????, I. N., Rachid, C. T. C. C. & Alves, F. R. F. (2016) Microbiome in the apical root canal system of teeth with post-treatment apical periodontitis. *PLoS ONE*. [Online] 11 (9), 1–14.

Siqueira, J. F., Rôças, I. N., Santos, S. R. L. D., Lima, K. C., Magalhães, F. a C. & de Uzeda, M. (2002) Efficacy of instrumentation techniques and irrigation regimens in reducing the bacterial population within root canals. *Journal of endodontia*. [Online] 28181–184.

Siqueira, J. F., Rqas, N. & Favieri, A. (2000) Chemomechanical Reduction of the Bacterial Population in the Root Canal after Instrumentation and Irrigation with 1 %, Hypochlorite. *Journal of endodontics*. 26 (6), 331–334.

Sjögren, U., Figdor, D., Persson, S. & Sundqvist, G. (1997) Influence of infection at the time of root filling on the outcome of endodontic treatment of teeth with apical periodontitis. *International endodontic journal*. [Online] 30 (5), 297–306.

Sjögren, U., Figdor, D., Spångberg, L. & Sundqvist, G. (1991) The antimicrobial effect of calcium hydroxide as a short-term intracanal dressing. *International endodontic journal*. [Online] 24 (3), 119–125.

Smeets, R., Henningsen, A., Jung, O., Heiland, M., Hammächer, C. & Stein, J. M. (2014) Definition, etiology, prevention and treatment of peri-implantitis-a review. *Head & face medicine*. [Online] 10 (34), 1–13.

Solano, C., Echeverz, M. & Lasa, I. (2014) Biofilm dispersion and quorum sensing. *Current Opinion in Microbiology*. [Online] 18 (1), 96–104.

Stewart, P. S. & Costerton, J. W. (2001) Antibiotic resistance of bacteria in biofilms. *Lancet*. 358 (9276), 135–138.

Stewart, P. S. & Franklin, M. J. (2008) Physiological heterogeneity in biofilms. *Nature reviews. Microbiology*. [Online] 6 (3), 199–210.

Stewart, P. S., Roe, F., Rayner, J., Elkins, J. G., Lewandowski, Z., Ochsner, U. A. & Hassett, D. J. (2000) Effect of catalase on hydrogen peroxide penetration into Pseudomonas aeruginosa biofilms. *Applied and Environmental Microbiology*. [Online] 66 (2), 836–838.

Stuart, C. H., Schwartz, S. a, Beeson, T. J. & Owatz, C. B. (2006) Enterococcus faecalis: its role in root canal treatment failure and current concepts in retreatment. *Journal of endodontics*. [Online] 32 (2), 93–98.

Takenaka, S., Trivedi, H. M., Corbin, A., Pitts, B. & Stewart, P. S. (2008) Direct visualization of spatial and temporal patterns of antimicrobial action within model oral biofilms. *Applied and environmental microbiology*. [Online] 74 (6), 1869–1875.

Tan, K. S., Yu, V. S. H., Quah, S. Y. & Bergenholtz, G. (2015) Rapid Method for the Detection of Root Canal Bacteria in Endodontic Therapy. *Journal of endodontics*. [Online] 41 (4), 447–450.

Tastepe, C. S., van Waas, R., Liu, Y. & Wismeijer, D. (2012) Air powder abrasive treatment as an implant surface cleaning method: a literature review. *The International journal of oral & maxillofacial implants*. 27 (6), 1461–1473.

Tawakoli, P. N., Al-Ahmad, A., Hoth-Hannig, W., Hannig, M. & Hannig, C. (2012) Comparison of different live/dead stainings for detection and quantification of adherent microorganisms in the initial oral biofilm. *Clinical oral investigations*. [Online] 3 (17), 841–850.

Taylor, P. K., Yeung, A. T. Y. & Hancock, R. E. W. (2014) Antibiotic resistance in Pseudomonas aeruginosa biofilms: Towards the development of novel anti-biofilm therapies. *Journal of Biotechnology*. [Online] 191121–130.

Teughels, W., Van Assche, N., Sliepen, I. & Quirynen, M. (2006) Effect of material characteristics and/or surface topography on biofilm development. *Clinical oral implants research*. [Online] 17 Suppl 268–81.

Thaler, C. & Vogel, S. S. (2006) Quantitative Linear Unmixing of CFP and YFP from Spectral Images Acquired with Two-Photon Excitation. *Cytometry. Part A : the journal of the International Society for Analytical Cytology*. [Online] 69 (8), 904–911.

Toole, G. O., Kaplan, H. B. & Kolter, R. (2000) Biofilm Formation as Microbial Development. *Annual review of microbiology*. 5449–79.

Toyofuku, M., Roschitzki, B., Riedel, K. & Eberl, L. (2012) Identification of Proteins Associated with the Pseudomonas aeruginosa Bio fi lm Extracellular Matrix. *journal of proteome research*. 11 (10), 4906–4915.

Umadevi, S., Joseph, N. M., Kumari, K., Easow, J. M., Kumar, S., Stephen, S., Srirangaraj, S. & Raj, S. (2011) Detection of extended spectrum beta lactamases, AmpC beta lactamases and metallobetalactamases in clinical isolates of ceftazidime resistant Pseudomonas aeruginosa. *Brazilian Journal of Microbiology*. [Online] 42 (4), 1284–1288.

Valeur, B. & Berberan-Santos, M. N. (2013) *Molecular Fluorescence*. Second Edi. Weinheim, Germany: WILEY-VCH Verlag GmbH & Co. KGaA.

Van Der Veen, M. H., Thomas, R. Z., Huysmans, M. C. D. N. J. M. & De Soet, J. J. (2006) Red autofluorescence of dental plaque bacteria. *Caries Research*. [Online] 40 (6), 542–545.

Wakamatsu, R., Takenaka, S., Ohsumi, T., Terao, Y., Ohshima, H. & Okiji, T. (2013) Penetration kinetics of four mouthrinses into Streptococcus mutans biofilms analyzed by direct time-lapse visualization. *Clinical oral investigations*. [Online] 18 (2), 625–634.

Wakamatsu, R., Takenaka, S., Ohsumi, T., Terao, Y., Ohshima, H. & Okiji, T. (2014) Penetration kinetics of four mouthrinses into Streptococcus mutans biofilms analyzed by direct time-lapse visualization. *Clinical oral investigations*. [Online] 18 (2), 625–634.

Wu, H., Moser, C., Wang, H.-Z., Høiby, N. & Song, Z.-J. (2015) Strategies for combating bacterial biofilm infections. *International journal of oral science*. [Online] 7 (1), 1–7.

Xi, C., Marks, D., Schlachter, S., Luo, W. & Boppart, S. A. (2006) High-resolution three-dimensional imaging of biofilm development using optical coherence tomography. *Journal of biomedical optics*. [Online] 11 (3), 34001/1-6.

Xiao, J., Klein, M. I., Falsetta, M. L., Lu, B., Delahunty, C. M., Yates, J. R., Heydorn, A. & Koo, H. (2012) The exopolysaccharide matrix modulates the interaction between 3D architecture and virulence of a mixed-species oral biofilm. *PLoS pathogens*. [Online] 8 (4), e1002623.

Yao, Y., Berg, E. A., Costello, C. E., Troxler, R. F. & Oppenheim, F. G. (2003) Identification of protein components in human acquired enamel pellicle and whole saliva using novel proteomics approaches. *Journal of Biological Chemistry*. [Online] 278 (7), 5300–5308.

Yin, R. & R. Hamblin, M. (2015) Antimicrobial Photosensitizers: Drug Discovery Under the Spotlight. *Current Medicinal Chemistry*. [Online] 22 (18), 2159–2185.

Young, G., Turner, S., Davies, J. K., Sundqvist, G. & Figdor, D. (2007) Bacterial DNA Persists for Extended Periods after Cell Death. *Journal of Endodontics*. [Online] 33 (12), 1417–1420.

Zehnder, M. & Belibasakis, G. N. (2015) On the dynamics of root canal infections-what we understand and what we don't. *Virulence*. [Online] 6 (3), 216–222.

Zhang, D. & Zheng, L. (2015) 'Dental Implants', in *Emerging Trends in Oral Health Sciences and Dentistry*. [Online]. InTech. p. 852.

Zimmermann, T. (2005) Spectral imaging and linear unmixing in light microscopy. *Advances in Biochemical Engineering/Biotechnology*. [Online] 95245–265.

Zimmermann, T., Rietdorf, J. & Pepperkok, R. (2003) Spectral imaging and its applications in live cell microscopy. *FEBS Letters*. [Online] 546 (1), 87–92.

Zipfel, W. R., Williams, R. M. & Webb, W. W. (2003) Nonlinear magic: multiphoton microscopy in the biosciences. *Nature biotechnology*. [Online] 21 (11), 1369–1377.

Ziuzina, D., Boehm, D., Patil, S., Cullen, P. J. & Bourke, P. (2015) Cold plasma inactivation of bacterial biofilms and reduction of quorum sensing regulated virulence factors. *PLoS ONE*. [Online] 10 (9), 1–21.